Understanding the Role of Contrails and Contrail Cirrus in Climate Change: A Global Perspective

Dharmendra Kumar Singh, Swarnali Sanyal, Donald J. Wuebbles

Department of Climate, Meteorology & Atmospheric Sciences (CliMAS), University of Illinois Urbana-Champaign, Urbana, IL 61802, Illinois, USA

Correspondence to: Dharmendra Kumar Singh (dksingh8@illinois.edu)

Abstract

Globally, emissions from aviation affect Earth's climate via complex processes. Contrail cirrus and carbon dioxide emissions are the largest factors contributing to aviation's radiative forcing on climate. Contrail cirrus, like natural cirrus clouds, impacts Earth's climate. While contrail cirrus enhances the influence of natural clouds on climate, uncertainties persist regarding their characteristics and life cycle. Despite extensive research on contrails, significant uncertainties remain. Contrail cirrus encompasses linear contrails and the associated cirrus clouds; these are characterized by ice particle properties, e.g., size, concentration, mixing, extinction, ice water content, optical depth, geometrical depth, and cloud coverage. The climate impact of contrails may intensify due to projected increases in air traffic. The radiative forcing from global contrail cirrus has the potential to triple and could reach as much as 160 mW m^{-2} by 2050. This projection is based on anticipated growth in air traffic and a potential shift to higher altitudes. The future climate impact of contrail cirrus is influenced by factors like the magnitude and geographical spread in air traffic, advancements in fuel efficiency, the effects of the use of alternative fuels, and the effects of the changing climate on the background atmosphere. This study reviews the microphysical processes affecting contrail formation and the aging of contrails and contrail-cirrus. Furthermore, the study explores global observational datasets for contrails, current analyses, and future projections and will aid in evaluating the effectiveness and trade-offs associated with various mitigation strategies. The research highlights gaps in knowledge and uncertainties while outlining research priorities for the future.

Keywords: Aviation, contrails, contrail cirrus, radiative forcing, climate model, climate change

1 Introduction

The increase in the atmospheric carbon dioxide (CO_2) concentration has had the most substantial impact on human-induced climate change over recent decades (IPCC, 2021). Emissions from aviation are a minor but significant contributor to these changes in climate, especially because of emissions of CO_2 and the effects of contrail formation from emitted water vapor (H_2O). Aviation expansion is outpacing economic growth, with projections indicating that over the next two decades, the demand for aviation could grow to about 3 times its present level (Wuebbles et al., 2007), with the International Civil Aviation Organization having previously projected a 4.3% annual growth to 2050 (ICAO 2012). Recent analyses by Boeing and Airbus suggest slightly lower rates of increase of 3.6-3.8% (Boeing, 2022; Airbus, 2023). These analyses suggest that aviation could become an even more important contributor to climate change in the future. Taking both CO_2 and non-CO_2 effects into account, The global aviation industry comprises about 3.5-4% of the current human-made (anthropogenic) activities forcing on climate (Lee et al., 2020; Klöwer et al., 2021; Grewe et al., 2021).

Aviation-induced cirrus is one of the most significant radiative forcing contributors from the aviation sector. (IPCC, 1999; Lee et al., 2009, 2021; Brasseur et al., 2016). However, considerable ambiguities persist, stemming from various origins, such as our incomplete understanding of cirrus cloud characteristics, their geographical distribution, and their life span. (Kärcher 2018; Burkhardt et al., 2018; Schumann and Heymsfield 2017). With current aircraft largely burning fossil fuel, CO_2 emissions are the other major forcing. Additionally, NO_x (oxides of nitrogen) emission also has a notable impact through the production of tropospheric ozone, but this is partially counteracted by chemical feedback effects on concentrations of atmospheric methane (CH_4). Fig. 1 (Lee et al., 2021) provides the most current assessment of the climate-forcing effects resulting from different aviation emissions on a global scale, spanning from 1940 to 2018; these effects are shown in terms of radiative forcing (RF) and effective radiative forcing (ERF). Radiative forcing in the context of contrails is due to the net radiative energy flux at the top of the atmosphere (TOA) caused by the presence of contrails in the atmosphere (Fuglestvedt et al., 2010). A positive radiative forcing (RF) signifies an increase in atmospheric warming, as depicted by the red bars in Figure 1. ERF, on the other hand, adjusts the RF by accounting for rapid responses occurring within the Earth's climate system. While RF and ERF provide valuable insights, it's important to acknowledge that these are global metrics. Contrails primarily affect the upper troposphere and are short-lived, leading to potentially larger regional effects, particularly in densely populated areas with high air traffic.

In the scientific literature, contrail cirrus is defined as encompassing both linear contrails and the resulting formation of cirrus clouds. Figure 2 provides an overview of aviation exhaust plume emissions and factors influencing contrail formation. The characteristics of contrail cirrus include average ice particle sizes and concentrations, extinction, ice water content, optical depth, geometrical depth, and contrail coverage. Integral contrail properties involve parameters such as contrail cirrus volume, total number of ice particles, overall ice water content, and total extinction (area integral of extinction) per contrail length.

Many global climate chemistry models used to study the physics and chemistry affecting the Earth's climate system typically do not incorporate the impacts. Models that do account for contrails estimate contrail cirrus coverage based on simplified treatments of contrail aging and spreading mechanisms in ice-supersaturated regions (ISSRs) (Burkhardt et al., 2010; Burkhardt and Kärcher, 2011; Bock and Burkhardt, 2016; Bier and Burkhardt, 2022; Chen and Gettelman

2013; Bickel et al., 2020; Schumann et al., 2015). The generation of persistent contrails depends on coming across ice-supersaturated conditions along a flight path, and these conditions show variability in both space and time within the troposphere and tropopause region (Irvine et al., 2013; Lamquin et al., 2012; Bier et al., 2017). Estimating the RF from contrail cirrus requires knowledge of complex microphysical processes, radiative transfer, and the interaction of contrails with background cloudiness (Burkhardt et al., 2010).
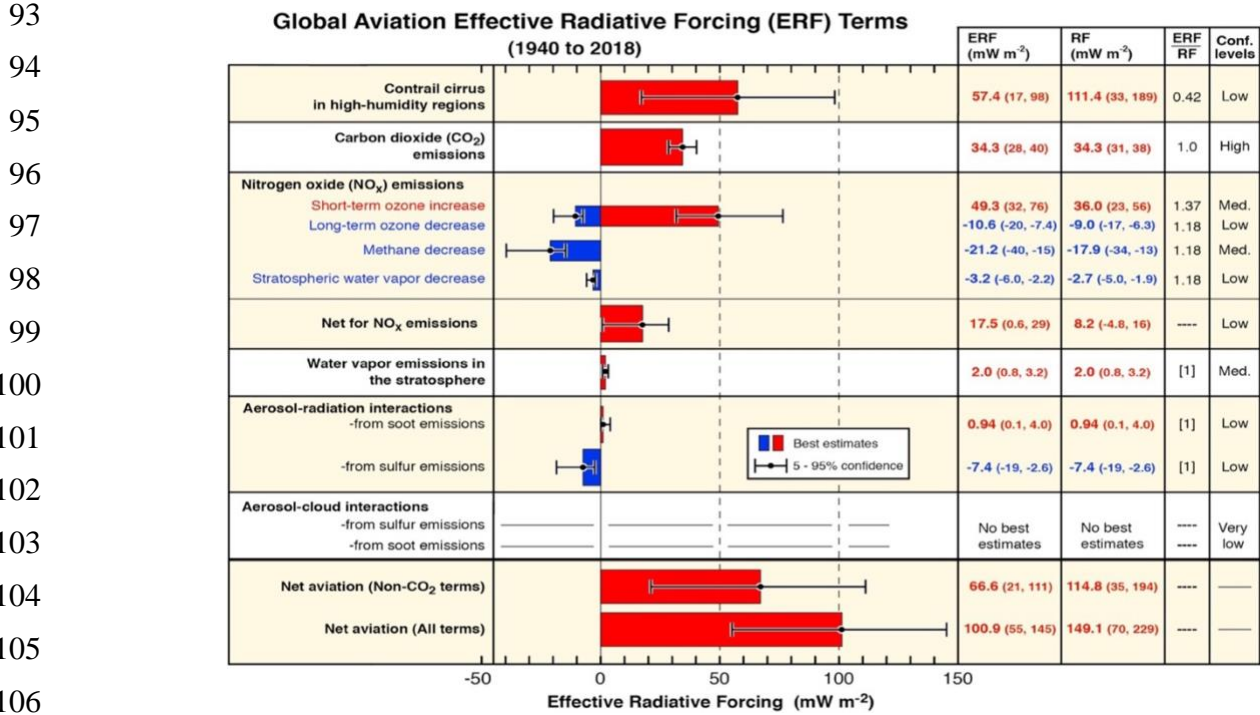
Figure 1. Current best evaluation of the climate forcing between 1940 and 2018 from commercial aviation for different types of emissions. ERF accounts for short-term feedback in the climate system not accounted for in the traditional RF evaluation. Adapted with permission from Lee et al. (2021).
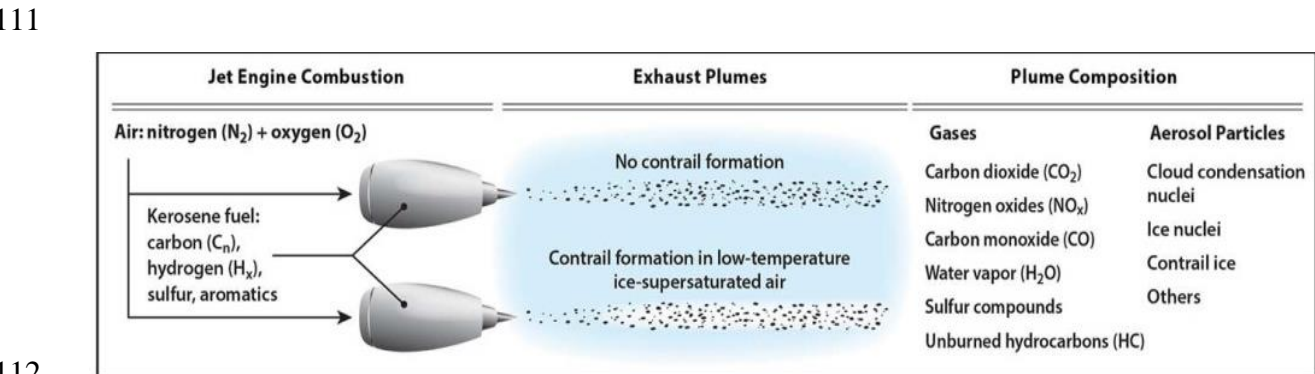
Figure 2. Schematic overview of exhaust plumes (contrail formation in low temperature) and their composition. Adapted with permission from Lee et al. (2021).

116 This review article aims to provide a comprehensive overview of our understanding of contrails,
117 encompassing their formation, progression, and the consequent repercussions on Earth's climate
118 system. In the process, the microphysical processes underlying contrail formation are explored
119 along with their representation in the simulation of contrails in current climate-chemistry models
120 of the global atmosphere. Furthermore, we address the uncertainties surrounding this topic and
121 identify areas requiring further research in the future.

122 2 Microphysics of Contrail Formation, Aging, And Transition to Contrail Cirrus

123 Microphysical processes play a pivotal role in the formation of contrails and their evolution in the
124 atmosphere. This section is aimed at discussing these processes, their effects on the lifetime of
125 contrails, and the possible transition of contrails to contrail cirrus in the upper troposphere.

126 2.1 The Physics of Contrail Formation and Aging

127 The fundamental principles for determining the formation of contrails were independently
128 developed by E. Schmidt in 1941 and H. Appleman in 1953. Contrails appear when the hot and
129 moist exhaust from aircraft quickly mixes with the cold and humid surrounding air, causing the
130 humidity in the exhaust gases to exceed the saturation point for liquid water (Appleman, 1953;
131 Schmidt, 1941; Schumann, 1996). A schematic representation of the Schmidt-Appleman criterion
132 for contrail formation is shown in Figure 3. In this diagram, the two solid curves depict saturation
133 levels concerning liquid water (upper curve) and ice (lower curve). The phase trajectory of the
134 mixture, consisting of exhaust gases and ambient air, follows a straight line from the upper right
135 to the lower left in the e-T diagram, where 'e' represents the partial pressure of water vapor in the
136 mixture, and 'T' represents its absolute temperature (as denoted by the dashed lines). The path that
137 lines up with the water saturation curve (dotted) specifies the highest temperatures at which
138 contrail formation can take place. When the trajectory terminates in an ice-supersaturated state,
139 the persisting contrails have the potential to disperse and transform into contrail cirrus.

140 In cases where the conditions do not meet the criteria, the contrail formed will have a brief lifespan,
141 lasting only a few minutes. The mixing process is presumed to occur isobarically, resulting in a
142 straight-line mixing (phase) trajectory on an e-T diagram. The Schmidt–Appleman criterion
143 (SAC), which is primarily based on thermodynamics, establishes the threshold temperature for
144 contrail formation. This threshold is determined by several factors, such as ambient air pressure,
145 humidity, the amount of water and heat released by the aircraft per unit of fuel, and the overall
146 efficiency of the aircraft engine's propulsion system. (Jensen et al., 1998; Schumann, 1996).
147 Accurate assessments of contrails necessitate precise data on ambient meteorological conditions.
148 The persistence of contrails is contingent on meeting a specific humidity threshold, as defined
149 below.

150 The persistence of contrails hinges on the atmospheric-specific humidity. Temperature and vertical
151 motions within the atmosphere play key roles in determining this humidity. Additionally, the
152 optical characteristics and lifespan of contrails are key aspects of contrail formation and are
153 influenced by various meteorological factors. These factors include turbulence, vertical motions,
154 wind shear, and the presence of ambient cirrus clouds. Furthermore, soot emissions from aircraft
155 engines can also influence these meteorological factors. The size and duration of the ice-
156 supersaturated region, the availability of water vapor for ice crystal growth, and consequently, the
157 sedimentation of these ice crystals within the contrail are also essential considerations (Bock and
158 Burkhardt, 2016). Crucially, the radiative forcing (RF) and the ensuing climate impacts depend on
159 a multitude of meteorological parameters. Additionally, factors such as the albedo and the

160   brightness temperature of the atmosphere in the absence of contrails play a significant role, as
161   outlined by Schumann et al. (2012).

162   Upon reaching the ambient temperature through the process of mixing with the surrounding air,
163   contrails undergo changes in size depending on the ambient humidity. When the ambient relative
164   humidity remains supersaturated concerning ice (RHice >100%), contrails experience growth in
165   ice water content and can remain detectable for up to 5 hours or even longer, as highlighted in
166   various studies (Gierens and Vázquez-Navarro, 2018; Schumann and Heymsfield, 2017; Bier et
167   al., 2017). This extended persistence contrasts with the mean lifetime of contrails, typically noted
168   to be around 2-3 hours (Schumann et al., 2015; Vázquez-Navarro et al., 2015; Tesche et al.,
169   2016; Sausen et al., 1998). Contrails, under such conditions, have the potential to disperse and
170   transform into thin cirrus layers. On the other hand, when the ambient relative humidity is not
171   supersaturated concerning ice, contrail ice particles sublimate and dissipate. The timescale of this
172   sublimation and dissipation process is contingent on the sizes of the contrail ice particles and the
173   ambient air RHice (Schumann, 2012).

174   Combinations of satellite information and ground-based lidar measurements, such as in the Atlas
175   et al. (2006) case study, showed a lifetime of more than 2 hours and a mean optical thickness
176   (integrated extinction coefficient over a vertical column of unit cross section) of 0.35. Duda et al.
177   (2004) studied the development of contrail clusters over the Great Lakes and derived optical
178   thickness (optical depth, τ) from 0.1 to 0.6 for contrails that lasted several hours (Kärcher et al.,
179   2009). Graf et al. (2012) studied the cirrus cover cycle and observed timescales between 2.3 to
180   4.1 hours for contrail cirrus and 1.4 to 2.4 hours for linear contrails.
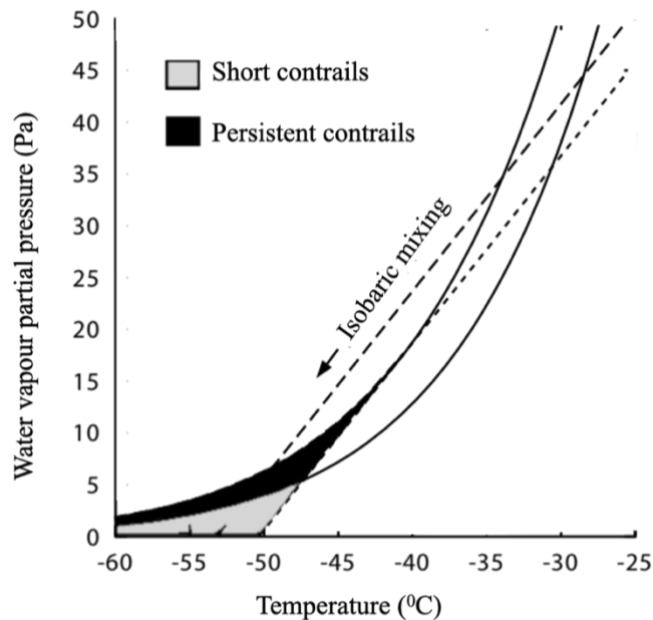
192   **Figure 3.** Phase diagram with mixing lines for aircraft exhaust Adapted from Gierens et al. (2008)
193   (Licensed under CC BY 4.0).

194   The critical factor influencing this contrasting behavior lies in the concept of ice supersaturation.
195   Ice supersaturation refers to conditions where the ambient humidity exceeds the saturation point

for ice, even at temperatures below freezing. These conditions are essential for the persistence and growth of contrails. While the initial formation process might occur at varying humidity levels, studies like Ovarlez et al. (2002) highlight the presence of ice supersaturation within cirrus clouds, which can significantly impact contrail persistence. Jensen et al. (2001) revealed a surprisingly high frequency of ice supersaturation in the upper troposphere, even in the absence of visible ice clouds. This finding highlights the importance of considering ice supersaturation for accurate assessments of contrail persistence and its potential transformation into cirrus clouds.

Upon reaching the ambient temperature through the process of mixing with the surrounding air, contrails undergo changes in size depending on the ambient humidity. When the ambient relative humidity remains supersaturated concerning ice (RHice >100%), contrails experience growth in ice water content and can remain detectable for up to 5 hours or even longer. The microphysical properties of contrails, including ice crystal size distribution and habit, significantly influence their radiative effects and persistence. These properties are determined by the initial conditions during contrail formation and subsequent processes. Ice crystal shapes in contrails are primarily randomly oriented, small ice crystals, with a possibility of some horizontally oriented plates existing as well. This finding is supported by Iwabuchi et al. (2012) who analyzed contrails using a combination of MODIS and CALIPSO satellite data. Their study showed that contrails have larger backscattering coefficients than neighboring cirrus clouds, indicative of smaller ice crystals. The analysis also suggested a tendency for stronger depolarization when ice crystals are small, with a mean linear depolarization ratio (LDR) of approximately 0.4-0.45 for young contrails and contrail cores (Iwabuchi et al., 2012).

There has been ongoing uncertainty regarding whether persistent contrails exclusively form in cloud-free supersaturated areas or if they can also develop within existing cirrus clouds (Burkhardt et al. 2008). Subsequent modeling work (Tesche et al. 2016) suggested that persistent contrails indeed have the potential to form within cirrus clouds. While the formation of contrails is commonly observed in clear skies, they also emerge in conditions where the sky is covered with thin or even subvisible cirrus clouds (Immler et al. 2008).

The temperature threshold for contrail formation, known as the SAC threshold, is slightly higher in cirrus clouds compared to clear air (Gierens, 2012). This difference is attributed to the additional humidity introduced by the ice water content (IWC) from cirrus clouds (Verma and Burkhardt 2022). In situ measurements have indicated high ice supersaturation both inside and outside cirrus clouds (Comstock et al. 2004). Moreover, observational evidence suggests that contrails embedded within cirrus clouds are not significantly thinner than contrails forming in clear air (Poellot et al. 1999).

A reliable estimation of the radiative effects stemming from contrail cirrus relies heavily on their optical properties, which are intricately linked to their microphysical properties and age, as well as their geographical distribution. The microphysical characteristics of contrail cirrus at various plume ages, as observed in diverse airborne campaigns, have been systematically compiled and detailed (Schröder et al. 2000; Schumann et al. 2017; Chauvigné et al. 2018). Fresh contrails, typically observed in plumes around 2 minutes old, exhibit distinct features, including an ice crystal number concentration reaching thousands per cubic centimeter and ice crystals measuring up to a few micrometers in diameter. This characterization is consistent with observations (Märkl et al., 2024, Bräuer et al., 2021a; Petzold et al., 1997). Contrails in their initial 2-5 minutes of existence have been frequently measured (Voigt et al., 2011; Gayet et al., 2012). The distinctive feature of these young contrails lies in their notably high ice crystal number concentration of small

ice particles, making them easily discernible from natural cirrus formations. However, contrails often coexist with natural cirrus and may be incorporated into thin or subvisible cirrus (Kübbeler et al., 2011; Gierens, 2012; Unterstrasser et al., 2017). This coexistence poses a challenge in distinguishing between aged contrails and natural cirrus, complicating efforts to clarify the contribution of contrail cirrus to the radiative balance. Contrail cirrus is characterized by a low ice water content (IWC) ranging from 0.1 to about 10 mg m^{-3}, a feature it shares with natural cirrus of in-situ origin, as observed by Schumann et al. (2017). Ice crystals within these clouds have formed and enlarged in an ice-cloud environment (Luebke et al., 2016; Krämer et al., 2020). In contrast to contrail cirrus and in situ-origin cirrus, cirrus clouds initiating from liquid often yield a higher IWC since their ice crystals originally form as liquid drops (Krämer et al., 2016, 2020) in a warmer atmosphere with an ambient temperature exceeding 235 K (-38°C), particles undergo freezing as they are lifted into the cirrus temperature region of the atmosphere.

Chauvigné et al. (2018) applied a method based on principal component analysis to differentiate between particles in contrail cirrus at various stages and those observed in natural cirrus during the CONCERT 2008 campaign (Voigt et al., 2010). The success of the campaign stemmed from the fact that contrails sampled during the CONCERT initiative were relatively young and exhibited greater distinctiveness compared to natural cirrus formations. Despite this success, the comprehensive acquisition of all necessary optical and microphysical parameters proved challenging during single aircraft campaigns, limiting the widespread application of this method. The CONCERT dataset is relatively small, encompassing approximately 4.0 hours of sampling time in total (Kübbeler et al., 2011). A commonly held assumption regarding the formation and evolution conditions of contrail cirrus is that it tends to persist particularly in ice-supersaturated regions (ISSRs) (Kärcher, 2018).

The collective presence of commercial, military, and other aircraft contributes to a global increase in cloudiness, primarily facilitated by the formation of persistent contrails when the surrounding atmosphere reaches supersaturation. Contrail cirrus exhibits both cooling and warming effects, with the nighttime impact being predominantly warming. Previous assessments of aviation's influence on climate (IPCC, 1999; Lee et al., 2009; Brasseur et al., 2016) were limited by the challenge of accurately quantifying the role of cloudiness arising from aging and spreading contrails (Minnis et al., 2013). The formation of a persistent contrail necessitates ice-supersaturated conditions along the aircraft's flight path. The life cycles of contrail cirrus are contingent upon the temporal and spatial scales of ice-supersaturated regions, which exhibit high variability in the troposphere and tropopause region (e.g., Lamquin et al., 2012; Irvine et al., 2013; Bier et al., 2017). Estimating the impact of contrail cirrus on upper tropospheric cloudiness requires the simulation of complex microphysical processes, contrail spreading, overlap with natural clouds, radiative transfer, and interaction with background cloudiness (Burkhardt et al., 2010).

Petzold et al. (2020) conducted a study investigating the frequency distribution of ice-supersaturated regions (ISSRs) through regular in-situ observations made by passenger aircraft across northern mid-latitude areas. Their research underscores the seasonal and geographical variability of ISSRs, indicating a higher likelihood of occurrence during winter and in specific geographic regions. This variability underscores the significance of considering the spatial and temporal distributions of ISSRs when assessing the potential for contrail formation.

Reutter et al. (2020) delved into the characteristics of ice-supersaturated regions using a combination of in-situ water vapor measurements obtained from the IAGOS research program and

286 data from ERA-Interim reanalysis. Their findings showcase the potential for validating reanalysis
287 data with high-resolution aircraft observations. This validation process is critical for enhancing the
288 accuracy of global models utilized in evaluating contrail formation and their subsequent climatic
289 impacts.

290 The ERF of contrail cirrus was estimated for 2011 (relative to an atmosphere without contrails) as
291 50 mWm^{-2} by Boucher et al. (2013), with uncertainty ranging from 20-150 mWm-2. Lee et al.
292 (2021) presented a new estimate derived from the outcomes of global climate models
293 implementing process-based contrail cirrus parameterizations. Recent analyses by Lee et al. (2021)
294 of the current aviation fleet emissions evaluate the ERF through 2018 as 57 mWm^{-2}, with an
295 uncertainty range of 17-98 mWm^{-2}. Given the limited availability of independent estimates,
296 assessing uncertainty becomes crucial. This necessitates analyzing the sensitivities of relevant
297 processes and incorporating the uncertainties associated with the underlying parameters and fields.

298 Contrails are created in the early exhaust plumes of airplanes during cruise (Kärcher et al., 2015;
299 aufm Kampe, 1943, Weickmann, 1945; Schumann and Wendling, 1990; Schumann, 1996). This
300 occurs when a large number of supercooled water droplets are activated and freeze into ice
301 particles. At cruising altitudes, the atmospheric relative humidity (RH) typically falls too low to
302 support the presence of liquid water droplets. However, it is conducive to the existence of ice-
303 phase particles (Gettelman et al., 2006; Lamquin et al., 2012). Therefore, freezing must occur
304 shortly after droplet formation within the moist exhaust plume to produce persistent contrails.
305 Appleman (1953) proposed a critical requirement for contrail formation, suggesting that a
306 significant amount of aerosol particles in the plume act as centers for water condensation (referred
307 to as the "water-saturation constraint"). The formation of contrails also has a visibility constraint,
308 which estimates a minimum number of nucleated ice particles in the contrails at around 10^4 cm^{-3}
309 within a plume age of 0.3s for a small-scale research aircraft (Appleman, 1953; Kärcher et al.,
310 1996). These are the crucial constraints for contrail formation.

2.2 Transition of contrails into contrail cirrus and contrail-cirrus-soot interaction

312 Contrail cirrus consists of elongated contrails trailing high-altitude aircraft and thin cirrus patches
313 formed by the dispersion of persistent contrails. The morphology of contrails evolves based on
314 factors such as humidity, shear, stratification, waves, turbulence, and radiative heating. Contrails,
315 individually and collectively, interact with other cirrus formations, giving rise to what is termed
316 "contrail cirrus" (Schumann and Wendling, 1990). The total extinction is less pronounced when
317 contrails overlap due to humidity competition. Consequently, the climate impact does not always
318 exhibit a linear correlation with air traffic density (Unterstrasser and Sölch, 2012; Bickel et al.,
319 2020). The transformation of a single contrail into a contrail cirrus is observable during aircraft
320 spiral flights, as depicted in Figure 4 (Haywood et al., 2009). "Contrail outbreaks" describe
321 scenarios where numerous aged and young contrails coexist, often spanning expansive areas within
322 the same airspace (Duda et al., 2001).

323 Soot emissions, composed of black carbon particles from aviation, have the potential to alter cirrus
324 properties independently of contrail processing, leading to the formation of "soot cirrus" (Lee et
325 al., 2010). Climate impact assessments of aviation-induced soot cirrus remain inconclusive due to
326 uncertainties in soot abundance and their ice-nucleating properties (Gettelman and Chen, 2013;
327 Zhou and Penner, 2014; Righi et al., 2021). Increased concentrations of small-sized cirrus particles
328 resembling aviation soot emissions have been detected in cirrus regions with dense air traffic
329 (Kristensson et al. 2000). It remains uncertain whether the soot enters the ice during the initial

330 nucleation process or at a later stage through scavenging. The exact mechanism of soot
331 incorporation into cirrus ice remains unclear. Uncertainties persist regarding whether the soot
332 enters the ice during the initial nucleation process or at a later stage through scavenging.

333 A recent study by Testa et al. (2024) examines the processing of aviation soot within contrails and
334 offered further insights into the potential influence of soot on ice nucleation. They specifically
335 investigate the ice nucleation ability of contrail-processed soot particles at cirrus temperatures and
336 found that these particles were generally poor ice nucleating agents. This suggests that soot cirrus
337 formed from processed aviation soot may have a weaker influence on cirrus cloud formation than
338 previously thought.

339 Dischl et al. (2024) demonstrate a significant reduction in non-volatile particle emissions from
340 aircraft engines using sustainable aviation fuel (SAF) compared to traditional jet fuel. This finding
341 indirectly supports the notion that some soot particles might remain dry throughout contrail
342 formation or that some ice particles might sublimate, as these processes could be influenced by
343 particle properties.

344 The sublimation of cirrus particles containing soot and sulfate may lead to the formation of soot
345 aggregates that can potentially act as efficient ice nuclei. A cirrus pattern observed near Munich,
346 Germany, on November 3, 2012, displayed characteristics suggesting an association with aged
347 soot plumes. The cirrus observed between 9.1 and 9.5 km in height, 8-10 km wide, and 35-50 km
348 long, exhibited a distinctive pattern resembling parallel line clouds. Back trajectories indicated that
349 soot was emitted upstream approximately 12 hours before the event by aircraft. The air ascended,
350 forming a cirrus about 4 hours before the event, lasting for about 1-2 hours before subsiding or
351 sublimating. Analyses propose that this could be cirrus formed on preactivated aircraft soot, but
352 certainty is limited, and it cannot be ruled out that the same pattern might have formed without air
353 traffic. (Schumann and Heymsfield, 2017).
354
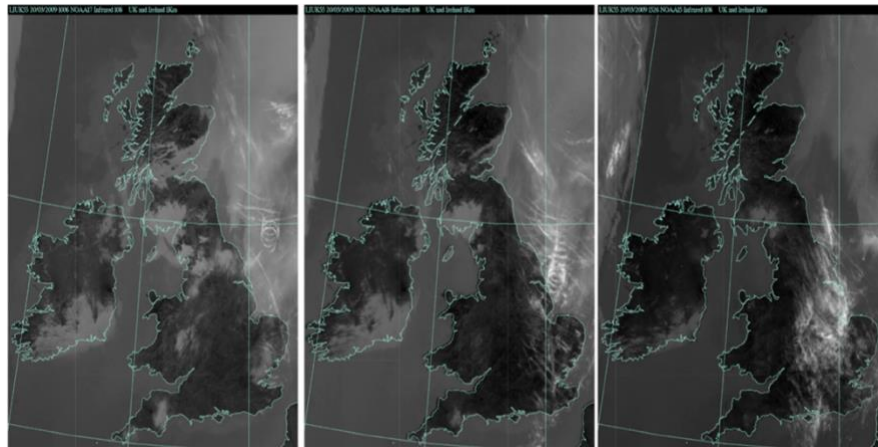
Figure 4. Evolution of contrail cirrus over 1, 3, and 6.5 hours. Contrail cirrus is identified by bright white areas with low infrared (10.8 mm) brightness temperature. The satellite scenes are from NOAA AVHRR for 3 UTC times: (left) 1006 (age after emission = 1 hour), (middle) at 1202 (elapsed time: 3 hours), and (on the right) 1526 (elapsed time: 6.5 hours). Adapted with permission from Haywood et al. (2009).

355

356 A comprehensive understanding of the interplay between contrails, cirrus clouds, and aircraft
357 emissions is essential for accurate assessments of their combined effect on Earth's climate. Recent
358 investigations have illuminated this complex relationship, providing valuable scientific insights.
359 Notably, Urbanek et al. (2018) documented ice clouds exhibiting atypical characteristics over
360 Europe, suggesting potential deviations from standard ice crystal behavior. Additionally, these
361 clouds displayed lower ice supersaturation, hinting at a possible modification in the usual ice
362 formation processes (Urbanek et al., 2018). Intriguingly, the spatial distribution of these cloud
363 formations appeared to correlate with regions experiencing high air traffic. While a definitive
364 causal link between these observations and contrail cirrus formation remains elusive, they do
365 suggest a potential indirect influence stemming from aircraft emissions (Urbanek et al., 2018).

366 In contrast, Kärcher and colleagues (2021) examine the impact of soot particles emitted by aircraft.
367 Kärcher et al. (2021) use modeling to study how these soot particles influence the birth of new
368 cirrus clouds. they found that only a tiny fraction of the soot particles played a role in cloud ice
369 formation via the freezing of liquid aerosol droplets. Consequently, cirrus clouds affected by soot
370 displayed negligible deviations in overall cloud ice content and optical depth compared to their
371 naturally formed counterparts (Kärcher et al., 2021). These findings question the accuracy of
372 current climate models, suggesting they might be overestimating the global radiative impact of
373 interactions between aircraft soot and expansive cirrus clouds.

374 In a related study, Wolf et al. (2023) delve into the radiative effect (RE) of cirrus clouds, shedding
375 light on the pivotal role played by ice crystal properties. Their investigations unveiled that ice
376 crystal size and concentration are the linchpins dictating the overall RE of cirrus clouds.
377 Intriguingly, smaller ice crystals, often associated with contrails, wield a dual-edged radiative
378 effect, inducing both cooling and warming influences. This intricate interplay generally tips the
379 scale towards an overall warming effect exerted by cirrus clouds (Wolf et al., 2023).

380 Beyond the realm of ice crystal properties, Wolf et al. (2023) underscores the importance of other
381 variables. Surface albedo emerges as a contributing factor, with cirrus clouds potentially inducing
382 cooling effects over highly reflective surfaces, like ice, while warming effects over less reflective
383 ones. Additionally, the presence of underlying liquid water clouds and the solar zenith angle also
384 influence the radiative effect. Though their focus primarily centered on plane-parallel clouds, Wolf
385 et al. (2023) acknowledge the potential significance of three-dimensional scattering effects,
386 particularly under high sun angles.

387 **2.3 Evolution of contrails and stages of aviation-induced cloud evolution**

388 The review by Paoli and Shariff (2016) examined the primary physical processes and simulation
389 efforts involved in four distinct phases of contrail evolution. These phases are commonly
390 categorized as the jet, vortex, vortex dissipation, and diffusion phases. Contrail evolution is
391 conveniently divided into these four regimes for clarity (Gerz et al., 1998) (see Fig.5).

392 In the initial seconds after emission (the jet regime), the vortex sheet shed by the wings rolls up
393 into a pair of counter-rotating vortices known as the primary wake. Simultaneously, newly formed
394 ice crystals in the engine exhaust become entrapped around the cores of these vortices. Following
395 this, in the minutes that follow (the vortex regime), the vortices descend into the atmosphere due
396 to their mutually induced downward velocity.
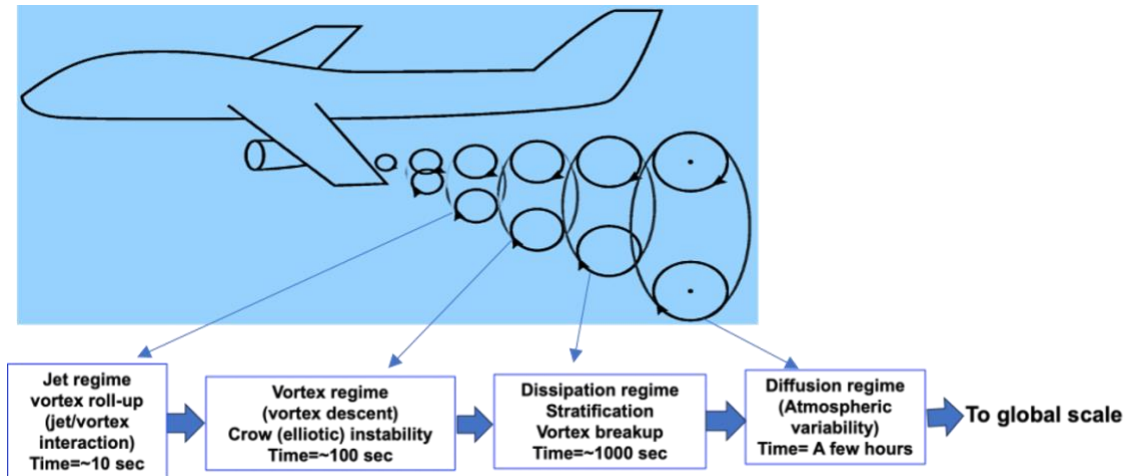
Figure 5. Schematic classification of aircraft wakes evolution into four regimes. Adapted from Paoli and Shariff (2016).

The descent of vortices effects in a contrast in density between the air contained within the vortices (within an oval-shaped region) and the ambient air. This process leads to the generation of vortices with opposite signs (in a stable stratified atmosphere) along the oval boundary. The vorticity shed in the upward direction gives birth to a "secondary wake." Within this secondary wake, a portion of the exhaust gases and ice particles becomes incorporated. Within the regime of vortex dissipation, the primary vortex pair and secondary vorticity disintegrate and disperse, releasing both exhaust and ice crystals that eventually endure sublimation. Ice crystals released in the secondary wake can endure for a longer duration due to the lower temperature. In the fourth regime, known as the diffusion regime, the horizontal and vertical spreading of the contrail is influenced by atmospheric turbulence, particle sedimentation, radiative processes, and wind shear until complete mixing takes place, typically within a few hours.

Figure 6 illustrates the processes that influence the various stages of contrail formation. Exhaust plumes, generated by burning fuel-air mixtures at high temperatures and pressure within turbofan jet engines, contain both gaseous and particulate matter. In the freely expanding and cooling plumes (jet regime), particle types include emitted soot particles and aqueous aerosol particles formed within the exhaust, along with entrained ambient aerosol particles. In scenarios where turbulent mixing occurs, leading to cooling and generating plume supersaturation over liquid water, a significant number of plume particles transform water droplets (depicted as gray circles in Fig. 6).

Water droplets rapidly freeze and increase in size by absorbing water vapor from their surroundings, eventually leading to the formation of a visible contrail. This occurs when the ambient temperature drops below the formation threshold. In exhaust rich in soot, most droplets contain soot inclusions. While droxtals, frozen water droplets with faceted surfaces, and hexagonal prisms and columns likely emerging from them may offer a realistic depiction of small ice crystals in fresh contrails, there is currently no direct observational evidence for their specific shapes.

Plumes from multiple aircraft engines combine with the two wingtip vortices, creating an inhomogeneous wake. The subsequent evolution of ice crystals is contingent upon fluid-dynamical processes, particularly in the vortex regime. The downward movement of the vortex pair warms

425 the surrounding air, resulting in the sublimation of ice crystals in the lower portion of the wake. A
426 small fraction of contrail is amplified by the detrainment of air from the lower wake. Ice crystals
427 present in the upper wake continue to grow by the uptake of entrained ice-supersaturated ambient
428 water vapor. A few minutes past emission, the organized flow pattern collapses and mixes with
429 ambient air (dissipation regime). Tables 1 and 2 summarize the qualitative and quantitative
430 comparisons of contrail characteristics across different stages of evolution, including measurement
431 techniques and modeling considerations.

432
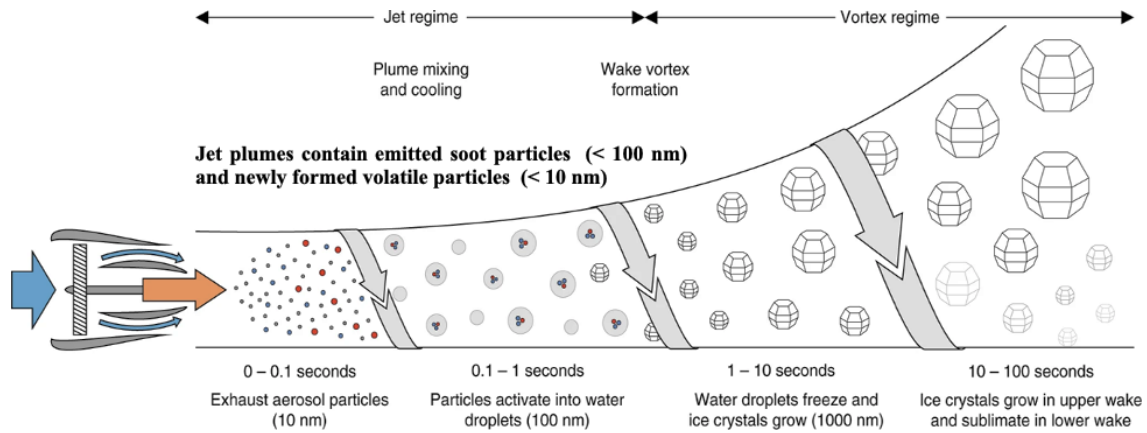
Figure 6. Processes influencing the contrail formation stage. Figure adopted with permission from Kärcher (2018). (Licensed under CC BY 4.0)

433 **Table 1.** Overview of qualitative comparison of contrail characteristics across different stages
434 of evolution

Stage	Ice crystal size	Number density	Extinction properties	Width	Length	Optical depth
Jet	Large and concentrated	High	High	Wide	Long	High
Vortex	Smaller and more dispersed than jet	Moderate	Moderate	Variable	Variable	Moderate
Dissipation	Small and faint	Low	Low	Narrow	Short	Low
Diffusion	Very small and spread out	Very low	Very low	NA	NA	Extremely low

435

2.4 Contrail coverage

437 The radiative forcing (RF) for contrails, as determined by Lee et al. (2010), is defined by the
438 product of contrail coverage and optical depth. For a single contrail segment, this product equates
439 to total extinction. However, defining contrail coverage presents challenges for several reasons.
440 Assessing contrail coverage separately from optical depth introduces difficulties. The
441 identification of young contrails versus other cirrus clouds often relies on their distinctive line

shape. Yet, using geometric characteristics for contrail coverage classification introduces uncertainty, particularly when contrails undergo deformation or shape changes (Mannstein et al., 1999). Only a small fraction of all linear contrails is detectable from satellites (Kärcher et al., 2009; Mannstein et al., 2010; Minnis et al., 2013).

Earlier studies examined global contrail coverage using regional satellite observations, estimating potential contrail coverage based on specific temperature and humidity data and traffic density (Sausen et al., 1998). The integration of observations to achieve hemispheric coverage has only recently become available (Duda et al., 2013). The coverage by contrail cirrus may be significantly higher than determined by line-shaped contrails, and uncertainty factors around an order of 10 have been reported (Burkhardt and Kärcher, 2011). However, this ratio is highly uncertain due to detection issues. Burkhardt and Kärcher (2011) conducted a quantification of contrail cirrus using the ECHAM contrail cirrus global climate model (CCmod), which incorporates a subgrid-scale cloud class representing young contrails. This model captures the life cycle of artificial clouds and simulates their global coverage, along with the changes in natural cloudiness they induce. Their calculations revealed contrail cirrus coverage to be approximately 0.23%. Similar results were obtained from recent attempts to quantify contrail cirrus using MODIS data, accounting for more diffuse contrail contributions (Minnis et al., 2013).

Table 2. Estimated changes in contrail properties during different stages with measurement techniques and modeling consideration.
(This table presents estimated changes in contrail properties (ice crystal size, number density, etc.) during the different stages of their lifecycle. The values are not based on specific references but represent a general understanding derived from contrail studies.)

Stage	Ice Crystal Size (μm)	Number Density (cm^{-3})	Extinction Coefficient (km^{-1})	Width (m)	Length (km)	Optical Depth
Jet	1-10	10^2 - 10^4	10^{-2} - 10^{-1}	10 - 20	10 - 100	0.01 - 0.1
Vortex	10 - 30	10 - 10^2	10^{-3} - 10^{-2}	10^2 - 10^3	1 - 10	0.001 - 0.01
Dissipation	30-100	1 - 10	10^{-4} - 10^{-3}	10^3 - 10^4	0.1 - 1	0.0001 - 0.001
Diffusion (Early)	1000-3000	0.1 - 1	10^{-5} - 10^{-4}	10^4 - 10^5	1 - 10	0.00001 - 0.0001
Diffusion (Mature)	3000-10000	0.01 - 0.1	10^{-6} - 10^{-5}	10^5 - 10^4	NA	NA

Stage	Measurement Techniques	Modeling Considerations
Jet	Lidar, satellite imagery	Microphysics, Ice Nucleation rates
Vortex	Lidar, In-situ probes	Turbulence, Wind shear effects
Dissipation	Lidar, Ground-based observations	Sedimentation, evaporation rates
Diffusion (Early)	Lidar, satellite imagery	Radiative transfer, ice crystal habit
Diffusion (Mature)	Lidar, Satellite imagery	Radiative transfer, cloud macrophysics

Observations during the COVID-19 pandemic lockdowns provide valuable insights into the relationship between air traffic and contrail coverage. Dauda et al. (2023) documented a significant decrease in contrail coverage (up to 41%) over the conterminous United States during the lockdown period compared to pre-pandemic levels. This decrease highlights the direct impact of air traffic on contrail formation and underscores the potential for mitigating climate impact through air traffic management strategies. However, the study also emphasizes the importance of considering environmental factors alongside air traffic when assessing contrail coverage. While

473 the reduction in air traffic was the primary driver of the observed decrease in contrail formation,
474 changes in atmospheric conditions at cruise altitudes likely played a secondary, but significant,
475 role.

476 In a modeling study, Huszar et al. (2013) adjusted the concentration of a tracer for contrails by
477 multiplying it with a specific factor and then adding it to the large-scale cloud ice mixing ratio.
478 They fine-tuned this factor through annual simulations spanning 2005 to achieve an appropriate
479 global value of the top-of-the-atmosphere radiative forcing attributable to contrails and contrail-
480 induced cirrus for that year, aiming for a target value of 31 mWm^{-2} as reported by Burkhardt and
481 Kärcher (2011). The distribution of this forcing aligns with Burkhardt and Kärcher (2011) findings,
482 showing peak values exceeding 300 mWm^{-2} over central Europe and the eastern U.S., with
483 significant parts of Europe and the U.S. experiencing a contrail-induced cirrus radiative forcing
484 above 100 mWm^{-2}. However, their estimates for eastern Asia surpass those of Burkhardt and
485 Kärcher (2011), with maximum values exceeding 300 mWm^{-2}, while ranging between 100 and
486 300 mWm^{-2} elsewhere. They suggested these differences could be attributed to how contrail cirrus
487 is handled (a simpler parameterization in this study versus the more complex contrail-cirrus
488 module used by Burkhardt and Kärcher), variations in simulated thermodynamic conditions over
489 East Asia, and differences in emission inventories.

490 Schumann (2012) developed the Contrail Cirrus Prediction (CoCiP) tool based on a Lagrangian
491 approach. In this model, global contrail coverage is computed by combining the optical depth (τ)
492 contributions from individual contrails and ambient cirrus, counting fractions of areas where
493 contrails cause the optical depth of the total cirrus to surpass a specific threshold (Schumann 2012).

494 Contrails not only augment cloud coverage but also thicken existing cirrus, consequently
495 influencing coverage (Minnis et al., 2013; Schumann and Graf, 2013). This thickening occurs by
496 generating more ice particles with smaller effective radii at constant ice water content (Kristensson
497 et al., 2000). While it is acknowledged that contrails consume humidity and may reduce natural
498 cirrus (Burkhardt and Kärcher, 2011; Unterstrasser and Görsch, 2014; Schumann et al., 2015;
499 Bickel et al., 2020), the prevailing evidence suggests that the thickening effect caused by numerous
500 additional small ice crystals tends to dominate.

501 **2.5 Contrail ice crystal nucleation**

502 Kärcher and Yu (2009) systematically investigated the relationship between nucleated contrail ice
503 crystal numbers and soot particle emissions. In exhaust rich in soot, there is a nearly proportional
504 increase in both ice crystal and soot particle numbers. Close to the contrail threshold, the formation
505 of ice crystals is limited as the low plume supersaturation hinders the activation of water on soot
506 particles, resulting in only a few ice crystals forming. Under conditions rich in soot, the quantity
507 of ice crystals reduces by about one hundred times compared to soot-poor conditions, reaching
508 constant low levels regulated by the number of particles present in the contrail environment. In
509 soot-poor exhaust at low ambient temperatures, there is an increase in ice crystal numbers due to
510 the activation of water and subsequent freezing of abundant aqueous plume particles. Figure 7
511 illustrates the ice crystal number emission index (per kilogram of fuel burnt) in the jet regime,
512 correlating with the number emission index of emitted soot particles as simulated by a parcel model
513 (Kärcher and Yu, 2009). Two sets of results are presented, one for an ambient temperature (T)
514 close to a contrail formation threshold temperature, $\Theta \approx 225$ K (-48°C), commonly encountered in
515 extratropical cruise conditions, and another for a lower temperature of Θ -12 K ≈ 213 K (-60°C).

516   At intermediate ambient temperatures, nucleated ice crystal numbers increase due to enhanced
517   water activation of either soot or ultrafine aqueous plume particles.

518   The hatched area in Figure 7 represents the approximate range of current in-flight soot emission
519   indices. In exhaust rich in soot, the number of soot particles capable of water activation and
520   freezing increases with decreasing ambient temperature. This, in turn, raises plume cooling rates
521   and levels of plume supersaturation over liquid water. It's important to note that the primary driver
522   of the increased cooling and supersaturation is the decreasing ambient temperature, with soot
523   particles acting as additional ice nuclei under these cooler conditions. As the ambient temperature
524   (T) approaches the contrail formation threshold (Θ) in soot-poor exhaust, ambient aerosol particles
525   mixed into exhaust plumes become the sole source of contrail ice crystals. This is because fewer
526   plume particles can be activated due to declining plume supersaturation. The number
527   concentrations of ambient particles in contrails are significantly lower than current levels of soot
528   emissions.

529   The plume cooling rate plays a crucial role in determining the timing of water activation of
530   entrained ambient particles and, consequently, the number of ice crystals derived from them
531   (Kärcher 2015). In soot-poor exhaust, a substantial number of ultrafine aqueous plume particles
532   are formed in the fresh exhaust, especially if the fuel contains condensable vapors besides water
533   vapor. These small particles are anticipated to contribute significantly to ice crystal formation at
534   low ambient temperatures well below average values at cruise levels ($T \approx 218$ K in the extratropic
535   and $T \approx 228$ K in the tropics). If the formation of ultrafine particles cannot be mitigated, ice crystal
536   numbers are expected to be lowest in an intermediate range of soot emissions, specifically between
537   10^{13} and 10^{14} (kg-fuel)$^{-1}$.

538   The ice crystal number (Ni) holds significant importance in the context of contrail formation. Ni
539   quantifies the concentration of ice crystal particles present in the surrounding atmosphere. The
540   significance of Ni in contrail formation lies in its direct influence on various contrail properties.
541   Key aspects such as contrail persistence, the extent of spreading, and the optical characteristics of
542   contrails are closely tied to the ice crystal number (Ni). In essence, Ni serves as a fundamental
543   factor in understanding and characterizing contrail behavior and its impact on the atmosphere. A
544   higher Ni value implies a higher concentration of ice particles in the contrail, which can have
545   several implications, for instance, contrails with a higher Ni tend to persist for longer periods. This
546   means they remain visible in the sky for extended durations before dissipating or spreading. Higher
547   Ni values are associated with greater contrail spreading. As the ice particles in the contrail interact
548   with the surrounding atmospheric conditions, they can spread out and cover a larger area, which
549   may lead to contrail cirrus. The optical properties of contrails, for instance, their brightness and
550   ability to scatter sunlight, are affected by the ice crystal number. Higher Ni values can result in
551   brighter and more reflective contrails, which can contribute to increased cloudiness and affect the
552   Earth's energy balance.

553   The signs of variation in the number of ice crystals refer to the alteration in the ice particle
554   concentration within a contrail, such as increased ice particle concentration in the contrail, greater
555   persistence, and spreading of the contrail. Increased optical effects, such as increased brightness
556   and reflectivity. The decreased ice crystal particle concentration in the contrail leads to reduced
557   persistence and spreading of the contrail, and weaker optical effects. These variations in Ni may
558   occur due to several factors, comprising changes in atmospheric conditions, aircraft engine
559   emissions, and the presence of ice nuclei or other particles that impact ice particle formation.

560 Lewellen (2014) elucidates the pivotal role of initial ice crystal concentration (Ni) in contrail
561 dynamics through extensive simulations and the proposition of a simplified model. Their
562 simulations elucidate a discernible correlation between elevated Ni values and several significant
563 effects on contrails. First, contrails characterized by higher Ni values demonstrate prolonged
564 lifetimes, persisting for considerably extended durations, with simulations even indicating
565 lifetimes surpassing 40 hours (Lewellen, 2014). This protracted residence within the atmosphere
566 translates to amplified influence on radiative forcing, as contrails with higher Ni values possess
567 increased temporal opportunities for interaction with incident solar radiation. Second, heightened
568 ice particle concentration within the contrail leads to augmented contrail spreading. As Ni
569 escalates, interactions with atmospheric conditions become more conspicuous, potentially
570 precipitating the formation of contrail cirrus, a prevalent cirrus cloud type intimately associated
571 with contrail genesis (Lewellen, 2014). Finally, higher Ni values correlate with intensified optical
572 effects. A greater abundance of ice crystals within the contrail facilitates more efficient scattering
573 of incident sunlight, engendering brighter and more reflective contrails that perturb the radiative
574 equilibrium in the atmosphere (Lewellen, 2014).

575 Lewellen (2014) delineates a valuable framework for understanding the influence of Ni on contrail
576 significance through their simplified model: $S_\Sigma = \alpha N \times D$, where S_Σ represents the lifetime-
577 integrated ice crystal surface area, a metric for contrail impact, N is the total crystal number per
578 length of flight path (i.e., ice crystal concentration), and D represents the number-averaged fall
579 distance of ice crystals before sublimation. The coefficient 'α' is approximately constant in the
580 regime of interest. This equation underscores the critical role of Ni (N) in determining the overall
581 radiative forcing exerted by contrails. A higher Ni value translates to a larger S_Σ, indicating a more
582 significant impact on the atmosphere due to increased light scattering and longer contrail
583 persistence.

584 **2.6 Stages of aviation-induced cloud evolution and spreading stage**

585 The microphysical and optical characteristics of ice crystals within contrails undergo alterations
586 as they disperse or transform into contrail cirrus, contingent upon the prevailing meteorological
587 conditions and microphysical processes (Fig. 8). Over time, persistent contrails undertake a
588 transformation from their initial linear form to become contrail cirrus. In regions of heavy air
589 traffic, these contrail cirrus formations overlap and merge, giving rise to extended layers of ice
590 clouds characterized by alterations in shape, depth, and longevity. These patterns differ from
591 natural cirrus clouds in terms of microphysical, and optical, additionally, geometric properties also
592 play a role. The ice-supersaturated layers that sustain these properties exhibit variations in both
593 vertical structure and horizontal extent, impacting the exchange of water molecules between vapor
594 and ice phases within them. Collectively, these factors contribute to the radiative forcing (RF)
595 potential of aviation-induced cirrus (AIC). Figure 8 illustrates the augmentation in cloud coverage
596 area attributed to the vertical shear of horizontal wind components.

597 The turbulent mixing or entrainment processes result in a gradual reduction (dilution) of ice crystal
598 concentrations over time. The sizes of ice crystals grow through the absorption (deposition) of
599 water vapor from layers that are supersaturated with ice. Continuous deposition growth causes
600 deviations in the shapes (habits) of ice crystals from their initial isometric forms.

601
602
603
604
605
606
607
608
609
610
611
612
613
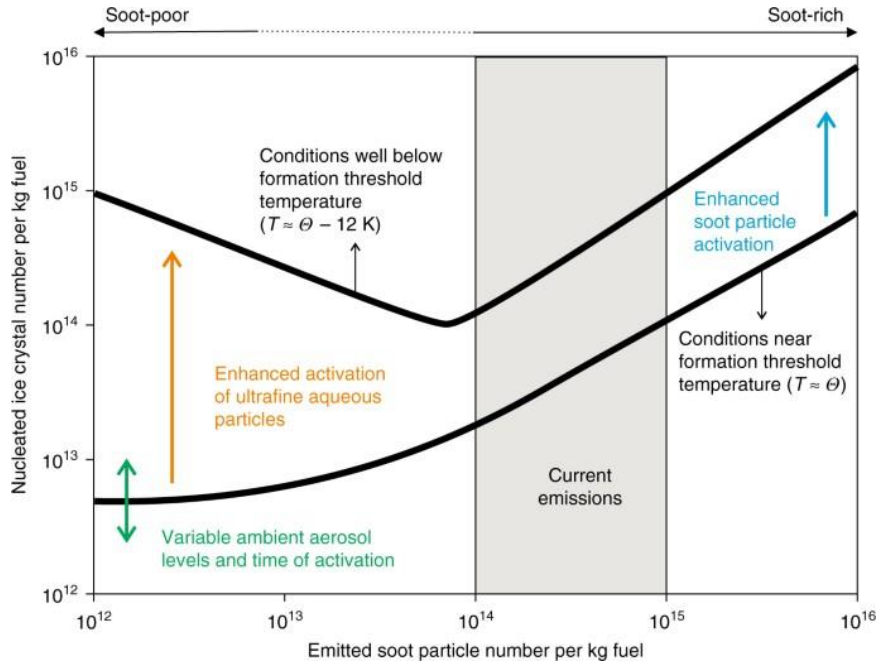
Figure 7. Nucleation of ice crystals in jet aircraft exhaust plumes. Figure adapted with permission from Kärcher (2018). (Licensed under CC BY 4.0)

The shapes and sizes of ice crystals in cirrus clouds significantly impact their growth rates, fall speeds, and optical properties. Larger ice crystals (>30 micrometers) tend to settle due to gravity with fall speeds exceeding 100 meters per hour and are more likely to sublimate in warmer or drier environments. Smaller ice crystals remain suspended around the flight levels due to their negligible fall speeds, provided that some degree of supersaturation can be maintained, which depends on the prevailing meteorological conditions.

The efficiency of sedimentation, the process by which ice crystals fall from clouds, is influenced by the depositional growth rate, which in turn is affected by ice supersaturation, the rate of air cooling, and the characteristics of the ice crystals themselves, including their size, shape, and number concentration. Sedimentation increases the vertical extent of cirrus clouds, enhancing their spreading rate and coverage under sheared flow conditions.

The settling of ice crystals, known as sedimentation, is a critical factor in determining the lifespan of contrails. As the contrail ages, larger ice particles, due to their increased mass, fall out of the plume more rapidly. This phenomenon can be explained by the concept of terminal velocity (Spichtinger and Gierens, 2009). Researchers have explored methods to calculate this velocity, considering the distribution of ice crystal sizes within the plume (Spichtinger and Gierens, 2009). This approach provides a more comprehensive understanding of the sedimentation process.

The size of an individual ice crystal directly influences its falling speed. Larger crystals, typically associated with persistent contrails, descend from the plume quicker than their smaller counterparts found in ephemeral contrails. This sedimentation process significantly impacts the vertical distribution of ice crystals within the contrail and affects its overall persistence. Ice crystals lofted higher, potentially due to weaker updrafts, may experience slower sedimentation and persist for longer durations, especially in colder atmospheric regions.

2.7 Lessons learned from observations of contrails and their properties

Contrails, as well as cirrus clouds, are frequently observed in air that lacks saturation (Kübbeler et al., 2011; Krämer et al., 2009). The prevailing explanation suggests that these clouds consist of large ice particles formed under supersaturated conditions, which then descend to lower and drier levels, undergoing slow sublimation. Notably, instances of contrails and contrail cirrus have been documented in ice-sub-saturated air across various scenarios, extending beyond dedicated contrail research flights (Schumann et al., 2017; Voigt et al., 2011; Kübbeler et al., 2011; Gayet et al., 2012; Chauvigné et al., 2018). Such observations have been derived not only from contrail-specific research endeavors but also from In-service Aircraft for a Global Observing System (IAGOS) commercial aircraft data collected in the North Atlantic region (Petzold et al., 2017).

Apart from a high number of small contrail ice particles, large particles (ice particle diameter greater than 100 µm) were also detected but at relatively low concentrations (Voigt et al., 2010). Such large ice crystals were also observed in contrail cirrus during the ML-CIRRUS (Midlatitude Cirrus experiment) campaign (Voigt et al., 2017). However, attention to contrail cirrus in ice-sub-saturated environments and the role that large ice particles play in contrail cirrus was raised by Kübbeler et al. (2011) and Schumann (2012).
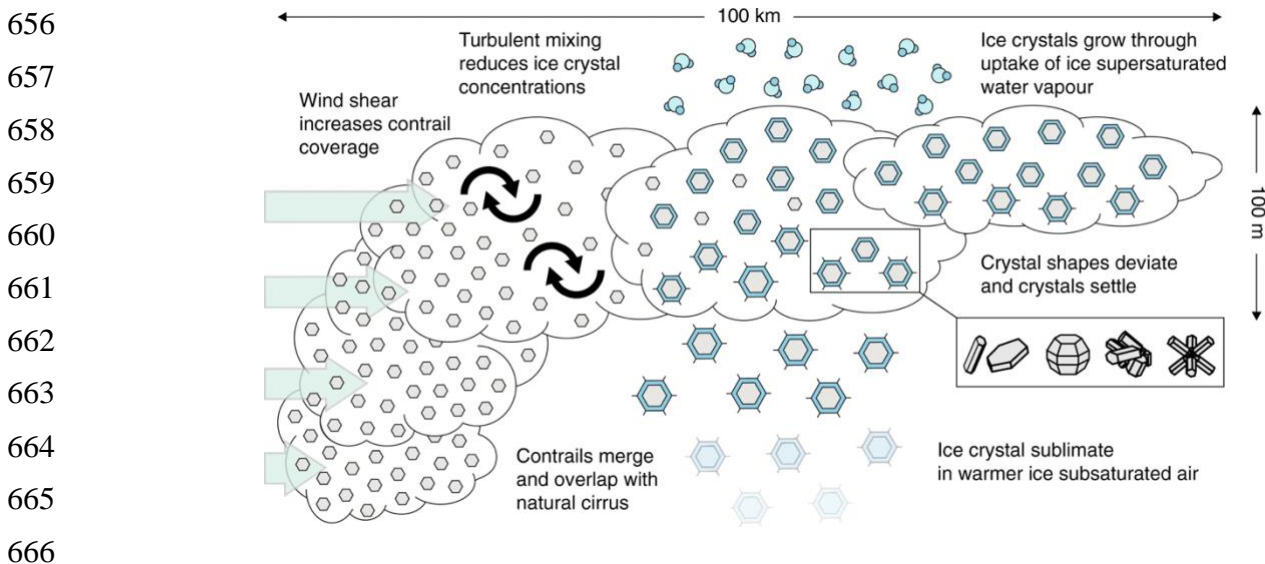
Figure 8. Influential factors in aircraft-induced cloud formation. Figure adopted with permission from Kärcher (2018). (Licensed under CC BY 4.0)

Kübbeler et al. (2011) suggested that the subsaturation observed in contrail cirrus during the CONCERT campaign is caused by the sublimation of large ice particles that may have fallen from higher altitudes after forming under ice supersaturated regions (ISSRs). However, due to the limited contrail cirrus data available, it is difficult to confirm whether contrail cirrus commonly occurs in ice-subsaturated environments.

Li et al. (2023) explored an extended dataset derived from 14.7 hours of cirrus cloud sampling conducted at a frequency of 1 Hz, with a maximum speed of approximately 290 m s^{-1}, obtained during the ML-CIRRUS 2014 campaign. Utilizing readily available parameters that characterize cirrus microphysical properties-including ice number concentration, ice crystal sizes, and ice water content (IWC)-they employed a more straightforward statistical method to distinguish aviation-induced cirrus from natural cirrus, in contrast to the approach adopted by Chauvigné et al. (2018).

680 It consists of the SAC, covering the most common aircraft cruising altitude range, and a recently
681 developed algorithm for detecting aircraft exhaust plumes to identify matured contrail cirrus (>0:5
682 h lifetime; Voigt et al., 2017; Schumann et al., 2017), and natural cirrus. Contrail cirrus showed
683 sharp differences from natural cirrus during the stages of formation and in the corresponding
684 microphysical properties and occurrence conditions.

685 **Observational Constraints**
686 While there is growing evidence regarding contrail observations in ice-subsaturated
687 environments, it is imperative to acknowledge the inherent limitations associated with measuring
688 contrail properties. These limitations stem from various factors, including:
689 *Spatial and temporal resolution of instrumentation:* The comprehensive depiction of contrail
690 phenomena may be impeded by the restricted range or sampling frequency of instruments
691 employed for in-situ or remote sensing observations. For instance, satellite-based observations
692 might fail to capture minute-scale contrail features, while in-situ measurements conducted via
693 research aircraft may not fully encompass the spatial extent of a contrail layer.
694 *Discriminating contrails from natural cirrus formations:* The differentiation between contrails
695 and natural cirrus clouds, particularly in ice-subsaturated conditions, presents a significant
696 challenge and often necessitates sophisticated analytical techniques. Both varieties of ice clouds
697 can exhibit comparable characteristics concerning size and ice crystal properties, rendering the
698 definitive identification of their origin based on limited observations a challenging endeavor.
699 *Restricted data availability:* Observational datasets, particularly those focusing on fully
700 developed contrail cirrus, may be scarce. This scarcity impedes the ability to draw definitive
701 conclusions regarding the prevalence of contrails in sub-saturated environments and their
702 enduring influence on the climate system.
703

704 **3 Modeling of Contrails and their Impacts**

705 Understanding the multifaceted impacts of contrails necessitates employing models at various
706 scales. Local-scale process and fluid-dynamic models offer valuable insights into how plume
707 turbulence and wake dynamics influence the nucleation and properties of contrail ice crystals.
708 These simulations can then be validated against in-situ aircraft measurements of nucleated ice
709 crystal concentrations and sublimation losses (Kärcher, 2018). For broader-scale analysis, cloud-
710 resolving and regional models are utilized. These models incorporate meteorological boundary
711 conditions and leverage optical parameterizations to capture the shortwave radiative response of
712 micron-sized ice crystals. By co-locating these simulations with data from aircraft and satellite
713 observations, scientists can gain a more comprehensive understanding of the radiative forcing (RF)
714 exerted by contrail cirrus and its potential influence on pre-existing cirrus clouds (Kärcher, 2018).

715 The limitations of current instrumentation in measuring the microphysical and optical properties
716 of contrail cirrus elevate the importance of models (Table 3) for estimating their RF. To provide
717 robust predictions of climate change driven by aircraft emissions, models simulating ice nucleation
718 and sublimation must effectively translate the current understanding of contrail formation and
719 evolution processes into frameworks that lack the spatial or temporal resolution to explicitly
720 capture the formation stage. This objective can be achieved by synergistically integrating findings
721 from observations with local-scale, process-oriented models.

722

723

Table 3. Modeling the complexities of aircraft-induced cloud radiative effects (Adapted from Kärcher 2018).

Model scale	Spatial resolution		Contrail stages	Major challenges	Approach/solution
	Horizontal	**Vertical**			
Local	<10 m	<10 m	Formation stage	Ice crystal number and size distribution	Turbulence microphysics coupling
Regional	<1000 m	<100 m	Spreading stage	Radiative flux changes and interaction with natural clouds	Contrail to contrail cirrus transition
Global	<1000km	<1km	Full life cycle	Ice crystal formation and ice supersaturation	Parameterization and high resolution

Improvements in a hierarchy of local- to global-scale models to be realized in conjunction with observations providing data for cloud and radiation parameterization development and overall model validation.

3.1 Modeling of individual contrails

Individual contrails have been studied by various authors through approaches ranging from simplified parameterizations to more complex numerical models. Parameterization approaches normally depend on simplified assumptions to estimate contrail properties based on simplified atmospheric and emission conditions. On the contrary, more sophisticated numerical models, such as the Contrail Cirrus Prediction model (CoCiP), utilize detailed representations of atmospheric processes, ice particle growth, and radiative transfer to simulate the formation and evolution of contrails.

3.1.1 Contrail Cirrus Prediction Tool (CoCiP) for individual contrails

Schumann et al. (2017) compiled a dataset of contrail properties from various sources, including previous publications, additional information gathered from experimenters, reanalysis of existing data, and comparisons with the CoCiP database. The dataset expands upon the work of Schumann and Heymsfield (2017) by incorporating data from the ML-CIRRUS campaign (Voigt et al., 2016). The data includes both in-situ measurements of contrails, such as ice particle size spectra obtained using optical particle spectrometers (Baumgardner et al., 2011; Wendisch and Brenguier, 2013), and remote sensing data from ground-based and airborne lidar, spectroradiometers, satellites, cameras, and visual observations. Remote sensing data provides information on contrail properties such as width and optical depth (Spinhirne et al., 1998; Duda et al., 2004).

3.1.2 MIT Aircraft Plume Chemistry, Emissions, and Microphysics Model (APCEMM)

APCEMM is applied to assess the impact of non-linear plume chemistry and to deliver an initial estimate of the effects of contrails on atmospheric chemistry. Accurately determining the intricate relationship between contrail microphysics and chemistry often necessitates the use of costly large eddy simulations (LESs). APCEMM, through simplified assumptions about plume dynamics, strives to close the disparity between Gaussian plume models and LESs, as outlined by Fritz et al. (2020). APCEMM simulates the growth and chemical progression of an individual aircraft plume. It computes chemical concentrations and aerosol characteristics for a two-dimensional cross-section of the plume, angled perpendicular to the flight path. Dynamics, chemistry, and microphysics are explicitly modeled within the plume, using two different approaches depending on the age of the plume.

755

3.1.3 NASA's global model for evaluation of individual linear contrails

The NASA Ames Research Center developed a computationally efficient aircraft contrail model designed to simulate aircraft-induced contrail formation. This model relies on the Appleman criterion and operates under static atmospheric conditions (Sridhar et al., 2010; Neil et al., 2010). Subsequently, researchers from NASA Ames extended this model to simulate the dynamic transport of contrails by incorporating a Lagrangian dispersion model and a cloud microphysics model (Li et al., 2013). The computational methods employed are grounded in well-established approaches utilized in other aircraft contrail models (Pruppacher and Klett, 2000; Schumann et al., 1995).

In comparison with models from Stanford (Naiman et al., 2009; Naiman et al., 2011; Jacobsen et al., 2011) and DLR (Burkhardt and Kärcher, 2009; Burkhardt and Kärcher, 2011; Bier and Burkhardt, 2022), this dynamic contrail model diverges primarily in two aspects: (1) It excludes the initial contrail ice particles down-wash process caused by airplane wake vortex turbulence. This process, typically lasting less than a minute, is crucial in determining contrail ice nucleation, initial contrail ice particle sizes, and displacements through a complex fluid dynamic process dependent on atmospheric, aircraft, and fuel parameters. In this model, the average initial ice particle size is predefined, and the initial contrail location is set based on the cell where contrail formation conditions are met. (2) The results from this model do not yet include additional radiative forcing caused by aircraft contrails. The researchers are in the process of adding a contrail radiative forcing module capable of computing the total aircraft contrail radiative forcing using inputs from the model, such as ice particle size and linear contrail cloud cover area.

3.1.4 DLR's ICON-LEM regional model

Verma and Burkhardt (2022) developed and implemented a model for contrail formation into the ICON-LEM (ICOsahedral Non-hydrostatic Large-Eddy Model; Zängl et al., 2014; Dipankar et al., 2015). This model includes parameterizations for ice nucleation in the jet phase and ice crystal loss during the contrail's vortex phase. It facilitates the investigation of modifications to cirrus clouds resulting from contrail formation. ICON is the new German Numerical Weather Prediction/Climate Model co-developed by DWD and MPI. It solves a set of equations on an unstructured triangular grid based on successive refinement of a spherical icosahedron (Zängl et al., 2014).

The model asserts high horizontal resolution coupled with a vertical resolution of approximately 150 m in the upper troposphere, enabling the resolution of pertinent cloud processes. Within ICON-LEM, a contrail scheme has been developed and implemented, incorporating the parameterization of contrail ice nucleation as proposed by Kärcher et al. (2015) and accounting for the survival of ice crystals within the vortex phase. (Unterstrasser, 2016), to study changes in cloud variables due to contrail formation within cirrus. Contrail formation, dependent on atmospheric as well as aircraft and fuel parameters, is calculated, and contrail ice nucleation and ice crystal loss in the contrail's vortex phase are estimated.

3.1.5 Large-eddy simulations covering the entire life cycle, from initiation to termination

Lewellen et al. (2014) outlined the utilization of large-eddy simulations with size-resolved microphysics to model persistent aircraft contrails and the resulting contrail-induced cirrus clouds. These simulations aim to depict the dynamic evolution of contrails, spanning from a few wing spans behind the aircraft to their dissipation over an extended period. The emphasis of the study lies in the modeling approach, discussing the development of schemes for efficient numerical computation. The authors introduced dynamic local ice binning and updating, along with coupled radiation, to accurately capture microphysical processes and radiative properties within individual columns. The paper also addresses the challenge of maintaining realistic ambient turbulence over extended simulation times, proposing a "quasi 3D" approach as a computationally feasible approximation of the full dynamics, allowing for exploration across a broader parameter space.

Lewellen (2014) provides an extensive analysis encompassing over 200 instances of long-lived contrails, spanning from their formation at several seconds old to their termination. The study investigated the complete lifespan of long-lived contrails originating from a single aircraft. Various factors were explored, including the effective ice crystal number emission index, temperature, relative humidity concerning ice, stratification, shear, supersaturated-layer depth, uplift/subsidence, and coupled radiation. The analysis delved into the scaling behaviors of contrail lifetime, width, ice mass, and surface area. The simulations unveiled contrail lifetimes exceeding 40 hours, widths surpassing 100 kilometers, and ice masses exceeding 50 kg per meter of the flight path. The paper identified distinct behavioral regimes influenced by radiative forcing and proposed a simplified model to predict these regimes.

Key insights from the simulations highlight the notable impact of ice crystal number loss resulting from competition among different crystal sizes, influencing both young contrails and aging contrail cirrus. The sensitivity of contrail properties to the initial number of ice crystals decreases over time, highlighting the importance of uncertainties in ice crystal deposition coefficients and the Kelvin effect. The influence of atmospheric turbulence on contrail properties and lifetime is also emphasized. Additionally, the paper discusses the effects of ice crystal shape, coupled radiation, precipitation dynamics, and the role of water from fuel consumption in reducing ice crystal loss in colder contrails.

Lewellen's simulations provide valuable insights into contrail behavior, shedding light on the significance of crystal number loss mechanisms, the interaction between shear and ice sedimentation, the depth of the supersaturated layer, and the potential impact of "cold" subvisible contrails. The findings from these simulations contribute to estimating the effects of intricate contrail scenarios, formulating mitigation strategies, and enhancing our comprehension of the dynamics of natural cirrus clouds.

3.2 Treatment of contrails in global models

The consideration of contrail cirrus in global climate models has greatly improved in recent years. Despite these advancements, notable uncertainties persist, particularly in the depiction of contrail microphysics and the interaction between contrail-cirrus and cirrus-radiation. As mentioned earlier, the characteristics of young contrail cirrus diverge from those of natural cirrus primarily due to the elevated ice crystal number concentration typical in contrails. Consequently, microphysical process rates in contrail cirrus, influencing its lifespan, can exhibit significant deviations from those observed in natural cirrus. In this section, we examine the treatments of contrail and contrail cirrus in global models. Very few models account for contrails, so our focus

838 is on those models that have been published extensively on contrail impacts, including modeling
839 studies done by the Institute for Atmospheric Physics (DLR), the National Center for Atmospheric
840 Research (NCAR), and Stanford University. The focus is on their modeling approaches and
841 findings. We start with a description of the approach used to treat contrails in these models.

3.2.1 DLR Contrail Cirrus Prediction Model (CoCiP)

843 CoCiP can be implemented within a GCM and used to study the global distributions of contrails
844 and contrail cirrus (Schumann et al., 2015). The model is specifically crafted for the estimation of
845 contrail cirrus coverage and the analysis of contrail climate impact, particularly in the context of
846 aviation system optimization processes. It is engineered to simulate the entire life cycle of
847 contrails. Contrail segments arise between waypoints along individual aircraft tracks in air masses
848 that are cold and humid enough. The initial characteristics of contrails are contingent upon the
849 specific aircraft involved. The advection and progression of contrails adhere to a Lagrangian
850 Gaussian plume model. This model treats the contrail life cycle using bulk contrail ice physics,
851 incorporating several simplifying assumptions. Notably, the model demonstrates efficiency in
852 handling mixing and cloud processes in a quasi-analytical manner (Schumann, 2012). Contrails
853 become extinct when the bulk ice content endures sublimation or precipitation.

854 The model takes into consideration the impact of both aircraft properties and ambient
855 meteorological conditions. This encompasses established contrail formation thresholds, the effects
856 of advection, turbulent mixing, and the formation of ice mass from both emitted and ambient
857 humidity. The number of ice crystals is contingent upon the quantity of soot particles emitted. The
858 model incorporates simplified approximations for the survival of ice particles in adiabatically
859 sinking wake vortices and the loss of particles in aged contrails (Schumann, 2012).

860 CoCiP (Contrail Cirrus Prediction) depicted in Figure 9 simulates the formation of contrails under
861 specific meteorological conditions, either regionally or globally. Numerical weather prediction
862 data are utilized to determine ambient meteorological conditions through linear interpolation at
863 given positions and times. The model has been effectively employed to simulate contrails in both
864 global and specific cases, and its results have been compared with outcomes from other models
865 and in-situ measurements (Schumann, 2012).

3.2.2 DLR version of the ECHAM5-HAM model

867 The global climate model ECHAM5-HAM (European Center for Medium-Range Weather
868 Forecasts (ECMWF) and Hamburg) was developed at the Max Planck Institute (MPI) for
869 Meteorology in Hamburg, Germany (Roeckner et al., 2003, 2006; Stier et al., 2005), and adapted
870 to study of aviation effects on climate, including the modeling of the effects from contrails. The
871 aerosol-climate modeling system ECHAM5-HAM is based on a flexible microphysical approach,
872 and it predicts the evolution of an ensemble of microphysically interacting internally and externally
873 mixed aerosol populations as well as their size distribution and composition. Bier and Burkhardt
874 (2022) applied the ECHAM5-HAM model, incorporating a two-moment microphysical scheme
875 that was expanded to introduce a novel cloud category-contrail cirrus. The contrail cirrus scheme
876 encompasses a parameterization addressing contrail ice nucleation, the loss of ice crystals during
877 the vortex phase, plume dilution, the spreading of contrails influenced by vertical wind shear, and
878 inclusive microphysical and macrophysical processes aligned with the natural cloud scheme.
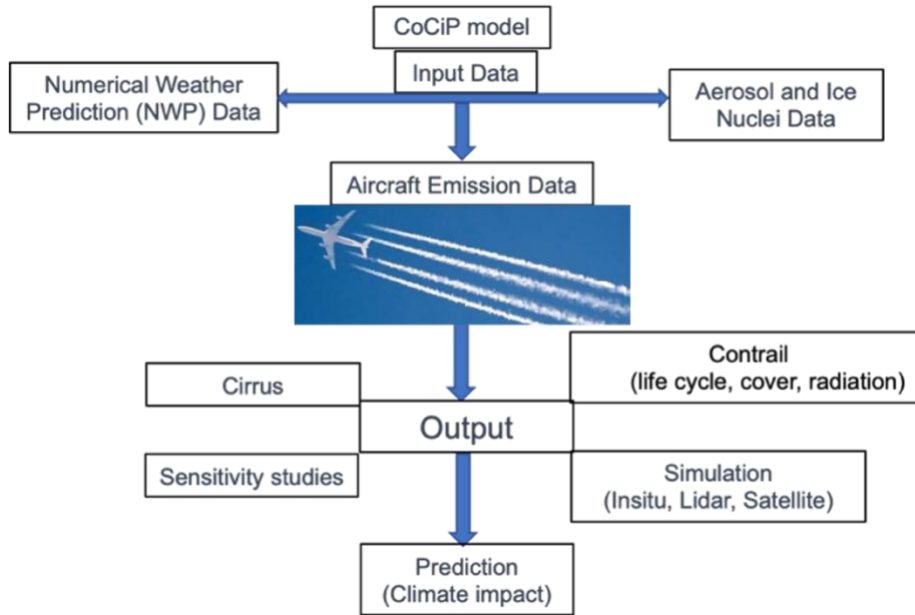
Figure 9. Schematic of the CoCiP model. Adapted from Schumann (2012). Contrail Image (Credit: Adrian Pingstone (public domain)

The contrail cirrus parameterization implemented in ECHAM5-HAM follows the framework established by Burkhardt and Kärcher (2009), who introduced contrail cirrus as a distinct cloud class alongside natural cirrus clouds within the model's natural cloud scheme. The water and heat budgets are balanced, with natural cirrus and contrails competing for available water vapor. Prognostic variables, including ice water content, contrail coverage, and the length of contrail cirrus, are computed based on factors such as persistence, advection, spreading, and deposition/sublimation.

Bock and Burkhardt (2016) extended this parameterization (CCMod) by incorporating a microphysical two-moment scheme (Lohmann et al., 2008). This enhancement significantly improved the representation of microphysical processes by introducing contrail cirrus ice crystal number concentration and volume as additional prognostic variables. This advancement is crucial for studies investigating the impact of aircraft particle number emissions on contrail cirrus properties and their overall climate influence.

Bier and Burkhardt (2022) describe the initialization of contrails within the model. However, the chosen initialization time of 450 seconds (7.5 minutes) warrants further discussion. This value represents half of a model time step, potentially suggesting computational efficiency as a factor in its selection. Nevertheless, a 450-second delay in contrail formation might be too long for accurate simulations, especially for studies focusing on the early stages of contrail evolution. Future investigations need to explore the sensitivity of model results to this initialization time and potentially refine it for a more realistic representation of contrail formation processes.

916

917

918

919

920

921

922

923

924

925

926

927

928
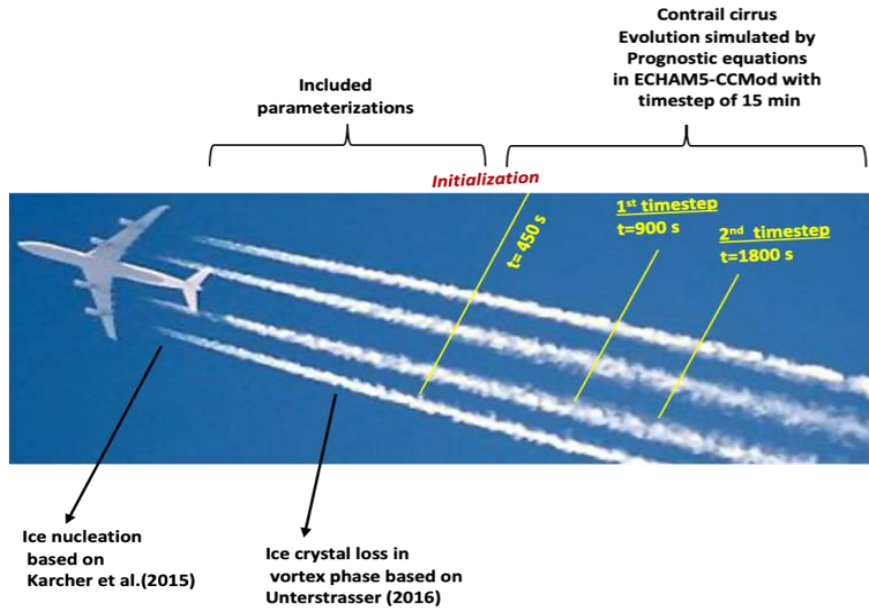
Figure 10. Stages of contrails and their corresponding treatment into the global climate model
ECHAM5-CCMod. [Adapted from Bier and Burkhardt (2022). Contrail Image (Credit: Adrian
Pingstone (public domain)

In instances of contrail cirrus volumes exhibiting very low ice crystal number concentrations, as
observed in aged contrails associated with heightened ice crystal sedimentation, the deposition of
ice water is constrained, aligning with the depositional growth of ice crystals (Bock and Burkhardt,
2016). In more recent iterations of the model, specifically, ECHAM5-CCMod, Bier and Burkhardt
(2019) incorporated the contrail ice nucleation parameterization proposed by Kärcher et al. (2015).
In their model approach, they suggest that the plume cools over time due to continuous mixing of
the exhaust with ambient air, eventually becoming water-supersaturated when the SAC criterion
is met. The number of activated aerosol particles, stemming from soot and ambient particles, is
computed based on ambient conditions, fuel/engine characteristics, and exhaust particle properties.
Additionally, Bier and Burkhardt (2022) introduced a parameterization for ice crystal loss during
the vortex phase and conducted a thorough evaluation of their model.

3.2.3 NCAR CAM6 model with Contrails

In the first NCAR study of the radiative forcing of linear contrails and contrail cirrus, Chen and
Gettelman (2013) used the Community Atmosphere Model version 5 (CAM5), the atmospheric
component of the National Center for Atmospheric Research (NCAR) Community Earth System
Model (CESM). More recently, they have used the updated atmospheric component from the new
version of CESM2 (Danabasoglu et al., 2020). The current atmospheric model implemented in
CESM2 is CAM, version 6.2 (CAM6; Gettelman et al., 2020). CAM6 incorporates a detailed two-
moment cloud microphysics scheme (Gettelman and Morrison, 2015) coupled with an aerosol
microphysics and chemistry model (Liu et al., 2016; Gettelman et al., 2019). The latest version of
the contrail parameterization (Chen et al., 2012) was utilized with CAM6 (Gettelman et al., 2021).
While the ice cloud microphysics and aerosols exhibit minimal differences between CAM5 and
CAM6, the aerosol activation in CAM6 significantly differs, impacting natural cirrus clouds but

955   not contrails. The assumed emission ice particle diameter was adjusted from the original
956   parameterization (10 µm) to 7.5 µm to better align with observations (e.g., Lee et al., 2021).

957   For contrail studies at NCAR, the standard version of CESM with 32 levels (to 3 hPa) vertical and
958   ~ 1∘ horizontal resolution was employed. Winds and optional temperatures were relaxed to
959   NASA's data assimilation analyses, specifically the Modern-Era Retrospective analysis for
960   Research and Applications, version 2 (MERRA2; et al., 2015), with wind nudging (Gettelman et
961   al., 2020, 2021). CESM2 features a fully interactive land surface model (the Community Land
962   Model, version 5; et al., 2020). Sea surface temperatures (SSTs) are fixed to MERRA2 SST, and
963   there is no interactive ocean.

964   These simulations allow for adjustments in atmospheric and surface temperatures, resulting in
965   radiative flux perturbations representing an Effective Radiative Forcing (ERF). Sensitivity tests
966   were conducted, with temperatures nudged to MERRA2. The results were compared with previous
967   contrail simulations using this model and others, as well as observational data. The pattern of
968   contrail-induced changes to cloud fraction closely resembled the previous model documented in
969   CAM5 (Chen and Gettelman 2013), with peak effects observed in the Northern Hemisphere at
970   mid-latitudes. The radiative forcing in the CAM6 simulations exceeded that of the earlier Chen
971   and Gettelman (2013) study due to a smaller initial contrail area (100 vs. 300 m) and smaller initial
972   ice crystal sizes (7.5 vs. 10 µm diameter). The radiative forcing pattern and magnitude were
973   qualitatively and quantitatively consistent with the analysis conducted by Lee et al. (2021),
974   aligning with the intercomparison between contrail simulation models.

975   **3.2.4 Stanford global model for contrail evaluation**

976   Although it is no longer actively utilized in aviation studies, Stanford University developed a low-
977   order contrail model and a Large Eddy Simulation (LES) model (Naiman et al., 2009; Naiman et
978   al., 2011; Jacobsen et al., 2011). In their work, Jacobsen et al. (2011) assessed mass-conservative,
979   positive-definite, unconditionally stable, and non-iterative numerical techniques for simulating the
980   evolution of discrete, size, and composition-resolved aerosol and contrail particles within
981   individual aircraft exhaust plumes. This simulation was conducted in a global or regional 3-D
982   atmospheric model, incorporating the coupling of subgrid exhaust plume information to the grid
983   scale (see Fig. 11). This approach represents a distinct method for simulating the impacts of aircraft
984   on climate, contrails, and atmospheric composition.

985   The microphysical processes addressed within each plume include size-resolved coagulation
986   among and between aerosol and contrail particles, aerosol-to-hydrometeor particle ice and liquid
987   nucleation, deposition/sublimation, and condensation/evaporation. Each plume is characterized by
988   its own emission and supersaturation, and the spreading and shearing of each plume's cross-section
989   are calculated over time. Aerosol and contrail-particle core compositions are tracked for each size
990   and affect optical properties within each plume. When linear contrails sublimate or evaporate, their
991   size and composition-resolved aerosol cores and water vapor are introduced to the grid scale,
992   where they influence large-scale clouds. The model's algorithmic properties were analyzed, and
993   the final model was evaluated against in situ and satellite data. Table 4 summarizes the cross-
994   model intercomparison of contrail simulation models covered in this study.

995

996
997
998
999
1000
1001
1002
1003
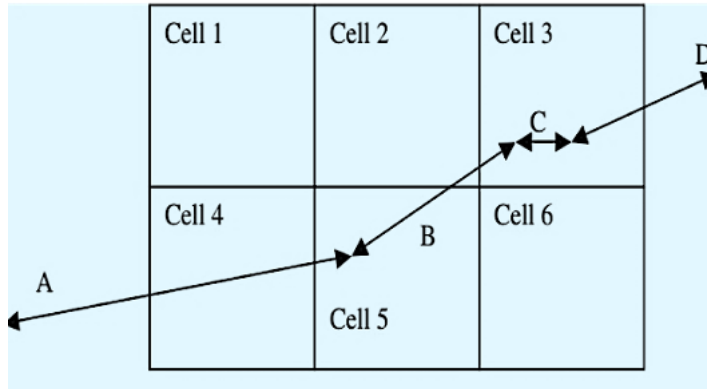
1004 **Figure 11.** Example of how flight segments cross grid cell boundaries in the Jacobsen et al., model.
1005 Segments A, B, C, and D are original segments. These are partitioned or aggregated into individual
1006 model grid cells 2, 3, 4, and 5 to form ''new'' segments. Adapted with permission from Jacobson
1007 et al. (2011).

1008

1009 **Table. 4** Cross-model intercomparison of contrail simulation models
1010
1011

Model Name	Developer	Simulations	Strengths	Weaknesses	Evaluation
CoCiP	DLR	Full life cycle	Efficient computation, considers aircraft/fuel	Simplified mixing, neglects radiation	In-situ measurements, remote sensing data
APCEMM	MIT	Individual microphysics/chemistry	Detailed microphysics	High computational cost, limited global use	Primarily theoretical, limited observations
NASA Global Contrail Model	NASA Ames	Individual formation/transport	Computationally efficient	Neglects downwash, excludes radiative forcing	Reanalysis data
ICON-LEM (Contrail Scheme)	DLR	Contrail formation (regional model)	Considers ice nucleation/survival	Relies on parameterizations, limited microphysics	Satellite data
LES Model	Stanford University	Full life cycle (individual & cirrus)	High-resolution microphysics	Computationally expensive, limited scalability	In-situ measurements

1012
1013

1014 4 Radiative Forcing for Contrail Cirrus in Global Models

1015 4.1 Contrail radiative forcing and efficacy

1016 Contrails during the day can warm or cool depending on optical depth, zenith angle, and ice crystal
1017 shape (Meerkötter et al., 1999; Stuber et al., 2006; Newinger and Burkhardt, 2012). Stuber et al.
1018 (2006) suggested that moving all air traffic to the day decreases RF. Newinger and Burkhardt
1019 (2012) stated that we need to consider the lifetime of the contrails since daytime air traffic can
1020 cause a large contrail coverage at night. After all, it is the long-lived contrail cirrus outbreaks that

1021 are responsible for a large part of the climate impact (Burkhardt et al., 2018). As illustrated in Fig.
1022 1, the overall effect reveals a positive net radiative forcing (RF), signifying a warming impact. The
1023 examination of this phenomenon is undertaken here in contrast to the comprehensive RF, the local
1024 RF (RF′) can be defined as the instantaneous change in net incoming radiation for 100% contrail
1025 coverage in a specific location.

1026 Contrail RF comprises both a long-wave (LW) and a short-wave (SW) component, with each
1027 influenced by flight characteristics and the time of day. Unlike the systematic dependency on
1028 optical depth (τ), the relationship between RF and ice water path (IWP) is less consistent (De Leon
1029 et al., 2012; Schumann et al., 2012). The LW RF is positive both day and night, with the largest
1030 impact observed for a cold contrail (located near the tropopause) over a warm, cloud-free Earth
1031 surface. The shortwave radiative forcing (RF) is predominantly negative, with the greatest impact
1032 observed for contrails over darker surfaces, such as cloud-free oceans (Meerkötter et al., 1999).
1033 Studies conducted by Schumann et al. (2012), utilizing both their model and observational
1034 evaluations, suggest the existence of substantial regional RF′ values. The calculation of contrail
1035 RF within a global model is contingent on factors such as the representation of contrails, the
1036 atmospheric conditions, and the radiation transfer model employed (Myhre et al., 2009).

1037 While radiative forcing (RF) provides a valuable measure of the impact of contrails on the radiative
1038 balance, it doesn't fully account for the efficacy of different forcing agents in driving surface
1039 temperature changes. Recent studies by Bickel et al. (2020) and Ponater et al. (2021) highlight the
1040 importance of effective radiative forcing (ERF) as a superior metric. ERF considers feedback
1041 mechanisms that can influence the ultimate climate impact of a forcing agent.
1042
1043 Bickel et al. (2020) analyzed the feedback processes and quantified the effective radiative forcing
1044 (ERF) of contrail cirrus, which refers to the cloud formations produced by aircraft engine exhaust.
1045 They highlighted that feedback analysis is a valuable tool for understanding climate sensitivity and
1046 the differences in efficacies between various climate-forcing agents. Previous climate model
1047 simulations have suggested a relatively low efficacy of contrails in forcing global mean surface
1048 temperature changes. They employed a climate model that incorporates a state-of-the-art
1049 representation of contrail cirrus and conducted the simulations with fixed sea surface temperatures
1050 to determine the ERF resulting from contrail cirrus.

1051 Bickel et al. (2020) noticed that significant scaling up of aviation density is necessary to obtain
1052 statistically significant results from the simulations. Their study found that the ERF of contrail
1053 cirrus is less than 50% of the respective instantaneous or stratosphere-adjusted radiative forcings.
1054 The best estimate of contrail cirrus ERF is approximately 35%. In comparison, the reduction of
1055 ERF is more substantial for contrail cirrus than for a similar magnitude increase in CO_2
1056 concentrations. They identified the main factor contributing to the reduction in contrail cirrus ERF
1057 as a compensating effect of natural clouds that provide negative feedback. Additionally, they
1058 observed that the combined water vapor and lapse rate adjustment, which affects the distribution
1059 of water vapor in the atmosphere and the lapse rate (temperature decrease with altitude), has a less
1060 positive impact on contrail cirrus ERF compared to the reference case of CO_2 forcing.
1061 Nevertheless, the negative feedback provided by natural clouds has a more pronounced effect in
1062 reducing contrail cirrus ERF compared to these adjustments.

1063 Overall, Bickel et al. (2020) suggested that contrail cirrus has a lower climate impact than initially
1064 thought, with the reduction in ERF attributed to the compensating effect of natural clouds.
1065 Understanding the specific feedback processes and quantifying the ERF of different climate

1066 forcing agents, such as contrail cirrus, is crucial for accurately assessing their contributions to
1067 surface temperature changes and overall climate dynamics.

1068 While radiative forcing (RF) provides a measure of contrail impact on radiative balance, it doesn't
1069 fully account for the efficacy of different forcing agents in driving surface temperature changes.
1070 Recent studies by Ponater et al. (2021) emphasize the importance of effective radiative forcing
1071 (ERF) as a superior metric. ERF considers feedback mechanisms that influence a forcing agent's
1072 ultimate climate impact. Their findings suggest a potentially lower climate impact from contrail
1073 cirrus than previously assumed based on ERF calculations. However, as acknowledged by Ponater
1074 et al. (2021), further research is needed to confirm the efficacy of ERF in assessing the complete
1075 surface temperature response to contrail cirrus. Direct simulations of this response would be
1076 crucial for validating ERF as a reliable metric for contrail cirrus impact.

1077 Similar to findings by Bickel (2023), this study highlights the potential limitations of using RF
1078 alone to estimate contrail cirrus impact. Here, climate model simulations revealed a significant
1079 reduction in the effective radiative forcing (ERF) of contrail cirrus compared to its conventional
1080 RF. This suggests a potentially lower climate impact from contrail cirrus than previously assumed
1081 based solely on RF calculations. The primary contributor to this reduced ERF is likely a negative
1082 cloud adjustment, where contrail cirrus formation leads to a decrease in natural cirrus cover.
1083 Further research is needed to confirm these findings across different climate models and refine our
1084 understanding of contrail cirrus efficacy in driving surface temperature changes.

1085 Long-lasting contrails contribute to global climate change. These contrails can form cirrus clouds,
1086 which are a type of high-altitude cloud that can trap heat in the atmosphere. This trapping of heat
1087 is known as radiative forcing. While the exact contrail contribution to radiative forcing remains
1088 uncertain, it is thought to be a significant factor in climate change (Brasseur et al., 2016). The RF
1089 metric is a backward-looking measure of the effect of emissions on the radiative flux balance and
1090 is commonly used to compare changes in climate forcings (Wuebbles et al., 2010). The RF linked
1091 to non-CO_2 aviation emissions arises from processes occurring over different time scales. Contrails
1092 generally exist for a few hours after an aircraft emissions occur, but other emissions can last much
1093 longer. Effects on the distribution of aerosols and on ozone produced from NOx emissions can
1094 remain for a few days to months, while changes in CH_4 can be affected for longer than a decade.
1095 The limitations of using RF as a comprehensive metric for global non-CO_2 aviation climate
1096 impacts are well-recognized due to such associated spatiotemporal variations (Wuebbles et al.,
1097 2007). The nonlinear interactions involved make it imprecise to represent the sum of RF for various
1098 non-CO_2 components as a single value. Similarly, distinct climate responses are observed for
1099 different forcing mechanisms.

1100 In 2016, Brasseur et al. investigated the radiative forcing (RF) through analyses involving seven
1101 global models (CAM4, CAM5, IGSM, GISS-E2, GEOSCCM, GATOR-GCMOM, and GEOS-
1102 CHEM) as part of the Federal Aviation Administration's (FAA) Aviation Climate Change
1103 Research Initiative (ACCRI) program. The assessment covered climate impacts for 2006, and the
1104 initial five models projected impacts for 2050 scenarios, specifically focusing on selected aircraft
1105 emission components. In a separate study, Chen and Gettelman (2016) used the CAM5 model to
1106 estimate RF for contrails and contrail cirrus in the 2050 future scenario, employing the 2006 AEDT
1107 dataset. Notably, the research highlighted the tendency to overestimate global linear contrail (LC)
1108 net RF when using the natural ice cloud optical property parameterization as a stand-in for contrail
1109 counterparts in modeling studies. Furthermore, the distribution of regional RF indicated that in

1110 densely trafficked airspaces, such as the United States, RF could be up to ten times higher than the
1111 global average (Brasseur et al., 2016).

1112 Schumann and Graf (2013) determined a more significant AIC impact by using both observational
1113 data and the contrail cirrus prediction model (CoCiP; Schumann, 2012). They found an "aviation
1114 fingerprint" ascribed to a daily air traffic cycle within the diurnal cycle of cirrus properties in the
1115 North Atlantic region (NAR), associating with the annual mean diurnal patterns of cirrus cover
1116 and outgoing longwave radiation (OLR) derived from Meteosat data (Graf et al., 2012).

1117 Figure 12 shows the global average annual radiative forcing (RF) values and uncertainty ranges
1118 for persistent contrails alone and together with contrail cirrus. The values are compiled from
1119 selected studies and assessments published since 1999 and include a recent development by
1120 Kärcher (2018). Over time, early assessments of contrail RF have been confirmed and the range
1121 of uncertainty has been narrowed down considerably.
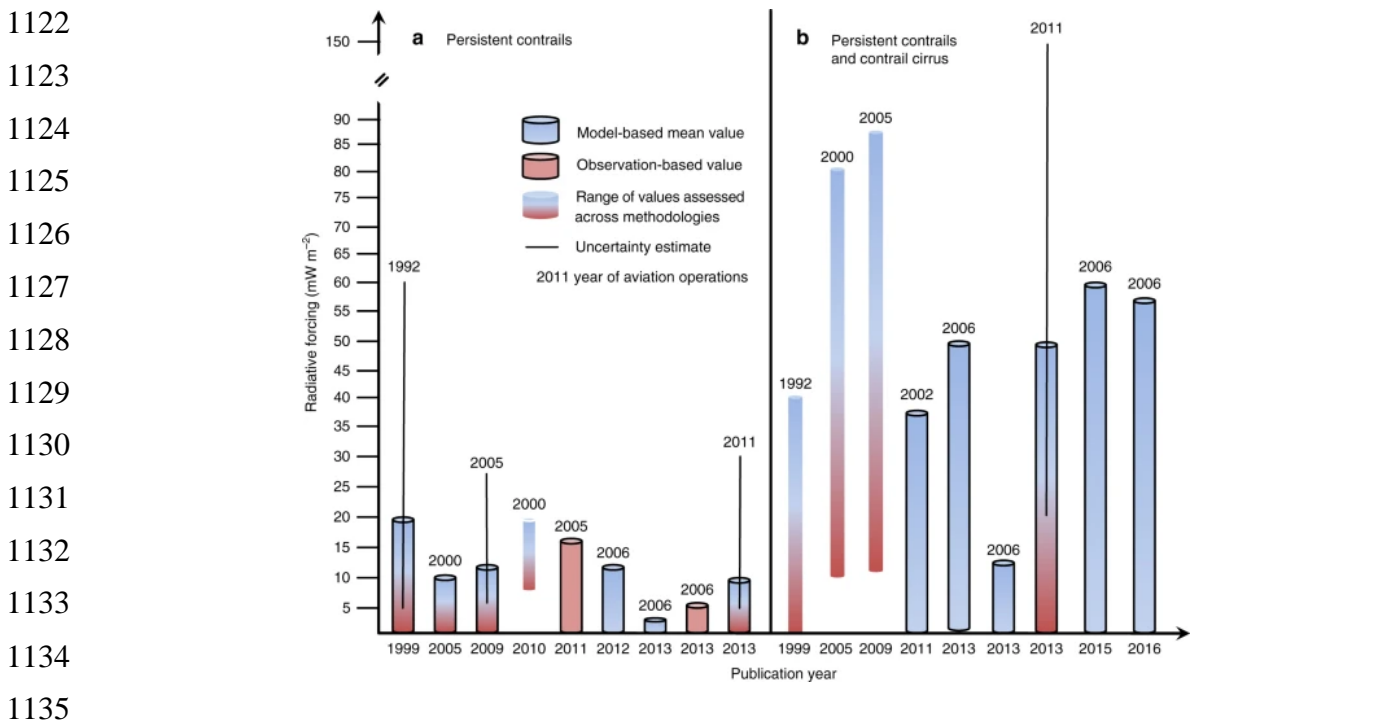
Figure 12. Global annual average amount of radiative forcing caused by aircraft-induced clouds
Figure adapted with permission from Kärcher (2018). (Licensed under CC BY 4.0)

1138 The figure shows that the RF due to persistent contrails alone is -0.01 W/m² (with an uncertainty
1139 range of 0.005-0.03 W/m²), and the RF due to persistent contrails together with contrail cirrus is
1140 ~0.05 W/m² (with an uncertainty range of 0.02-0.15 W/m²). (Kärcher, 2018). Figure. 12 shows
1141 that analyses accounting only for linear contrails underestimate the total RF for contrails. More
1142 recent analyses tend to show an overall warming of around ~45mWm⁻² (Bier and Burkhardt, 2022).

1143 The models applied by DLR and NCAR's groups are summarized in Table 5 (updated from. Bock
1144 and Burkhardt, 2016). Bock and Burkhardt (2016) evaluated the year 2002 using the AERO2k
1145 inventory and for year 2006 using the AEDT 2006 slant distance inventory. The corrected NCAR
1146 analyses and their more recent results are consistent with those from the DLR modeling studies
1147 (Lee et al., 2021). These findings further amplify the conclusions from Fig. 12.

1148 **Table 5.** Summary of existing contrail cirrus simulations and RF from the DLR and NCAR
1149 models. Adapted from of Bock and Burkhardt (2016).
1150

Model	Inventory	Flight distance	RF (mW/m^2)	References
ECHAM5-CCMod	AERO2k 2002	track	35	
ECHAM5-CCMod	AEDT 2006	track	49	*Burkhardt and Kärcher* (2011)
ECHAM5-CCMod	AEDT 2006	slant	56	
ECHAM4-CCMod	AERO2k 2002	track	38	
ECHAM4-CCMod	REACT4C 2006	track	45	*Schumann et al,* (2015)
COCIP	AEDT 2006	flight vectors	63	*Schumann et al.* (2015)
CAM5	AEDT 2006	slant	13 (57)*	*Chen and Gettelman* (2013)
CAM6	AEDT 2006	slant	62 (ERF)**	*Gettelman et al.* (2021)

* The approximation of Chen and Gettelman (2013) was revised.

**ERF (the scaling technique was derived from Lee et al.2021 for 2006 to 2018 and then 9% per year scaled (2018 to 2019) by Gettelman et al. (2021)

AERO2k – Global aircraft emissions data project for climate impacts evaluation

AEDT- Aviation Environmental Design Tool

REACT4C- Reducing Emissions from Aviation by Changing Trajectories for the benefit of Climate

1151 **4.2 Future RF projections**

1152 **4.2.1 DLR's study for future RF projections**

1153 Bock and Burkhardt (2019) investigated how changes in air traffic between 2006 and 2050,
1154 including both volume increase and upward shift in flight altitudes (0.3-1.5 km), would impact
1155 contrail cirrus properties and radiative forcing. Table 6 shows their simulations considering this
1156 combined scenario. It projects a fourfold increase in air traffic and a maximum flight density at a
1157 lower altitude (200 hPa in 2050 compared to 240 hPa in 2006), which has climate implications.

1158 In Table 6, the air traffic distance is specified as the ground-projected track distance. The coverage
1159 is sketched out for all contrail cirrus, and the visibility of contrail cirrus (visible optical depth >
1160 0.05) is indicated in brackets (Bock and Burkhardt, 2016). Radiative forcing estimates exist for
1161 both track distance and slant distance within brackets (Table 6). Remarkably, Bock and Burkhardt
1162 (2019) determined that the projected future increase in air traffic, coupled with a minor shift to
1163 higher altitudes, outcomes in a substantial rise in contrail cirrus coverage, optical depth, and
1164 radiative forcing. Particularly, air traffic contrail cirrus radiative forcing is estimated to increase
1165 threefold, from 49 to 159 mW m^{-2} (Fig. 13). The findings are a result of a future air traffic
1166 inventory, where the measurement of air traffic is signified in terms of track distance (ground
1167 projected) rather than slant distance (3-D). Declining the initial contrail ice particle number by
1168 50% results in a substantial drop in the climate impact of contrail cirrus, leading to a global decline
1169 in radiative forcing for the year 2050. The reduction is significant, amounting to a 14% reduction
1170 from 160 to 137 mWm^{-2} (Fig. 13).

1171 **4.2.2 RF projections from the NCAR model**

1172 The study conducted by Chen and Gettelman (2016) investigated the radiative forcing curbing
1173 from aviation-induced cloudiness, using the Community Atmosphere Model Version 5 (CAM5)
1174 for both present (2006) and future (up to 2050) scenarios. The researchers found a projected four-

1175 fold increase in global flight distance from 2006 to 2050. Despite this, the simulated radiative
1176 forcing from contrail cirrus in 2050 is predicted to reach 87 mWm^{-2}, representing a seven-fold rise
1177 compared to 2006. This underlines a non-linear correlation between radiative forcing and fuel
1178 emission mass, accredited to non-uniform regional escalations in air traffic and changes in contrail
1179 radiative forcing sensitivity through different regions.

1180 **Table 6.** Overview of the model simulations: Air traffic distance exists as ground-projected track
1181 distance. Coverage is furnished for all contrail cirrus, with coverage for visible contrail cirrus
1182 (visible optical depth > 0.05) shown in brackets (Bock and Burkhardt, 2016). The radiative
1183 forcing is represented for both track distance and slant distance, with values enclosed in brackets.
1184 (Adapted from Bock and Burkhardt (2019)

Background	Inventory	Air traffic volume (km yr^{-1})	Propulsion efficiency	Initial ice number concentration (cm^{-3})	Coverage (%)	RF (mW m^{-2})
2006	2006	3.7×10^{10}	0.3	150	1.1 (0.7)	49 (56)
2006	2050 Baseline	15.4×10^{10}	0.3	150	2.9 (2.0)	159 (182*)
2050 (RCP6)	2050 Baseline	15.4×10^{10}	0.3	150	2.8 (2.0)	160 (183*)
2050 (RCP6)	2050 Scenario1	15.4×10^{10}	0.42	75	2.98(1.7)	137 (157*)

RCP6-Representative Concentration Pathway 6.0

*Asterisks denote extrapolated values resultant from the factor resolute by the radiative forcing in 2006, which is connected to air traffic volume and computed using slant distance and track distance (Bock and Burkhardt, 2016).

1185 The CAM5 simulations also indicate that the negative radiative forcing resulting from the indirect
1186 effect of aviation sulfate aerosols on liquid clouds in 2050 could be as large as -160 mWm^{-2}, a
1187 four-fold increase from 2006. Consequently, when considering both aviation aerosols and contrail
1188 cirrus, the total radiative forcing in 2050 could possibly employ a cooling impact on the planet.
1189 Aerosols, particularly aviation sulfate aerosols distributed at cruise altitudes, may be transferred
1190 to the lower troposphere. This procedure raises aerosol concentrations and consequently enhances
1191 the cloud drop number concentration and persistence of low-level clouds. On the other hand, the
1192 study suggests that aviation black carbon aerosols have an insignificant net forcing affect globally,
1193 both in 2006 and 2050.

1194 The researchers focus on specific regions, for instance, Central Europe, eastern North America,
1195 and East Asia, and recommend quantitative evaluations of the forcing in each region for several
1196 scenarios. For example, in Central Europe, the predicted contrail cirrus radiative forcing in 2050
1197 is anticipated to locally peak at 2 Wm^{-2}, marking a 2 to 3-fold increase compared to 2006. In the
1198 eastern United States, the contrail cirrus radiative forcing could reach 800 mWm^{-2} in 2050,
1199 revealing a higher percentage increase compared to 2006. The most prominent rise in contrail
1200 cirrus radiative forcing is estimated in East Asia, where a 6-fold increase is projected for 2050,
1201 associated with the region's anticipated significant rise in consumption of aviation fuel. The
1202 inclusion of aviation aerosols in the simulations suggests a slight reduction in positive forcing over
1203 land, as compared to the forcing solely caused by contrail cirrus. On the other hand, over the ocean,
1204 a negative forcing rising from aviation emissions is measured. This can be accredited to the lower
1205 surface albedo and cleaner environment (fewer aerosols) in comparison to land areas. In the three

1206 regions with the highest projected air traffic in 2050 (eastern United States, Central Europe, and
1207 East Asia), aviation aerosols reduce the regionally averaged positive radiative forcing induced by
1208 contrail cirrus by approximately 50%, as indicated by the blue boxes in Fig. 14. The peak positive
1209 forcing within each of these regions is also reduced by 50% due to aviation aerosols. The study
1210 provides detailed regional estimates of these effects (Table 7).

1211 The negative radiative forcing result from aviation aerosols, as detected in this study, supports the
1212 inferences represented by Righi et al. (2013). The extent of the cooling effect is estimated to be
1213 affected by the background cloud drop number concentration.
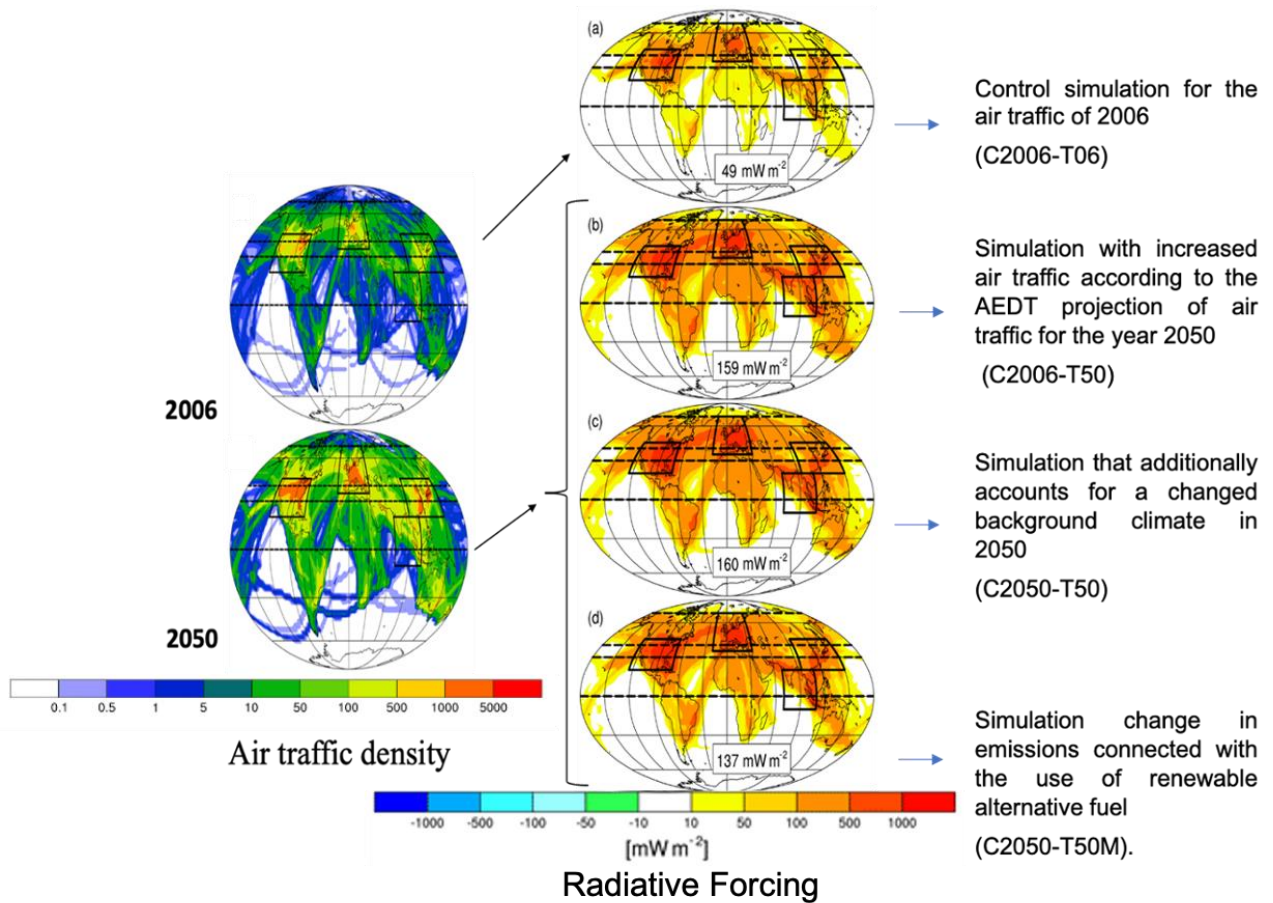
Figure 13. The horizontal distribution depicts the vertically incorporated air traffic density (km
$m^{-2}s^{-1}$) for the years 2006 and 2050, along with the radiative forcing in scenarios C2006-T06 (a),
C2006-T50 (b), C2050-T50 (c), and C2050-T50M (d) Figure adapted with permission from Bock
and Burkhardt (2019). (Licensed under CC BY 4.0).

Table 7. Radiative forcing (mWm^{-2}) attributed to aviation H_2O emissions, with uncertainties derived from 2 standard deviations of the four-member ensemble. (Adapted from Chen and Gettelman, 2016)

Meteorology	Scenario	Global	North America	Central Europe	East Asia
Present	2006 AIR	12 ± 4	195 ± 30	483 ± 69	41 ± 8
2050 RCP4.5	2050 BL	87 ± 6	798 ± 152	1682 ± 535	272 ± 39
2050 RCP4.5	2050 SC1	76 ± 7	724 ± 136	1568 ± 489	231 ± 36
2050 RCP4.5	2050 SC2	76 ± 7	724 ± 136	1568 ± 489	231 ± 36
2050 RCP4.5	2050 SC3	80	681	1952	213
2050 RCP8.5	2050 BL	83 ± 3	852 ± 92	1558 ± 226	248 ± 25
2050 RCP8.5	2050 SC1	73 ± 4	777 ± 96	1442 ± 235	211 ± 24
2050 RCP8.5	2050 SC2	73 ± 4	777 ± 96	1442 ± 235	211 ± 24
2050 RCP8.5	2050 SC3	75	865	1597	221

RCP4.5-Representative Concentration Pathway 4.5

RCP8.5 -Representative Concentration Pathway 8.5. BL-Base line

SC1. SC2, and SC3- Scenarios 1, 2 and 3

4.3 Issues representing cloud-contrail and contrail-contrail overlaps in modeling studies

A thorough examination of past methodologies for modeling cloud layer overlaps and several modeling studies recommends that overlapping with other cloud layers is prone to reduce both the shortwave (cooling) and longwave (warming) radiative forcing linked to contrails (Sanz-Morère et al., 2021). However, there is inadequate agreement on how the overlap between clouds and contrails might modify the net radiative forcing due to uncertainties regarding whether it would more strongly mitigate the shortwave or longwave components. Particularly, the precise impact of contrail-contrail overlap on global contrail radiative forcing has yet to be measured. In this section, we review previous literature referring to the treatment of multiple-layer overlap in the context of contrail radiative forcing calculations.

Schumann et al. (2012) determined that the net radiative forcing may augment if contrails overlap with low-level clouds but could go through significant variations when passing under natural cirrus clouds. This underscores the significance of precisely modeling natural clouds in contrail simulations. Nevertheless, when utilizing this method to simulate single contrails, accounting for the radiative interactions among multiple contrails turns into a challenging task. In prior examples of modeling contrail-contrail overlap, when simulating contrails in global climate models, various treatments have been utilized, as outlined in Table 8. Contrail parametrizations have been formulated for ECHAM4 (Ponater et al., 2002; Burkhardt and Kärcher, 2009), where maximum-random overlap is presumed between contrail and cloud layers, as well as among different contrails (Burkhardt and Kärcher, 2011; Marquart et al., 2003; Bock and Burkhardt, 2016; Frömming et al., 2011). Rädel and Shine (2008) and Rap et al. (2010) also use this parameterization, calibrating the outcomes by using satellite observations.
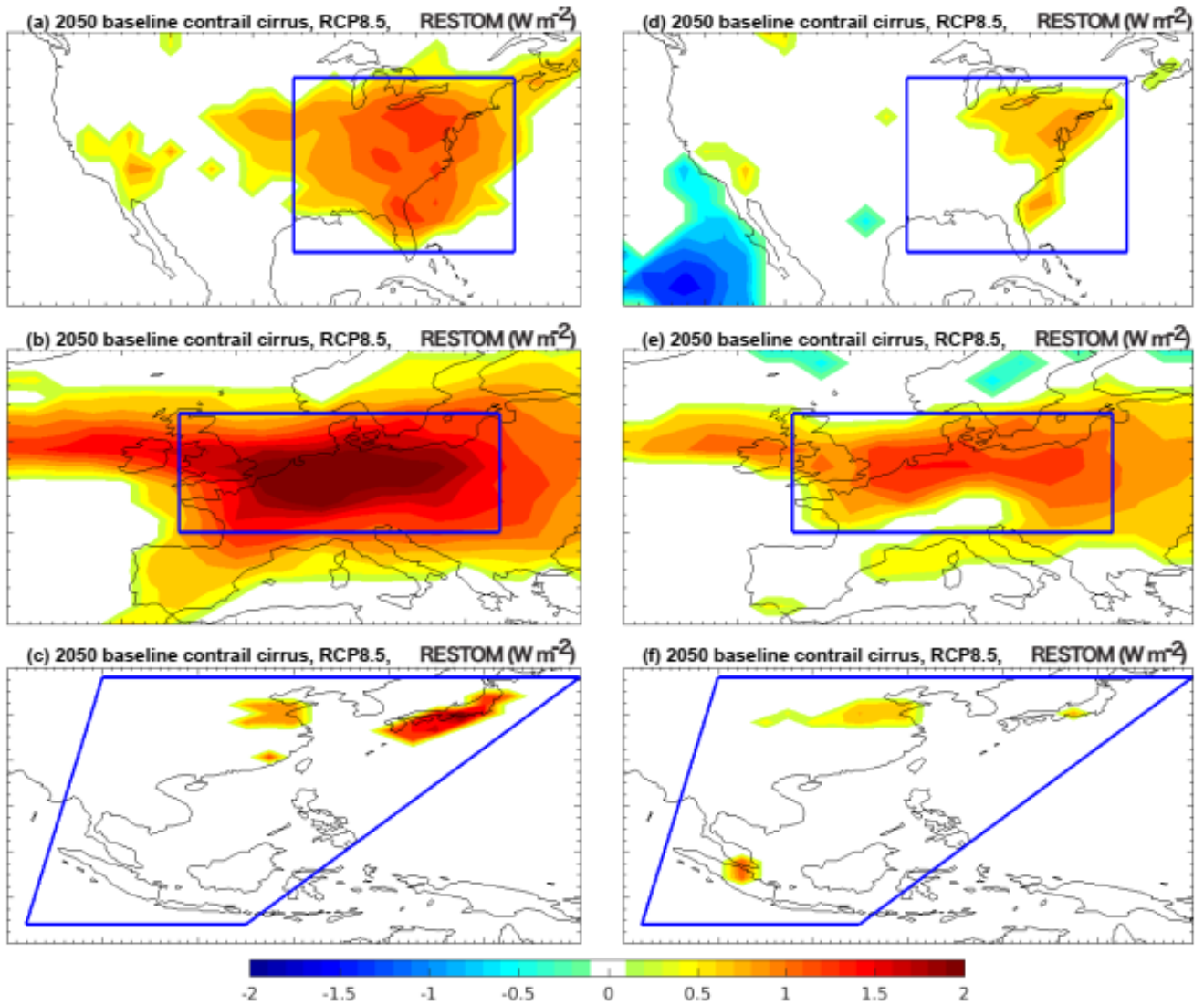
1267

Figure 14. Ensemble of the average regional radiative forcing in Wm^{-2}, utilizing the baseline emission scenario for the year 2050 with RCP8.5 meteorology, focusing on contrail cirrus alone (a–c) and contrail cirrus combined with aviation aerosols (d–f). The term "RESTOM" represents the alteration in the net residual radiative flux at the top of the model. The plot includes only ensemble-mean perturbations that surpass 2 standard deviations of the averaged control simulations. (Figure adopted with permission from Chen and Gettelman, 2016) (Licensed under CC BY 4.0)

1275

1276

1277

1278

1279

Table 8. Existing methods for modeling contrail–contrail overlap when estimating global contrail RF. MRO: maximum-random overlap, defined by Geleyn and Hollingsworth (1978) as assuming that clouds in adjacent layers maximally overlap, while clouds separated by one or more clear layers randomly overlap (Adapted from Sanz-Morère et al. 2021).

Source	Model used to represent contrail–contrail overlap
Minnis et al. (1999)	No overlap considered (fractional coverage from observations)
Marquart et al. (2003)	MRO in the vertical for each column
Rädel and Shine (2008)	Random overlap
Rap et al. (2010)	Random overlap
Frömming et al. (2011)	MRO in the vertical for each column
Burkhardt and Kärcher (2011)	MRO in the vertical for each column
Chen and Gettelman (2013)	Zero contrail–contrail overlap in grid box
Schumann and Graf. (2013)	Linear RF addition
Bock and Burkhardt (2016)	MRO in the vertical for each column

Chen and Gettelman (2013) included contrails in the CAM5 model by portraying them as an increase in the 3-D cloud fraction, where the model presumes maximum-random overlap. Nevertheless, in their method, they considered zero overlaps between newly formed contrails when placed at the same vertical level (approximately 1 km). Finally, the CoCiP Lagrangian contrail model (Schumann, 2012) reports contrail-contrail overlaps indirectly by linearly summing the radiative forcing of all contrails, taking into consideration any observed cirrus present above the simulated contrail. Nonetheless, this method does not clearly consider the overlap between simulated contrails. Inconsistencies rise in how contrail-contrail overlaps are modeled across various studies. The most efficient approach remains uncertain, and as of now, no analysis has measured the impact of contrail-contrail overlaps on global contrail RF. Since further expansion of the aviation sector is expected, it is anticipated that an increased number of instances of contrail overlap will occur. Hence, a more inclusive understanding of the degree and dynamics of contrail-contrail overlap is a necessity. Table 9 summarizes the agreement and disagreement between climate models on contrail cirrus radiative forcing.

5 Observation Datasets for Contrail Studies

The vast majority of observations, comprised of airborne, satellite, and ground-based approaches, encompass jet aircraft exhaust contrails from 1972 onward. Nevertheless, it is remarkable that records of contrail observations date back to as early as 1915, as published by Ettenreich in 1919.

Early measurements performed behind a propeller-driven aircraft offered data supporting the concept that contrail ice formation requires liquid saturation to originate, associating with the Schmidt-Appleman criterion that is now well-established (Schmidt, 1941, Appleman,1953 and Schumann, 1996.). These remarks, which encompassed the collection of ice particles on impactors and halo observations, also furnished initial insights into the size and shape of both contrail and cirrus ice particles (Weickmann, 1945).

1312   Table 9 Agreement and disagreement between climate models on contrail cirrus radiative forcing
1313

Aspect	Agreement	Disagreement	Potential Causes	Recommendations for Future Research
Net Radiative Forcing (RF)	Likely positive net RF, signifying warming			
Longwave vs. Shortwave RF		Models show some variation in the relative contribution of longwave (warming) and shortwave (cooling) components to the net RF depending on factors like ice crystal shape and optical depth.	Complexity of ice crystal parameterizations Treatment of solar radiation transfer	Improve ice crystal parameterizations in models to better capture the variation in radiative properties. Conduct studies to refine the treatment of solar radiation transfer in contrail simulations.
Regional Variations	Models concur on significant regional variations in RF			
High-traffic vs. Low-traffic areas		Models show discrepancies in the magnitude of the regional variations.	Input data on air traffic patterns	Improve the quality and resolution of air traffic data used in climate models.
Future RF Projections	Models predict a significant increase in contrail cirrus RF by 2050 due to rising air traffic and flight altitude			
Impact of aviation aerosols		Models show variations in the projected net effect (warming vs. cooling) due to the counteracting impact of aviation aerosols on low-level clouds.	Uncertainties in how models represent aviation aerosol properties and their interactions with clouds.	Conduct dedicated studies to improve the representation of aviation aerosols and their interactions with clouds in climate models.
Cloud Overlap	Overlap with other clouds (natural cirrus, low-level clouds) can affect RF, but the extent of impact (shortwave vs. longwave dominance) is uncertain.	Contrail-contrail overlap is not well understood and might be more frequent in the future.	Need for a better understanding of cloud-contrail and contrail-contrail overlap and their impact on global RF.	Develop improved methods for simulating cloud-contrail and contrail-contrail overlap in climate models. Conduct observational studies to quantify the frequency and radiative effects of contrail overlap.

1314

1315   The precise testing of models necessitates reliable quantitative data, covering not only information
1316   on contrail and plume properties but also on contrail age, the generating aircraft, atmospheric
1317   conditions during contrail formation, and the observational methods employed (Schumann et al.,
1318   2017). Mean properties of individual contrails are characterized for a wide range of jet aircraft as
1319   a function of age during their life cycle from seconds to 11.5 h (7.4-18.7 km altitude, -88 to -31°C

1320 ambient temperature), based on a compilation of about 230 in-situ and remote sensing
1321 measurements (Schumann et al., 2017). Contrails from individual aircraft can remain visible for
1322 extended periods, as reported in analyses by Minnis et al. 1998, 2013) and Vázquez-Navarro et al.
1323 (2015). Schumann et al. (2017) furnished a brief description of individual datasets, integrating new
1324 analyses for their study, and combined them to create a "contrail library" (COLI). This dataset was
1325 then compared with the outcomes of the Contrail Cirrus Prediction (CoCiP) model. The
1326 observations corroborate that the quantity of ice particles in contrails is controlled by both the
1327 engine exhaust and the formation process in the jet phase. Some particle losses ensue in the wake
1328 vortex phase, with succeeding gradually diminishes over time.

1329 Publicly available air traffic data are usually limited, but certain projects have gathered flight data
1330 from sources such as air traffic control or ground-based observations (Schumann et al., 2013;
1331 Schumann et al., 2017). Distinguishable projects with air traffic subsets since 2005 are accredited.
1332 Garber et al. (2005) compiled traffic data for the United States and southern Canada for the years
1333 2000-2005. In Germany, the Deutsche Flugsicherung (DFS) has been gathering and filing away
1334 traffic data from 2006 onwards for more new projects. The Aviation and Climate Change Research
1335 Initiative (ACCRI; Brasseur et al., 2016) furnished a global waypoint dataset for the year 2006 to
1336 researchers included in the ACCRI project.

1337 The existing observation datasets on contrail properties and formation conditions are constantly
1338 expanding with the inclusion of innovative resources. The recently developed Global Aviation
1339 Emissions Inventory based on ADS-B (GAIA) (Teoh et al., 2024). leverages historical flight paths
1340 derived from Automatic Dependent Surveillance-Broadcast (ADS-B) technology, coupled with
1341 reanalyzed weather data from 2019 to 2021. GAIA paints a detailed picture of global aviation
1342 activity, encompassing the spatial and temporal variations in flight patterns, fuel consumption, and
1343 emissions of key pollutants like CO_2, NOx, and particulate matter. This information proves
1344 particularly valuable for contrail research by offering insights into the connections between aircraft
1345 types, flight routes, and the potential for contrail formation in diverse regions. For example, by
1346 analyzing short-haul versus long-haul flight emissions within GAIA, researchers can glean insights
1347 into the contribution of various aircraft categories to contrail formation patterns across different
1348 geographical areas.

1349 By seamlessly integrating GAIA with existing observation datasets like COLI (Schumann et al.,
1350 2017), researchers can cultivate a more nuanced understanding of the interplay between aviation
1351 activity, atmospheric conditions, and contrail occurrence. This enhanced knowledge ultimately
1352 empowers the improvement of contrail prediction models and informs strategies to mitigate their
1353 impact on climate.

1354 Particulars about aircraft assets, including size, mass, speed, fuel consumption, and propulsion
1355 efficiency, were tracked from various references, including the BADA (EUROCONTROL, 2009).
1356 Added engine properties, such as fuel consumption and emissions at surface pressure, can be
1357 attained from the ICAO Aircraft Engine Emissions Databank (EASA, 2023) and the 2006 AEDT
1358 emissions inventory (Barrett, 2010; Wilkerson, 2010).

1359 Poll (2018) devised a straightforward model to estimate fuel burn for commercial aircraft, offering
1360 a transparent, publicly accessible option apart from the BADA and PIANO codes (Piano-X,
1361 software, Lissys Ltd., 2008)). Utilizing this method necessitates understanding the Mach number
1362 and flight level where an aircraft, under specific conditions, achieves its absolute minimum fuel

1363 burn rate. Yet, acquiring this data proves challenging, although an initial effort is outlined in Poll
1364 and Schumann (Poll, 2018), where input files are supplied for 53 aircraft types.

1365 Two sets of observational-based capabilities exist that can provide the coverage needed to help
1366 evaluate the global modeling analyses for treating the effects of contrails, the Contrail Library
1367 (COLI) and the satellite-based record. The Contrail Library results are useful for evaluating limited
1368 areas of contrails but not for global analyses.

5.1 Contrail Library (COLI)

1370 The COLI database includes 236 entries describing properties of contrails with known ages,
1371 including mean data for one hundred cases of in-situ measurements, more than 70 cases from
1372 ground-based and airborne lidar observations, 50 cases from satellites, and a few camera
1373 observations. The data come from 33 observation projects during the last 45 years. The comparison
1374 of the data from various measurements shows notable differences among the various instruments
1375 utilized across the dataset. Nevertheless, a notable accord endures among each approach, as well
1376 as uniformity between in-situ and remote sensing results, along with agreement with Schumann et
1377 al (2017) model outcomes. Moreover, in-situ data resultant from contrail measurements, the
1378 investigation integrates remote sensing data found from ground-based or airborne lidar and
1379 spectroradiometer, satellites, cameras, and visual interpretations. Table 10 summarizes some of
1380 the projects that contributed to the COLI database, including the aircraft used and the primary
1381 location, the mode of reference, and the primary reference of the study.

1382 Accurate forecasting of contrail occurrence and persistence holds significant importance in
1383 addressing their potential climate impact. For this purpose, research conducted by Gierens et al.
1384 (2020) underscores the limitations of reanalysis data, primarily due to their coarse vertical
1385 resolution. This study shows the necessity for high-resolution observational data, especially
1386 concerning temperature and relative humidity in the upper troposphere and tropopause region, to
1387 understand contrail formation and behavior better. Initiatives such as the In-service Aircraft for a
1388 Global Observing System (IAGOS) (Gierens et al., 2020) are pivotal in providing such data by
1389 utilizing advanced instruments installed on passenger aircraft. The assessment of contrail
1390 formation models demands dependable data encompassing both contrail characteristics and
1391 atmospheric conditions during their formation. While the study by (Gierens et al., 2020) evaluates
1392 the predictability of contrails using the Schmidt-Appleman criterion based on reanalysis data, it
1393 underscores the critical role of high-resolution data in assessing more advanced contrail prediction
1394 models. The availability of observational datasets containing parameters such as temperature,
1395 relative humidity, and air traffic data, as discussed in this section, is indispensable for such model
1396 assessments.

5.2 Satellite-based datasets

1399 Over the past two decades, the detection of contrail in satellite imagery has primarily depended on
1400 the algorithm developed by Mannstein et al. (2003) (e.g., Palikonda et al., 2005; Vazquez-Navarro
1401 et al., 2010). This algorithm contains a series of convolution and thresholding operations related
1402 to brightness temperature images and, subsequently the detection of linear associated components
1403 of fitting size. While the algorithm has been fine-tuned to attain either high precision or high
1404 remembrance in contrail detections, no single model has simultaneously surpassed in both aspects.
1405 Subsequently, empirical observations of contrail coverage often need broad lower-bound/upper-
1406 bound approaches (Duda et al., 2013). Minnis et al. (2013) reported the properties of contrail cirrus

clouds formed during 11 different contrail outbreaks, in the context of objectively determined linear contrails and their properties. It was observed that the ratio of contrail cirrus to linear contrails is substantially affected by the satellite analysis algorithm utilized to allocate linear contrails. Furthermore, this ratio seems to be affected by the presence of overlapping contrails, which can obscure individual contrails.

The contrail cirrus optical depths were found to be 2-3 times greater than their linear contrail counterparts and the associated ice crystal particle diameters were 20% greater than the contrail particle sizes. The analyses of such satellite datasets are likely to be useful for evaluating global models of contrail radiative effects.

An exception to the application of the Mannstein et al. (2013) algorithm is prominent in Kulik (2019) and Meijer et al. (2021). These analyses employed a deep learning model for pixel-level contrail detection using GOES-16 satellite imagery. Upon detecting a contrail, these studies facilitate the assessment of its lifetime impact and the ascription of potentially relevant flights (Vazquez-Navarro et al., 2010; Vazquez-Navarro et al., 2013; Vazquez-Navarro et al., 2015. Mutually, these practices furnish a means to evaluate the efficacy of flight diversions in avoiding contrail formations. McCloskey et al. (2021) officially released the first large dataset of pixel-level contrail locations in Landsat-8 satellite imagery labeled by humans. Labelers should be able to accurately differentiate contrails from naturally occurring cirrus due to Landsat-8's high spatial resolution and the advected flight history information provided. This dataset will be useful in benchmarking contrail detection models and validating contrail research in collocated geostationary satellite imagery.

Satellite-based datasets offer valuable insights into global contrail occurrence and variability, although challenges arise when estimating contrail radiative forcing. Retrieving contrail optical thickness, a crucial parameter for such calculations, from current satellite observations, is particularly difficult. Moreover, distinguishing contrails from overlapping features and natural cirrus clouds remains challenging, especially with limited spatial resolution. Addressing these challenges is essential for enhancing the contribution of satellite observations to contrail radiative forcing estimations. Advancements in retrieval algorithms for contrail optical thickness and methods to differentiate contrails from overlapping features are necessary for more accurate assessments.

Despite these challenges, satellite-based contrail datasets have significant potential for monitoring contrail occurrence and coverage over time. This information is valuable for evaluating the effectiveness of flight diversion strategies aimed at minimizing contrail formation. Furthermore, the emergence of human-labeled contrail datasets like McCloskey et al. (2021) provides a valuable resource for training and validating future advancements in contrail detection using deep learning and machine learning algorithms. Continuous collaboration among satellite data providers, atmospheric scientists, and AI researchers is vital for realizing the full potential of satellite-based contrail datasets for contrail mitigation and climate impact assessments.

Ng et al. (2023) presented a human-labeled dataset named open contrails to train and evaluate contrail detection models based on GOES-16 Advanced Baseline Imager (ABI) data. Ng et al. (2023) proposed and evaluated a contrail detection model that incorporates temporal context for improved detection accuracy. The human-labeled dataset and the contrail detection outputs are publicly available on Google Cloud Storage at gs://goes_contrails_dataset.

Persuading policymakers and airlines about the climate benefits of flight diversions becomes more reasonable with the availability of satellite corroboration capabilities. Geostationary satellites like GOES-16 and low-earth orbit satellites such as Landsat-8 present both complementary strengths and weaknesses when employed for the task of contrail detection (i.e., coverage versus persistence of the observations). An automated contrail detection system is essential for developing and evaluating contrail avoidance systems. Deep neural networks can be employed as an automated contrail detection system, a form of artificial intelligence (AI) and machine learning (ML), that has been advanced to connect and categorize contrails in satellite imagery or other relevant data sources. This system can effectively analyze complex patterns and features associated with contrails, by leveraging the competencies of deep neural networks. By utilizing deep neural networks and machine learning techniques, the automated contrail detection system offers an efficient and reliable solution for detecting and monitoring contrails, facilitating further research and analysis of their impact on climate and aviation.

Table 10. Observations from the year 2000 to 2014 were incorporated into the COLI for the study of contrail (Adapted from Schumann et al. 2016).

Year	Project name	Source aircraft	Carrier/location	Measurement	Reference
2000	Cluster	airliners	Great Lakes	satellite	Duda et al.,(2004)
2001	Shutdown	B747+C fighters	Northwestern USA	satellites	Minnis et al.,(2002)
2002	CRYSTAL-FACE	WB-57	NASA WB-57	in situ	Gao et al.,(2006)
2003	Fallstreaks 2003	airliners	Goddard	lidar	Atlas and Wang (2010)
2005	PAZI-2	airliners	DLR Falcon	in situ	Febvre et al.,(2009)
2006	CR-AVE	WB-57	NASA WB-57	in situ	Flores et al.,(2006)
2008	CONCERT	airliners	DLR Falcon	in situ	Voigt et al.,(2010)
2008	ACTA	airliners	Europe andNorth Atlantic	satellite	Vázquez-Navarro et al.,(2015)
2011	CONCERT2011	airliners	DLR Falcon	in situ	Kaufmann et al.,(2014)
2011	COSIC	Bae 146	FAAM Bae-146	in situ	Jones et al.,(2012)
2012	Cameras	airliners	Munich	cameras	Schumann et al.,(2013)
2014	ML-CIRRUS	B772 or F900	HALO	in situ	Voigt et al.,(2016)

Siddiqui (2020) conducted a study where a neural network was used to distinguish contrail cirrus clouds from regular cirrus clouds on TSI images. The study found that the neural network triumphed with a high accuracy of 98.5% on the validation set, implying that the model was able to learn significant visual features of contrails that differentiate them from regular cirrus clouds. The success of this model opens various practical applications for studying contrails. For instance, the model can be used to analyze images from different months of data, agreeing for researchers to investigate the frequencies of contrail occurrences. This can impart valuable insights into air traffic trends, as well as how physical conditions like temperature and humidity vary seasonally and their potential impact on contrail formation. Researchers can better understand contrail behavior and their relationship with various environmental factors by leveraging the neural network's ability to detect and classify contrails accurately. This knowledge can be used to refine models and predictions related to contrail formation and persistence and contribute to a more comprehensive understanding of aviation's impact on the atmosphere.

6 Supersonic contrails

Contrail studies have primarily focused on subsonic aviation due to the predominance of subsonic air traffic since the retirement of the Concorde in 2003. Contrail formation and persistence for

1484 supersonic commercial aircraft pose challenges -- persistent contrails are unlikely to form in the
1485 stratosphere when these aircraft are flying at supersonic speeds but societal requirements for flying
1486 at subsonic speeds over land to avoid noise issues would still potentially produce persistent
1487 contrails. The importance of understanding the global climate effect of contrails linked to
1488 supersonic aviation is well-established (Stenke et al., 2008). Matthes et al. (2022) recently
1489 published a comprehensive review on the climate effects of supersonic aviation, encompassing
1490 non-CO2 effects like contrail formation. Their work highlights the need for a thorough
1491 understanding of existing research in this area and uncertainties persist regarding parameters
1492 controlling contrail ice crystal distribution evolution for these aircraft. Consequently, the presence
1493 or absence of contrails becomes a discernible marker of the aircraft's speed regime. Additionally,
1494 limited research, such as observations by Schumann et al. (2017) suggested the possibility of
1495 contrail formation even at high altitudes (18.7 km) under specific atmospheric conditions. These
1496 factors highlight the need for a comprehensive understanding of contrail formation and persistence
1497 for future supersonic aircraft.
1498

7 Uncertainties and Research Gaps

7.1 Uncertainties

1501 There are several crucial areas of uncertainty and research gaps that require focused investigation
1502 to achieve a more comprehensive understanding of contrail formation, evolution, and their effects:

1503 • *Humidity Observations and Predictions:* An important uncertainty lies in the accuracy and
1504   reliability of humidity observations and predictions at different altitudes. Improved
1505   measurements and modeling of humidity are critical for assessing the conditions conducive to
1506   persistent contrail formation and their subsequent behavior. Addressing this uncertainty will
1507   lead to more precise insights into contrail persistence and its associated radiative impacts.
1508 • *Aircraft Plume Mixing:* Uncertainty persists in referring to how ambient air mixes with the
1509   aircraft plume during contrail formation, comprising uncertainties associated with the rate and
1510   extent of mixing.
1511 • *Interaction with Natural Cirrus Clouds:* The interplay between natural cirrus clouds and
1512   contrails initiates an additional level of uncertainty, fostering obscuring the understanding of
1513   their individual and mutual effects on radiative forcing (RF).
1514 • *Regional Variations in Atmospheric Conditions:* The sensitivity of contrail radiative impacts
1515   to regional variations in atmospheric conditions is not well understood and remains uncertain.
1516 • *Aerosols and Aircraft Emissions:* Uncertainties persist in understanding the role of aerosols
1517   and particles from aircraft emissions in contrail formation and properties.
1518 • *Uncertainties and Soot Particles*: The role of soot particles in contrail formation remains
1519   subject to uncertainties, particularly regarding their ability to nucleate ice. Despite the presence
1520   of numerous ice particles in fresh contrails, ongoing debates, as highlighted in recent studies
1521   such as Righi et al. (2021), question whether soot particles directly facilitate ice nucleation.
1522   Clarifying this relationship is essential for comprehending the impact of soot emissions on
1523   contrail formation and subsequent evolution. To address this knowledge gap, further research
1524   efforts are imperative to explore the influence of soot particles on ice nucleation processes
1525   within contrails.
1526 • *Radiative Transfer Scheme:* Schumann and Graf (2013) further highlight these complexities
1527   by demonstrating an observed "aviation fingerprint" in cirrus cover and outgoing longwave

1528   radiation (OLR) that aligns with air traffic patterns. Their study estimates a regional longwave
1529   radiative forcing of 600-900 mWm^{-2}, emphasizing the impact of aviation on cirrus cloud
1530   formation. Additionally, their analysis of the shortwave/longwave forcing ratio underscores
1531   the model's dependence on the global net forcing. These findings resonate with our discussion
1532   on radiative transfer scheme uncertainties, as variations in how models handle radiative
1533   processes can significantly influence the estimated impact of contrails on Earth's energy
1534   balance.
1535

1536   Significant uncertainties persist regarding the radiative forcing caused by aircraft contrails. These
1537   uncertainties arise from numerous factors, starting with uncertainties in the background
1538   meteorology and specific aircraft emissions. When assessing the climate impact of contrail cirrus,
1539   the primary uncertainties lie in (1) determining upper tropospheric water vapor concentrations and
1540   regions of supersaturation; (2) adequately representing contrail cirrus processes in global models;
1541   and (3) understanding the radiative response resulting from the contrail cirrus presence, typically,
1542   only approximate assessments of uncertainties associated with these processes are furnished.

1543   Assessing the radiative response of contrail cirrus involves handling several crucial uncertainties,
1544   including:
1545   *Uncertainties in Contrail Cirrus Radiative Forcing:* Estimating the radiative forcing (RF) of
1546   contrail cirrus clouds is inherently uncertain. Lee et al. (2021) categorizes these uncertainties into
1547   two main areas: (A) uncertainties related to the radiative response of contrail cirrus and (B)
1548   uncertainties associated with the upper-tropospheric water budget and the contrail cirrus scheme
1549   within climate models.

1550   (A) *Uncertainties in Radiative Response*

1551   Radiative Transfer Scheme (A1): Myhre et al. (2009) estimated an uncertainty of approximately
1552   35% arising from the radiative transfer scheme employed in climate models. This scheme
1553   simulates how different wavelengths of radiation interact with various atmospheric components,
1554   including contrail cirrus.

1555   *Cloud* Heterogeneity (A2*):* The inhomogeneity of ice crystals within a model grid box, vertical
1556   cloud overlap, and limitations of plane-parallel geometry contribute an estimated uncertainty of
1557   35% (Carlin et al., 2002; Pomroy and Illingworth, 2000; Gounou and Hogan, 2007).

1558   *Ice Crystal Habit* (A4): Variations in the shape and form (habit) of ice crystals within contrail
1559   cirrus can significantly impact how they interact with radiation. Markowicz and Witek (2011)
1560   suggest an uncertainty of 20% due to this factor.

1561   *Soot Core Impact* (A5): The radiative transfer uncertainty associated with soot cores embedded
1562   within contrail cirrus ice crystals is significant, particularly for shortwave albedo (reflectivity), but
1563   remains unquantified (Liou et al., 2013). Soot cores can absorb radiation, potentially leading to a
1564   warming effect that is not currently accounted for in models.

1565   (*B) Uncertainties in Water Budget and Contrail Cirrus Scheme*

1566   *Ice Supersaturation* (B1): Uncertainties in the representation of upper-tropospheric ice
1567   supersaturation (Lamquin et al., 2012) contribute an estimated 20% uncertainty.

1568   *Ice Crystal Number Density* (B2): and Radiative Transfer for Young Contrails (A3): Uncertainties
1569   in ice crystal number densities (Karcher et al., 2015, 2018) are linked to factors like water vapor
1570   saturation and soot emissions. Lee et al. (2021) recognized the dependence between A3 (radiative

1571 transfer for young contrails) and B2 (ice crystal number density). Consequently, they included the
1572 uncertainty from A3 within their overall category B uncertainty estimate.

1573 *Contrail Cirrus Lifetime* (B3): The effect of contrail cirrus lifetime on estimated RF is relatively
1574 small, with an associated uncertainty estimated at 5-10% (Chen and Gettelman, 2013; Newinger
1575 and Burkhardt, 2012). While Lewellen (2014) highlights the potential importance of lifetime
1576 through large-eddy simulations demonstrating contrail cirrus lifetimes exceeding 40 hours and
1577 widths exceeding 100 km, several factors contribute to the seemingly counterintuitive finding in
1578 this context of estimated RF. Lewellen's (2014) simulations highlight the potential significance
1579 of contrail cirrus with extended lifetimes, particularly for their ice crystal surface area and overall
1580 radiative impact. However, the study focuses on the integrated effect over the entire lifetime,
1581 whereas the uncertainty estimate (5-10%) pertains to the impact of variations in lifetime on the
1582 average RF. Further research is needed to better understand the complex interplay between contrail
1583 cirrus lifetime, ice crystal growth processes, atmospheric conditions, and their combined effect on
1584 radiative forcing.

1585 *Air Traffic Data Resolution* (B4): Sensitivity studies suggest an uncertainty of about 10% arising
1586 from the temporal resolution of air traffic data used in climate models (Lee et al., 2021).

1587 *Natural Cloud Feedback* (B5): The feedback mechanism by which contrail cirrus alters the upper
1588 tropospheric water budget, affecting natural clouds, introduces a significant uncertainty that
1589 remains unquantified (Burkhardt and Karcher, 2011; Schumann et al., 2015). Lee et al. (2021)
1590 assumed an uncertainty of 15% for this factor.

1591 *Initial Ice Crystal Assumptions* (B6): The estimation of RF by Chen and Gettelman (2013) is
1592 subject to uncertainties associated with assumptions about initial ice crystal radii and contrail
1593 cross-sectional areas, leading to an estimated uncertainty of 33%.

1594 Overall Uncertainty

1595 Following Lee et al. (2021), the uncertainty in the radiative response to contrail cirrus (excluding
1596 soot cores) is estimated to be around 55%, assuming independence of different uncertainties. This
1597 aligns with their findings and highlights the dominance of radiative response uncertainties
1598 (category A) in the overall uncertainty budget. Category B uncertainties (water budget and contrail
1599 cirrus scheme) remain significant and require further investigation, particularly the combined
1600 effect of ice crystal number density and radiative transfer for young contrails.

1601 **7.2 Research needs and gaps**

1602 In the pursuit of a comprehensive understanding of contrail impacts on climate, there is a critical
1603 need to establish clear research needs and requirements.

1604 Improving weather models demands better predictions of humidity and clouds with enhanced
1605 resolution in time, space, and altitude. The models must also adapt to evolving weather conditions.
1606 Accurate water vapor data during cruise altitudes is crucial, emphasizing the need for small, cost-
1607 effective humidity sensors. To achieve this, there is a need for the production, testing, and
1608 evaluation of precise sensors. Lidar technology and weather model assessments play a key role in
1609 advancing observational capabilities for more accurate predictions. Enhancing cirrus cloud
1610 forecasts requires a dual focus on data and artificial intelligence. Ensemble simulations are vital
1611 for estimating uncertainties in cirrus cloud predictions. Additionally, there is an urgent need for
1612 more climate and contrail models, ensuring a comprehensive understanding and evaluation of these
1613 complex atmospheric processes. Furthermore, research by Ovarlez et al. (2000) highlights

discrepancies between measured water vapor content and data from weather forecasts. Their findings emphasize the importance of accurate humidity measurements, particularly for studies on contrail formation and persistence. Weather forecasts might underestimate actual humidity, potentially leading to inaccurate assessments of contrail behavior. This underlines the need for ongoing research to improve the accuracy of humidity data in weather models.

Furthermore, high-quality observations, effectively integrated into weather models, are crucial for setting accurate starting points for forecasts (Bauer et al., 2015). This highlights the need for robust data collection strategies that combine information from diverse sources. These sources can include in-situ measurements taken directly within the atmosphere, radar systems that track precipitation patterns, and satellite sensors that provide a global view. Advanced data assimilation techniques then play a vital role by merging these observations with model outputs. This combined approach creates a more precise picture of the initial atmospheric state, ultimately leading to improved weather forecasts (Bauer et al., 2015).

Sun and Roosenbrand (2023) reported the limitations in traditional computer vision approaches for contrail detection, particularly in handling the complexity of satellite images under varying conditions. Earlier machine learning methods relied on simpler convolutional neural network models, primarily demanding extensive labeled data for contrail presence determination. Notably, there is a gap in the existing literature, lacking research specifically tailored to machine learning approaches for contrail detection, setting it apart from other image segmentation or detection tasks. A significant challenge lies in the absence of adequate loss functions optimized for linear features like contrails during training, making detection notably difficult at lower resolutions, especially when multiple contrails are close. Addressing these gaps is crucial for advancing the efficacy of contrail detection methods (Sun and Roosenbrand, 2023).

While a complete understanding of contrail effects on climate may not be achievable, further research is crucial to reduce uncertainties and improve our ability to predict and mitigate their impact. Here are some of the key areas of research gaps that should be explored to address existing uncertainties:

- *Properties of Contrail Particles*: Understanding contrail effects on climate requires reflection of key factors such as particle size, layer height, cloud overlap, and optical properties. Larger particles tend to have a different radiative impact than smaller ones. The altitude of contrail formation impacts their interaction with solar and terrestrial radiation. Precise climate modeling requires proper accounting for cloud overlap, impacting radiative calculations. Contrail optical properties, comprising albedo and emissivity, determine their reflective and trapping abilities for solar and terrestrial radiation. The concentration and size distribution of contrail particles affect their formation and radiative impact. Accurate estimation of contrail forcing, important for climate modeling and policy decisions, depends on understanding particle number, size, and layer height.
- *Assessment of Effective Radiative Forcing:* Effective Radiative Forcing (ERF) is a valuable tool for evaluating the global mean radiative impact of contrail cirrus on climate. However, it's important to recognize that ERF primarily focuses on this average effect and may not fully capture regional variations or complex feedback mechanisms associated with contrail formation and persistence.
- *Emissions and Alternative Fuels*: Corroborating a precise connection between soot and contrail ice crystal numbers is important for understanding the environmental impact of sustainable aviation fuels, such as biofuels. Biofuels are being studied as a more sustainable

1659   alternative to conventional aviation fuels, and evaluating their impact on contrail formation
1660   is crucial for assessing environmental benefits. Scientific research, notifying regulatory
1661   decisions, relies on the interpretation of the correlation between soot and ice crystal
1662   numbers. This connection is integral for complete visions of the environmental
1663   implications of alternative aviation fuels. Precise data on contrail formation, containing the
1664   impact of biofuels, is crucial for climate models predicting the impact of aviation emissions
1665   on climate. The experimental establishment of the soot-ice crystal connection gives this
1666   understanding.

1667   ▪   *Properties of Soot Particle*: A study into the bimodal size distributions of soot particles in
1668   aircraft emissions is critical for focusing uncertainties on contrail formation and properties,
1669   with inferences for climate science and aviation practices. In-flight measurements uncover
1670   that freshly emitted soot particles usually exhibit a single peak in number-size distributions,
1671   but some cases play a second, larger particle mode in near-field contrails and dry plumes.
1672   The source of this larger mode remains uncertain, signifying that the bimodal distribution
1673   may survive in unrefined jet engine emissions rather than be caused by contrail processing
1674   or coagulation during plume development. Precise data on soot particle properties is
1675   essential for climate models incorporating contrail outcomes, and resolving the origin of
1676   bimodal size distributions is crucial to improving model representations of contrail
1677   properties. Policymakers and regulatory bodies rely on scientific research for progressing
1678   aviation-related environmental policies, making an understanding of soot particle size
1679   distributions significant for up-to-date decision-making.

1680   A study into the bimodal size distributions of soot particles in aircraft emissions is critical
1681   for focusing uncertainties on contrail formation and properties, with inferences for climate
1682   science and aviation practices (Schumann et al., 2002). In-flight measurements typically
1683   show a single peak in the number-size distribution of freshly emitted soot particles
1684   (Schumann et al., 2002). However, some cases reveal a second, larger particle mode in
1685   near-field contrails and dry plumes. The source of this larger mode remains uncertain,
1686   suggesting that the bimodal distribution might be present in unrefined jet engine emissions
1687   rather than being solely caused by contrail processing or coagulation during plume
1688   development (Schumann et al., 2002). Precise data on soot particle properties, including
1689   any potential bimodal size distribution, is essential for climate models incorporating
1690   contrail effects. Resolving the origin of this bimodal distribution is crucial to improving
1691   model representations of contrail properties. Policymakers and regulatory bodies rely on
1692   scientific research for progressing aviation-related environmental policies, making an
1693   understanding of soot particle size distributions significant for up-to-date decision-making.

1694

1695   ▪   Examining the microphysical interaction between soot particles and contrail ice crystals
1696   emerges as a critical research priority. Laboratory experiments simulating contrail
1697   formation conditions offer valuable insights into the ice nucleating potential of soot
1698   particles under controlled environments. Moreover, field measurements focusing on the
1699   in-situ characterization of soot particles and ice crystals within nascent contrails provide
1700   indispensable data for validating models. By integrating these methodologies, researchers
1701   can advance their understanding of the role of soot particles in contrail formation and
1702   refine climate models accordingly.

1703

1704 ▪ *Remote Sensing for Contrail-Cirrus*: Organized regional campaigns are important for
1705 estimating key variables in aging contrail-cirrus and aircraft plumes. This contains in-situ
1706 and remote sensing to portray the growth, decay, and trajectories of contrail ice particles,
1707 delivering essential data for interpretation of transformation and radiative effects.
1708 Estimation of contrail particles, ambient aerosols, and gaseous aerosol precursors notifies
1709 climate modeling and environmental assessments, connecting emissions to contrail
1710 properties. Gathered data validates climate models, enhancing their accuracy and
1711 improving the representation of contrail-cirrus effects. Understanding contrail-cirrus
1712 development supports developing mitigation strategies, informing contrail avoidance, and
1713 reducing aviation's climate impact.
1714 In addition to these research issues, there is a need to bridge the gaps with the assessment of the
1715 above-reported uncertainties and to investigate and improve the understanding of contrail
1716 avoidance and climate tradeoffs. Research should explore how to mitigate the climate impact of
1717 contrails without compromising aviation safety and efficiency.

1718 **7.3 Contrail avoidance and climate tradeoffs**

1719 While existing studies explore contrail avoidance strategies and their impact on fuel burn and
1720 climate, a comprehensive large-scale evaluation remains elusive. Ideally, such an evaluation would
1721 encompass a significant number of routes, account for weather variations, enable full flight level
1722 optimization, quantify contrail impacts on individual flights, and compare results to a fuel-optimal
1723 baseline to isolate the specific effects of contrail avoidance. This comprehensive approach would
1724 provide a more definitive understanding of the fuel-climate tradeoffs associated with contrail
1725 avoidance strategies.

1726 Recent studies investigating targeted contrail avoidance strategies offer promising results. Teoh et
1727 al. (2020) suggest that focusing on a small percentage of flights with the highest contrail impact
1728 could be an effective approach, minimizing the overall increase in fuel consumption and CO2
1729 emissions. Additionally, advancements in engine design hold promise as a long-term solution for
1730 reducing contrail formation.

1731 Molloy et al. (2022) address a critical step towards implementing effective contrail avoidance
1732 strategies in practice. Their work outlines the practical considerations for conducting large-scale
1733 trials, which are essential for evaluating the feasibility and effectiveness of these strategies in real-
1734 world conditions. The proposed deployable options based on existing air traffic management
1735 processes offer a promising path forward for initiating such trials.

1736 Frias et al. (2024) present a compelling case for the practicality and economic viability of contrail
1737 avoidance. Their findings demonstrate that significant reductions in contrail climate impact can be
1738 achieved with minimal operational burdens. This study provides strong motivation for airlines and
1739 air traffic controllers to embrace contrail avoidance strategies as a means to reduce aviation's
1740 overall climate footprint.

1741 Gierens et al. (2008) proposed several potential ways to mitigate the impact of contrails,
1742 encompassing both technical and operational approaches. Regarding the technical aspect, they
1743 recognized the challenge of completely preventing contrail formation due to its primarily
1744 thermodynamic nature. However, they suggested the exploration of new engine cycles and
1745 technical infrastructures that might help suppress contrails. Additionally, reducing the number of
1746 emitted particles was considered to mitigate contrail formation. While such evaluations would not

eliminate contrails completely, they would produce thinner contrails with rarer but larger crystals. These heavier ice crystals would incline more rapidly on average, causing shorter contrail lifetimes. The analysis also investigated operational mitigation options. Striking strict constraints, such as fixed maximum flight levels, was studied unreasonably due to the significant challenges it would pose for air traffic controllers and the resulting safety concerns. Their proposed strategies focused on addressing contrail formation both at the technical level through engine and infrastructure improvements and at the operational level by implementing flexible measures that consider real-time weather conditions. These approaches aimed to strike a balance between contrail reduction and the practical needs of aviation.

In a recent study, Sausen et al. (2023) presented an experiment that aimed to avoid contrail formation during real-world operations. This experiment took place in the Maastricht Upper Area Control region, covering parts of Germany, the Benelux countries, and the North Sea, in the year 2021. The researchers highlighted that contrail avoidance could serve as an effective method for mitigating the climate impact of aviation. To conduct their trial experiment, air traffic was deliberately diverted every other day by adjusting the flight altitude, either increasing or decreasing it by up to 2000 ft, whenever potential persistent contrails were predicted. The effectiveness of these deviations was assessed by analyzing satellite images of high clouds and employing a contrail detection algorithm that utilized contrail properties. Despite the ongoing challenge of accurately forecasting persistent contrails, the trial achieved a significant level of success, reaching 97.5%, suggesting that on average, persistent contrails can be avoided during regular flights in the real world through minor adjustments in the vertical flight path. Contrail avoidance through minor adjustments in flight paths represents a practical approach to mitigate the formation of persistent contrails. It demonstrates the feasibility of implementing such measures within air traffic management to reduce the environmental impact of aviation. The study highlights the potential for real-world applications of contrail avoidance as a means of addressing the climate effects of contrails. The findings of this experiment mark an important milestone in implementing operational measures in air traffic management to decrease the impact of climate from aviation.

 The limitations of simply avoiding all contrails become evident when we consider their diverse climate effects. While some contrails can have a net cooling effect, others contribute to warming. This distinction necessitates a more nuanced approach to contrail avoidance. We should focus on mitigating the formation of contrails that contribute to warming, while potentially allowing or even encouraging the formation of those with a net cooling effect. This distinction requires reliable methods for differentiating between the two contrail types.

Future considerations: optimizing contrail avoidance.

The Sausen et al. (2023) study represents a significant step forward, demonstrating the feasibility of operational contrail avoidance through minor flight adjustments. To optimize this approach for maximum climate benefit, future research should focus on three key areas:

Distinguishing warming from cooling contrails: Developing robust methods to differentiate between these contrail types is crucial. Improved weather forecasting models and contrail prediction algorithms that consider factors like altitude, atmospheric conditions, and cirrus cloud cover can contribute to this goal.

Large-scale implementation: Evaluating the broader applicability of contrail avoidance strategies necessitates conducting large-scale trials across diverse airspace with varying weather patterns.

1790 This will provide a more comprehensive understanding of the effectiveness and potential trade-
1791 offs associated with contrail avoidance in different operational contexts.

1792 *Integration with air traffic management:* For widespread adoption, efficient protocols for
1793 integrating contrail avoidance measures within existing air traffic management systems are
1794 essential. This may involve developing streamlined decision-making tools and communication
1795 channels for air traffic controllers and pilots.

1796 By addressing these considerations, contrail avoidance can evolve from a general strategy to a
1797 targeted approach that maximizes its potential for mitigating aviation's climate impact. This
1798 approach would focus on reducing the formation of warming contrails while allowing for or even
1799 encouraging the formation of cooling contrails.

1800 In a recent Ph.D. thesis, Elmourad (2023) evaluated the fuel-climate tradeoffs arising from contrail
1801 avoidance strategies applied on a large scale. This study raises several key questions about
1802 contrails avoidance: What fraction of aviation's global total contrail length can be avoided using
1803 vertical re-routing exclusively? What is the fuel penalty of such an avoidance strategy? How does
1804 the fuel penalty or contrail reduction vary between flights or seasons? Can the fuel penalty be
1805 constrained? What effect does that have on the ability to do contrail avoidance? What net climate
1806 benefit can be achieved from contrail avoidance strategies? How does this differ from avoiding all
1807 contrails or only nighttime contrails? What are the relative orders of magnitude between the
1808 climate benefits from contrail avoidance and the climate damages from additional fuel burn? How
1809 does this difference compare with the uncertainties associated with contrail impacts?

1810 As the global volume of air traffic continues to rise, the aviation industry grapples with a
1811 significant challenge in mitigating its environmental impact on climate change. Contrails, which
1812 contribute to global warming by trapping terrestrial radiation, have the potential to counteract the
1813 benefits of reduced emissions resulting from optimized flight paths. In a study by Roosenbrand et
1814 al. (2023), the authors conducted a global assessment of flights that contribute to contrail formation
1815 and assessed the altitude adjustments required to avoid these contrail-prone areas. This analysis
1816 utilized a combination of data from the Integrated Global Radiosonde Archive (IGRA), which
1817 provides measurements from weather balloons with global coverage and high vertical resolution,
1818 and flight data from OpenSky. The study identified Mid-Western Europe, the Eastern United States
1819 of America, and Japan as regions characterized by both high air traffic volumes and a substantial
1820 percentage of flights forming contrails. Importantly, these regions offer opportunities for altitude
1821 adjustments of less than one kilometer to minimize contrail formation. The research also
1822 pinpointed other regions where relatively minor operational interventions could yield significant
1823 climate benefits.

1824 *Fuel-climate tradeoffs*: While there have been numerous studies on operational contrail avoidance,
1825 there are still some research gaps in the field when it comes to understanding the fuel-climate
1826 tradeoffs that would follow a large-scale global application of contrail avoidance strategies.

1827 *Sustainable Aviation Fuel (SAF)*: Much still needs to be understood about what SAF will look like
1828 as it becomes the dominant fuel of the future. The emissions of soot and other particles from SAF
1829 are still not well understood and will have a significant effect on future contrail production and
1830 lifetimes. According to Bräuer et al. (2021b), sustainable aviation fuels have been identified as
1831 capable of reducing both contrail ice numbers and the radiative forcing caused by contrail cirrus.
1832 Their study involved the measurement of apparent ice emission indices across different fuels with
1833 varying aromatic content at altitudes ranging from 9.1 to 9.8 km and 11.4 to 11.6 km. The data

were collected during the ECLIF II/NDMAX flight experiment in January 2018, encompassing a variety of fuels differing in aromatic quantity and type. A comparison between a sustainable aviation fuel blend and a reference fuel Jet A-1 revealed a maximum reduction of 40% in apparent ice emission indices, highlighting the potential impact of sustainable aviation fuels on mitigating contrail-related environmental effects.

Moore et al. (2017) investigated the effects of using a biofuel blend, as opposed to traditional jet fuel, on these aircraft emissions. Their findings revealed a notable decrease in both the quantity and weight of particles discharged from aircraft engines when the biofuel blend was employed. This discovery implies that integrating biofuels into aviation practices could offer a viable approach to mitigating the environmental footprint of air travel on climate change.

Moore et al. (2017) utilized measurements of particle size distributions to examine the variations between the reductions in number and mass emissions indices for the two types of fuels. A significant decrease in both total and non-volatile particle number and volume was observed with the biofuel blend, accompanied by a slight shift towards smaller sizes in the peak diameter of the mode, ranging from 3 to 5 nm for number distributions and 9 to 12 nm for volume distributions. This shift appears to be driven by a more substantial reduction in the number of larger soot-mode aerosols, which act as condensation nuclei for organic species and sulfuric acid. Since gas-to-particle condensation is proportional to particle size (specifically, to the square of the diameter in the free molecular regime), the reduced emission of the soot size mode from the biojet fuel blend decreases the condensational sink, thereby enhancing the nucleation of new particles in a compensatory manner. This interplay is evident in the size-dependent reductions in number emissions. Their study found that blending petroleum-based fuels with a HEFA biojet fuel leads to a reduction in both volatile and non-volatile particle emissions by 50%–70% under atmospheric cruise conditions. However, the emissions indices for soot particle numbers remain in the soot-rich regime (around $10^{14}\,\text{kg}^{-1}$) for the biofuel blend. Theoretical calculations suggest that the initial number of contrail ice particles increases linearly with the soot number emissions index in the soot-rich regime, and that ambient and ultrafine particles are unlikely to contribute significantly to contrail formation.

Alternative aircraft and new fuels: There is a lot of ongoing discussion about the potential development of aircraft using hydrogen as fuel. Such an aircraft engine would still emit water vapor and therefore could produce contrails. However, the major reduction in particulates, e.g., no soot, could affect the lifetime of the contrail and whether it could result in contrail cirrus. Research is needed to evaluate the potential for contrail production and resulting lifetimes. Other alternative fuels would also need to be evaluated.

There is a necessity for government research organizations as well as industry partners to venture into the investigation and establishment of sensor prototypes. An example is a humidity sensor prototype with a range of great precision covering 20 parts per million by volume to more than 10,000 ppmv. The purpose is to improve the accuracy of measurements, especially on parameters like temperature and relative humidity, at altitudes preserved during flight to counteract contrail mitigation. Additionally, improving measurement at lower altitudes is vital for improving the precision of weather forecasting. This accumulated data will play a pivotal role in evaluating and integrating these insights into forecast models, enhancing the robustness of these calculations. An additional area of focus is the refinement of model calculations on the impact of contrails, necessitating improved handling of variables such as clouds, aerosols, and specific aircraft characteristics.

Tackling the pressing challenge of climate change requires the exploration and adoption of effective contrail mitigation strategies. Recent studies show promise in the utilization of alternative fuels, particularly sustainable aviation fuels (SAFs), which boast lower soot particle emissions compared to conventional jet fuel. Initial flight trials have shown a marked decrease in contrail formation when SAFs are used, potentially attributed to the reduced concentration of ice nucleation particles in SAF exhaust. Moreover, ongoing research focuses on optimizing flight path planning and air traffic management (ATM) to minimize contrail formation and persistence. Research conducted by Sausen et al. (2023) demonstrates the feasibility of contrail avoidance through minor adjustments in flight paths during real-world operations. Continued progress and application of these strategies, coupled with advancements in contrail observation technologies such as high-precision humidity sensors, offer significant potential to mitigate the climate impact of aviation.

8 Conclusions

This study reviews the current understanding of the impacts of contrail formation by aircraft on the Earth's climate system; it provides insights into the current state of contrail research, offering perspectives on contrail formation, characteristics, life cycle, and potential future impacts. The study underscores the importance of confronting uncertainties in climate models and emphasizes the need for further research to enhance our understanding of contrail effects.

Aviation emissions, encompassing both contrail cirrus clouds and carbon dioxide emissions, exert an important influence on the Earth's climate. Extensive research efforts have significantly improved our understanding of contrail formation and aging; however, key microphysical processes remain a subject of ongoing investigation. Our examination of global observational data and projections highlights the potential for a significant increase in contrail cirrus radiative forcing by the mid-21st century, driven by factors such as anticipated growth in air traffic, potential improvements in fuel efficiency, and evolving atmospheric conditions. While uncertainties regarding the precise magnitude of this increase exist, the potential consequences necessitate proactive mitigation strategies. Several promising approaches are being explored, including operational measures to optimize flight paths, the development of new contrail suppression technologies, and the adoption of sustainable aviation fuels. Implementing a combination of these strategies, while continuously refining our understanding of contrail effects, is crucial for minimizing the overall climate impact of aviation.

Author contributions. DKS prepared the manuscript with support from SS and DJW

Competing interests. The author declares that they have no competing interests.

Acknowledgment.
This work was supported by the National Aeronautics and Space Administration (NASA) under award number NNA16BD14C for NASA Academic Mission Services (NAMS).
We thank Drs. Andrew Gettelman (Pacific Northwest National Laboratory, PNNL, USA), Ulrike Burkhardt (German Aerospace Center, DLR, Germany), Bernd Kärcher (DLR), Phillip J Ansell (University of Illinois at Urbana-Champaign, USA), D.S. Lee (Manchester Metropolitan University, UK), and Steven L Baughcum (The Boeing Company) for reviewing prior drafts of this report.

Financial support. The authors would like to thank for support from the Universities Space Research Association (USRA) through project subcontract 08600-031.

References

Airbus Global Market Forecast: 2023-2042. Retrieved from https://www.airbus.com/en/products services/commercial-aircraft/market/global-market-forecast), 2022.

Appleman, H.: The formation of exhaust condensation trails by jet aircraft. Bull. Amer. Meteor. Soc., 34(1), 14-20, https://doi.org/10.1175/1520-0477-34.1.14, 1953.

Atlas, D., Wang, Z., and Duda, D. P.: Contrails to cirrus: Morphology, microphysics, and radiative properties. J. Appl. Meteor., 45, 5–19, https://doi.org/10.1175/JAM2335.1, 2006.

Aufm Kampe, H. J.: Die Physik der Auspuffwolken hinter Flugzeugen, Luftwissen, 10, 171–173, 1943.

Barrett, S., Prather, M., Penner, J., Selkirk, H., Balasubramanian, S., Dopelheuer, A., Fleming, G., Gupta, M., Halthore, R., Hileman, J., Jacobson, M.: Guidance on the use of AEDT gridded aircraft emissions in atmospheric models. A technical note, Aug 17, https://doi.org/10.2172/993261, 2010.

Bauer, H.S., Schwitalla, T., Wulfmeyer, V., Bakhshaii, A., Ehret, U., Neuper, M. and Caumont, O.: Quantitative precipitation estimation based on high-resolution numerical weather prediction and data assimilation with WRF–a performance test. Tellus A: Dynamic Meteorology and Oceanography, 67(1), p.25047, https://doi.org/10.3402/tellusa.v67.25047, 2015.

Baumgardner, D., Brenguier, J. L., Bucholtz, A., Coe, H., DeMott, P., Garrett, T. J., Gayet, J. F., Hermann, M., Heymsfield, A., Korolev, A., Krämer, M.: Airborne instruments to measure atmospheric aerosol particles, clouds and radiation: A cook's tour of mature and emerging technology. Atmos. Res., 102(1-2), 10-29. Oct 1, https://doi.org/10.1016/j.atmosres.2011.08.010, 2011.

Bickel, M., Ponater, M., Bock, L., Burkhardt, U. and Reineke, S.,. Estimating the effective radiative forcing of contrail cirrus. Journal of Climate, 33(5), pp.1991-2005, https://doi.org/10.1175/JCLI-D-19-0531.1, 2020.

Bickel, M.: Climate Impact of Contrail Cirrus. Ph.D. Thesis, Ludwig-Maximilians-Universität München, 133 pp. doi: 10.57676/mzmg-r403., 2023.

Bier, A., and Burkhardt, U.: Variability in contrail ice nucleation and its dependence on soot number emissions. J. Geophys. Res. Atmos., 124(6), 3384–3400, https://doi.org/10.1029/2018JD030132, 2019.

Bier, A., and Burkhardt, U.: Impact of parametrizing microphysical processes in the jet and vortex phase on contrail cirrus properties and radiative forcing. J. Geophys. Res. Atmos., 127, e2022JD036677, https://doi.org/10.1029/2022JD036677, 2022.

Bier, A., Burkhardt, U., and Bock, L.: Synoptic control of contrail cirrus life cycles and their modification due to reduced soot number emissions. J. Geophys. Res. Atmos., 122(21), 11,584–11,603, https://doi.org/10.1002/2017JD027182, 2017.

Bock, L., and Burkhardt, U.: Reassessing properties and radiative forcing of contrail cirrus using a global climate model. J. Geophys. Res. Atmos., 121(16), 9717–9736, https://doi.org/10.1002/2015JD024688, 2016.

Bock, L., and Burkhardt, U.: The temporal evolution of a long-lived contrail cirrus cluster: Simulations with a global climate model, J. Geophys. Res. Atmos., 121, 3548–3565, https://doi.org/10.1002/2015JD024282, 2016.

Bock, L., and Burkhardt, U.: Contrail cirrus radiative forcing for future air traffic. Atmos. Chem. Phys., 19(12), 8163–8174, https://doi.org/10.5194/acp-19-8163-2019, 2019

Boeing: Commercial Market Outlook 2022–2041. https://www.boeing.com/commercial/market/commercial-market-outlook/index.page, 2022.

Bräuer, T., Voigt, C., Sauer, D., Kaufmann, S., Hahn, V., Scheibe, M., Schlager, H., Diskin, G. S., Nowak, J. B., DiGangi, J. P., Huber, F.: Airborne measurements of contrail ice properties-Dependence on temperature and humidity, Geophys. Res. Lett., 48(8), e2020GL092166, https://doi.org/10.1029/2020GL092166, 2021a.

Bräuer T, Voigt C, Sauer D, Kaufmann S, Hahn V, Scheibe M, Schlager H, Huber F, Le Clercq P, Moore RH, Anderson BE. Reduced ice number concentrations in contrails from low-aromatic biofuel blends. Atmos. Chem. Phys., 21(22), 16817-26., https://doi.org/10.5194/acp-21-16817-2021, 2021b.

Burkhardt, U., Kärcher, B., Ponater, M., Gierens, K., and Gettelman, A.: Contrail cirrus supporting areas in model and observations. Geophys. Res. Lett., 35, https://doi.org/10.1029/2008GL034056, 2008.

Burkhardt, U., and Kärcher, B.: Process-based simulation of contrail cirrus in a global climate model. J. Geophys. Res. Atmos., 114(D16), D16201, https://doi.org/10.1029/2008JD011675, 2009.

Burkhardt, U., Bock, L., and Bier, A.: Mitigating the contrail cirrus climate impact by reducing aircraft soot number emissions. npj Clim. Atmos. Sci., 1, 37, https://doi.org/10.1038/s41612-018-0044-x, 2018.

Burkhardt, U., and Kärcher, B.: Global radiative forcing from contrail cirrus. Nat. Clim. Change., 1, 54–58, https://doi.org/10.1038/nclimate1068, 2011.

Burkhardt, U., Kärcher, B., and Schumann, U.: Global modeling of the contrail and contrail cirrus climate impact. Bull. Am. Meteorol. Soc., 91(4), 479–484, https://doi.org/10.1175/2010BAMS2966.1, 2010.

Caiazzo, F., Agarwal, A., Speth, R. L., and Barrett, S. R. H.: Impact of biofuels on contrail warming. Environ. Res. Lett., 12, 114013, https://doi.org/10.1088/1748-9326/aa8c25, 2017.

Carlin, B., Fu, Q., Lohmann, U., Mace, G., Sassen, K., and Comstock, J.: High-cloud horizontal inhomogeneity and solar albedo bias. J. Climate, 15, 2321–2339, https://doi.org/10.1175/1520-0442(2002), 2002.

Chauvigné, A., Jourdan, O., Schwarzenboeck, A., Gourbeyre, C., Gayet, J. F., Voigt, C., Schlager, H., Kaufmann, S., Borrmann, S., Molleker, S., Minikin, A.: Statistical analysis of contrail to cirrus evolution during the Contrail and Cirrus Experiment (CONCERT). Atmos. Chem. Phys., 18(13), 9803-22, Jul 12, https://doi.org/10.5194/acp-18-9803-2018, 2018.

Chen, C.-C., Gettelman, A., Craig, C., Minnis, P., and Duda, D.: Global contrail coverage simulated by CAM5 with the inventory of 2006 global aircraft emissions. J. Adv. Model. Earth Syst., 4(4), https://doi.org/10.1029/2012MS000088, 2012.

Chen, C.-C., and Gettelman, A.: Simulated radiative forcing from contrails and contrail cirrus. Atmos. Chem. Phys. Discuss., 13, 10,939–10,959, https://doi.org/10.5194/acpd-13-10939-2013, 2013.

Chen, C.-C., and Gettelman, A.: Simulated 2050 Aviation Radiative Forcing from Contrails and Aerosols. Atmos. Chem. Phys., 16 (11), 7317–33, https://doi.org/10.5194/acp-16-7317-2016, 2016.

Comstock, J. M., Ackerman, T. P., and Turner, D. D.: Evidence of high ice supersaturation in cirrus clouds using ARM Raman lidar measurements. Geophys. Res. Lett., 31, L11106, https://doi.org/10.1029/2004GL019705, 2004.

Danabasoglu, G., Lamarque, J. F., Bacmeister, J., Bailey, D. A., DuVivier, A. K., Edwards, J., Emmons, L. K., Fasullo, J., Garcia, R., Gettelman, A., Hannay, C.: The community earth system model version 2 (CESM2). J. Adv. Model. Earth Syst., 12(2), e2019MS001916, https://doi.org/10.1029/2019MS001916, Feb, 2020.

De Leon, R. R., M. Krämer, M., Lee, D. S., and Thelen, J. C.: Sensitivity of radiative properties of persistent contrails to the ice water path. Atmos. Chem. Phys., 12, 7893–7901, https://doi.org/10.5194/acp-12-7893-2012, 2012.

Dischl, R. K., Sauer, D., Voigt, C., Harlaß, T., Sakellariou, F., Märkl, R. S., Schumann, U., Scheibe, M., Kaufmann, S., Roiger, A., Dörnbrack, A., Renard, C., Gauthier, M., Swann, P., Madden, P., Luff, D., Johnson, M., Ahrens, D., Sallinen, R., Schripp, T., Eckel, G., Bauder, U., and Le Clercq, P.: Measurements of particle emissions of an A350-941 burning 100 % sustainable aviation fuels in cruise, EGUsphere [preprint], https://doi.org/10.5194/egusphere-2024-1224, 2024.

Dietmüller, S., et al.: A new radiation infrastructure for the Modular Earth Submodel System (MESSy, based on version 2.51). Geosci. Model Dev., 9, 2209–2222, https://doi.org/10.5194/gmd-9-2209-2016, 2016.

Dipankar, A., Stevens, B., Heinze, R., Moseley, C., Zängl, G., Giorgetta, M., and Brdar, S.: Large eddy simulation using the general circulation model ICON. J. Adv. Model. Earth Syst., 7, 963–986, https://doi.org/10.1002/2015MS000431, 2015.

Duda, D. P., Minnis, P., Nguyen, L., and Palikonda, R.: A case study of the development of contrail clusters over the Great Lakes. J. Atmos. Sci., 61, 1132–1146, https://doi.org/10.1175/1520-0469(2004)061<1132:ACOTDO>2.0.CO;2, 2004.

Duda, D. P., Minnis, P., Khlopenkov, K., Chee, T. L., and Boeke, R.: Estimation of 2006 Northern Hemisphere contrail coverage using MODIS data. Geophys. Res. Lett., 40, 612–617, https://doi.org/10.1002/grl.50126, 2013.

Duda, D. P., Smith, W. L., Bedka, S., Spangenberg, D., Chee, T., and Minnis, P.: Impact of COVID-19-Related Air Traffic Reductions on the Coverage and Radiative Effects of Linear MicrphysicalPersistent Contrails Over Conterminous United States and Surrounding Oceanic Routes, J. Geophys. Res.-Atmos., 128, e2022JD037554, https://doi.org/10.1029/2022JD037554, 2023.

EASA (European Union Aviation Safety Agency) ICAO Aircraft Engine Emissions Databank 2023: http://www.easa.europa.eu/document-library/icao-aircraft-engine-emissions-databank.

Ettenreich, R.: Wolkenbildung über einer Feuersbrunst und an Flugzeugabgasen. Meteorol. Z., 36, 355–356, 1919.

Elmourad, J. A.: Evaluating Fuel-Climate Tradeoffs in Contrail Avoidance (Doctoral dissertation, Massachusetts Institute of Technology), 2023.

EUROCONTROL.: Aircraft Performance Summary Tables for the Base of Aircraft Date (BADA), 3.7, European Organisation for the Safety of Air Navigation, Brétigny-sur-Orge, 103, 2009.

Frias, A.M., Shapiro, M.L., Engberg, Z., Zopp, R., Soler, M. and Stettler, M.E.J.: Feasibility of contrail avoidance in a commercial flight planning system: an operational analysis.

Environmental Research: Infrastructure and Sustainability, 4(1), p.015013, doi 10.1088/2634-4505/ad310c, 2024.

Fritz, T. M., Eastham, S. D., Speth, R. L., and Barrett, S. R. H.: The role of plume-scale processes in long-term impacts of aircraft emissions. Atmos. Chem. Phys., 20, 5697–5714, https://doi.org/10.5194/acp-20-5697-2020, 2020.

Frömming, C., Ponater, M., Burkhardt, U., Stenke, A., Pechtl, S., and Sausen, R.: Sensitivity of contrail coverage and contrail radiative forcing to selected key parameters, Atmos. Environ., 45, 1483–1490, https://doi.org/10.1016/j.atmosenv.2010.12.039, 2011.

Fuglestvedt, J. S., and coauthors: Transport impacts on atmosphere and climate: Metrics. Atmos. Environ, 44, 4648–4677, https://doi.org/10.1016/j.atmosenv.2009.04.044, 2010.

Garber, D. P., Minnis, P., and Costulis, P. K.: A commercial flight track database for upper tropospheric aircraft emission studies over the USA and southern Canada, Meteorologische Zeitschrift, 14, 445–452, https://doi.org/10.1127/0941-2948/2005/0040, 2005.

Gayet, J. F., Shcherbakov, V., Voigt, C., Schumann, U., Schäuble, D., Jessberger, P., Petzold, A., Minikin, A., Schlager, H., Dubovik, O., Lapyonok, T.: The evolution of microphysical and optical properties of an A380 contrail in the vortex phase, Atmos. Chem. Phys., 12(14), 6629-6643, https://doi.org/10.5194/acp-12-6629-2012, 2012.

Geleyn, J. F., Hollingsworth, A.: An economical analytical method for the computation of the interaction between scattering and line absorption of radiation, Beiträge zur Physik der Atmosphäre, 52, 1–16, 1978.

Gerz, T., Durbeck, T., Konopka, P.: Transport and effective diffusion of aircraft emissions, J. Geophys. Res., 103, 25905–25914, https://doi.org/10.1029/98JD01819, 1998.

Gettelman, A., Chen, C. C., Bardeen, C. G.: The climate impact of COVID-19-induced contrail changes, Atmos. Chem. Phys., 21(12), 9405-9416, https://doi.org/10.5194/acp-21-9405-2021, 2021.

Gettelman, A., Chen, C.: The climate impact of aviation aerosols, Geophys. Res. Lett., 40(11), 2785-2789, https://doi.org/10.1002/grl.50539, 2013.

Gettelman, A., Morrison, H.: Advanced Two-Moment Bulk Microphysics for Global Models. Part I: Off-Line Tests and Comparison with Other Schemes, J. Climate, 28, 1268–1287, https://doi.org/10.1175/JCLI-D-14-00102.1, 2015.

Gettelman, A., Bardeen, C. G., McCluskey, C. S., Järvinen, E., Stith, J., Bretherton, C., McFarquhar, G., Twohy, C., D'Alessandro, J., Wu, W.: Simulating Observations of Southern Ocean Clouds and Implications for Climate, J. Geophys. Res., 125, https://doi.org/10.1029/2019JD031872, 2020.

Gettelman, A., Gagne, D. J., Chen, C.-C., Christensen, M. W., Lebo, Z. J., Morrison, H., Gantos, G.: Machine Learning the Warm Rain Process, J. Adv. Model. Earth Syst., 13, https://doi.org/10.1029/2020MS002273, 2021.

Gettelman, A., Hannay, C., Bacmeister, J. T., Neale, R. B., Pendergrass, A. G., Danabasoglu, G., Lamarque, J.-F., Fasullo, J. T., Bailey, D. A., Lawrence, D. M., Mills, M. J.: High Climate Sensitivity in the Community Earth System Model Version 2 (CESM2), Geophys. Res. Lett., 46, https://doi.org/10.1029/2019GL083978, 2019.

Gierens, K. M., Lim, L., Eleftheratos, K.: A review of various strategies for contrail avoidance, Open Atmos. Sci. J., 2, 1-7, https://doi.org/10.2174/1874282300802010001, 2008.

Gierens, K., Matthes, S., Rohs, S.: How Well Can Persistent Contrails Be Predicted?, Aerospace, 7, 169, https://doi.org/10.3390/aerospace7110169, 2020.

Gounou, A., Hogan, R. J.: A sensitivity study of the effect of horizontal photon transport on the radiative forcing of contrails, J. Atmos. Sci., 64, 1706–1716, https://doi.org/10.1175/JAS3943.1, 2007.

Graf, K., Schumann, U., Mannstein, H., Mayer, B.: Aviation induced diurnal North Atlantic cirrus cover cycle, Geophys. Res. Lett., 39, https://doi.org/10.1029/2012GL053403, 2012.

Grewe, V., Gangoli Rao, A., Grönstedt, T., Xisto, C., Linke, F., Melkert, J., Middel, J., Ohlenforst, B., Blakey, S., Christie, S., Matthes, S., Dahlmann, K.: Evaluating the climate impact of aviation emission scenarios towards the Paris agreement including COVID-19 effects, Nat. Commun., 12, 3841, https://doi.org/10.1038/s41467-021-24046-4, 2021.

Huszar, P., Teyssèdre, H., Michou, M., Voldoire, A., Olivié, D. J. L., Saint-Martin, D., Cariolle, D., Senesi, S., Salas Y Melia, D., Alias, A., Karcher, F., Ricaud, P., and Halenka, T.: Modeling the present and future impact of aviation on climate: an AOGCM approach with online coupled chemistry, Atmos. Chem. Phys., 13, 10027–10048, https://doi.org/10.5194/acp-13-10027-2013, 2013.

Haywood, J. M., Allan, R. P., Bornemann, J., Forster, P. M., Francis, P. N., Milton, S., Rädel, G., Rap, A., Shine, K. P., Thorpe, R.: A case study of the radiative forcing of persistent contrails evolving into contrail-induced cirrus. J. Geophys. Res. Atmos., 114(D24), https://doi.org/10.1029/2009JD012650, 2009.

ICAO Future Of Aviation 2012, 2012. Retrieved from https://www.icao.int/Meetings/FutureOfAviation/Pages/default.aspx

Immler, F., Treffeisen, R., Engelbart, D., Krüger, K., Schrems, O.: Cirrus contrails, and ice supersaturated regions in high-pressure systems at northern mid-latitudes, Atmos. Chem. Phys., 8, 1689–1699, https://doi.org/10.5194/acp-8-1689-2008, 2008.

IPCC: Climate Change 2021: The Physical Science Basis. Contribution of Working Group I to the Sixth Assessment Report of the Intergovernmental Panel on Climate Change, 2021.

IPCC: Summary for Policymakers 2018: In V. Masson-Delmotte, P. Zhai, H. O. Pörtner, et al. (Eds.), Global warming of 1.5°C. An IPCC Special Report on the Impacts of Global Warming of 1.5°C above Pre-industrial Levels and Related Global Greenhouse Gas Emission Pathways, World Meteorological Organization Technical Document, pp. 32, 2018.

IPCC: Aviation and the global atmosphere 1999: In: Penner, J.E., Lister, D.H., Griggs, D. J., Dokken, D.J., McFarland, M. (Eds.), Intergovernmental Panel on Climate Change Special Report. Cambridge University Press, Cambridge, UK, 1999.

Irvine, E. A., Hoskins, B. J., Shine, K. P.: A Lagrangian analysis of ice-supersaturated air over the North Atlantic, J. Geophys. Res.: Atmospheres, 119, 90–100, https://doi.org/10.1002/2013JD019843, 2013.

Iwabuchi, H., Yang, P., Liou, K.N. and Minnis, P.: Physical and optical properties of persistent contrails: Climatology and interpretation. J. Geophys. Res: Atmospheres, 117(D6), https://doi.org/10.1029/2011JD017003, 2012.

Jacobson, M. Z., Wilkerson, J. T., Naiman, A. D., Lele, S. K.: The effects of aircraft on climate and pollution. Part I: Numerical methods for treating the subgrid evolution of discrete size-and composition-resolved contrails from all commercial flights worldwide. J. Comput. Phys., 230(12), 5115-32, https://doi.org/10.1016/j.jcp.2011.03.021, Jun 1, 2011.

Jacobson, M. Z.: Short-term effects of controlling fossil-fuel soot, biofuel soot and gases, and methane on climate, Arctic ice, and air pollution health. J. Geophys. Res., 115, D14209, https://doi.org/10.1029/2009JD013795, 2010.

Jensen, E., Ackermann, A.S., Stevens, D.E., Toon, O.B., Minnis, P.: Spreading and growth of contrails in a sheared environment. J. Geophys. Res., 103, 13557–13567, https://doi.org/10.1029/98JD00642, 1998.

Jensen, E., Toon, O., Vay, S., Ovarlez, J., May, R., Bui, T., Twohy, C., Gandrud, B., Pueschel, R., and Schumann, U.: Prevalence of ice-supersaturated regions in the upper troposphere: Implications for optically thin ice cloud formation, J. Geophys. Res., 106, 17253–17266, https://doi.org/10.1029/2000JD900774, 2001.

Kärcher, B.: Formation and radiative forcing of contrail cirrus. Nat. Commun., 9, 1824, https://doi.org/10.1038/s41467-018-04272-2, 2018.

Kärcher, B., Burkhardt, U., Bier, A., Bock, L., and Ford, I. J.: The microphysical pathway to contrail formation. J. Geophys. Res. Atmos., 120, 7893–7927, https://doi.org/10.1002/2015JD023293, 2015.

Kärcher, B.: Formation and radiative forcing of contrail cirrus. Nat. Commun., 9(1), 1824, https://doi.org/10.1038/s41467-018-04272-2, 2018.

Kärcher, B., and Yu, F.: Role of aircraft soot emissions in contrail formation. Geophys. Res. Lett., 36(1), L01804, https://doi.org/10.1029/2008GL036649, 2009.

Kärcher, B., Burkhardt, U., Bier, A., Bock, L., and Ford, I. J.: The microphysical pathway to contrail formation. J. Geophys. Res. Atmos., 120(15), 7893–7927, https://doi.org/10.1002/2015JD023293, 2015.

Klöwer, M., Allen, M. R., Lee, D. S., Proud, S. R., Gallagher, L., and Skowron, A.: Quantifying aviation's contribution to global warming. Environ. Res. Lett., 16, 104027, https://doi.org/10.1088/1748-9326/ac24ff, 2021.

Krämer, M., Rolf, C., Spelten, N., Afchine, A., Fahey, D., Jensen, E., Khaykin, S., Kuhn, T., Lawson, P., Lykov, A., Pan, L. L. (2020 Nov 2). A microphysics guide to cirrus–Part 2: Climatologies of clouds and humidity from observations. Atmos. Chem. Phys., 20(21), 12569-608, https://doi.org/10.5194/acp-20-12569-2020, 2020.

Krämer, M., Schiller, C., Afchine, A., Bauer, R., Gensch, I., Mangold, A., Schlicht, S., Spelten, N., Sitnikov, N., Borrmann, S., de Reus, M., and Spichtinger, P.: Ice supersaturations and cirrus cloud crystal numbers, Atmos. Chem. Phys., 9, 3505–3522, https://doi.org/10.5194/acp-9-3505-2009, 2009.

Kristensson, A., Gayet, J.-F., Ström, J., and Auriol, F.: In situ observations of a reduction in effective crystal diameter in cirrus clouds near flight corridors, Geophys. Res. Lett., 27, 681–684, https://doi.org/10.1029/1999GL010858, 2000.

Kübbeler, M., Hildebrandt, M., Meyer, J., Schiller, C., Hamburger, Th., Jurkat, T., Minikin, A., Petzold, A., Rautenhaus, M., Schlager, H., Schumann, U., Voigt, C., Spichtinger, P., Gayet, J.-F., Gourbeyre, C., and Krämer, M.: Thin and subvisible cirrus and contrails in a subsaturated environment, Atmos. Chem. Phys., 11, 5853–5865, https://doi.org/10.5194/acp-11-5853-2011, 2011.

Kulik, L.: Satellite-based detection of contrails using deep learning, Master's thesis, Massachusetts Institute of Technology, 2019.

Kurz, C.: Entwicklung und Anwendung eines gekoppelten Klima-Chemie-Modellsystems: Globale Spurengastransporte und chemische Umwandlungsprozesse (Doctoral thesis), Ludwigs-Maximilians-University Munich, DLR Forschungsbericht, 2007.

Lamquin, N., Stubenrauch, C.J., Gierens, K., Burkhardt, U., and Smit, H.: A global climatology of upper tropospheric ice supersaturation occurrence inferred from the Atmospheric Infrared

Sounder calibrated by MOZAIC, Atmos. Chem. Phys., 12, 381–405, https://doi.org/10.5194/acp-12-381-2012, 2012.

Lee, D.S., Pitari, G., Grewe, V., Gierens, K., Penner, J.E., Petzold, A., Prather, M.J., Schumann, U., Bais, A., Berntsen, T. and Iachetti, D.: Transport impacts on atmosphere and climate: Aviation, Atmospheric environment, 44(37), pp.4678-4734, https://doi.org/10.1016/j.atmosenv.2010.06.045, 2010.

Lee, D. S., Fahey, D. W., Forster, P. M., Newton, P. J., Wit, R. C. N., Lim, L. L., Owen, B., and Sausen, R.: Aviation and global climate change in the 21st century, Atmos. Environ., 43, 3520-3537, https://doi.org/10.1016/j.atmosenv.2009.04.024, 2009.

Lee, D. S., Fahey, D. W., Skowron, A., Allen, M. R., Burkhardt, U., Chen, Q., Doherty, S. J., Freeman, S., Forster, P. M., Fuglestvedt, J., Gettelman, A., De León, R. R., Lim, L. L., Lund, M. T., Millar, R. J., Owen, B., Penner, J. E., Pitari, G., Prather, M. J., Sausen, R., and Wilcox, L. J.: The contribution of global aviation to anthropogenic climate forcing for 2000 to 2018, Atmos. Environ., 244, 117834, https://doi.org/10.1016/j.atmosenv.2020.117834, 2021.

Lewellen, D. C.: Analytic Solutions for Evolving Size Distributions of Spherical Crystals or Droplets Undergoing Diffusional Growth in Different Regimes, J. Atmos. Sci., 69, 417–434, https://doi.org/10.1175/JAS-D-11-0193.1, 2012.

Lewellen, D. C.: Persistent contrails and contrail cirrus. Part II: Full lifetime behavior, J. Atmos. Sci., 71, 4420–4438, https://doi.org/10.1175/JAS-D-14-0004.1, 2014.

Lewellen, D. C., Meza, O., Huebsch, W.: Persistent contrails and contrail cirrus. Part 1: Large-eddy simulations from inception to demise, J. Atmos. Sci., 71, 4399–4419, https://doi.org/10.1175/JAS-D-14-0003.1, 2014.

Li, J., Caiazzo, F., Chen, N. Y., Sridhar, B., Ng, H., and Barrett, S.: Evaluation of aircraft contrails using dynamic dispersion model, AIAA Guidance Navigation, and Control (GNC) Conf., 2013–5178 pp., https://doi.org/10.2514/6.2013-5178, 2013.

Li, Y., Mahnke, C., Rohs, S., Bundke, U., Spelten, N., Dekoutsidis, G., Groß, S., Voigt, C., Schumann, U., Petzold, A., and Krämer, M.: Upper-tropospheric slightly ice-subsaturated regions: frequency of occurrence and statistical evidence for the appearance of contrail cirrus, Atmos. Chem. Phys., 23, 2251–2271, https://doi.org/10.5194/acp-23-2251-2023, 2023.

Liou, K.N., Takano, Y., Yue, Q., and Yang, P.: On the radiative forcing of contrail cirrus contaminated by black carbon, Geophys. Res. Lett., 40, 778–784, https://doi.org/10.1002/grl.50214, 2013.

Liu, X., Ma, P.-L., Wang, H., Tilmes, S., Singh, B., Easter, R. C., Ghan, S. J., and Rasch, P. J.: Description and evaluation of a new four-mode version of the Modal Aerosol Module (MAM4) within version 5.3 of the Community Atmosphere Model, Geosci. Model Dev., 9, 505–522, https://doi.org/10.5194/gmd-9-505-2016, 2016.

Lohmann, U., Spichtinger, P., Heidt, S., Peter, T., and Smit, H.: Cirrus clouds and ice supersaturation regions in a global climate model, Environ. Res. Lett., 3(4), 045022, https://doi.org/10.1088/1748-9326/3/4/045022, 2008.

Luebke, A. E., Afchine, A., Costa, A., Grooß, J.-U., Meyer, J., Rolf, C., Spelten, N., Avallone, L. M., Baumgardner, D., and Krämer, M.: The origin of midlatitude ice clouds and the resulting influence on their microphysical properties, Atmos. Chem. Phys., 16, 5793–5809, https://doi.org/10.5194/acp-16-5793-2016, 2016.

Mahnke, C., Gomes, R., Bundke, U., Berg, M., Zereis, H., Sharma, M., Righi, M., Hendricks, J., Zahn, A., and Petzold, A.: Properties and processing of aviation induced aerosol within the UTLS observed from the IAGOS-CARIBIC Flying Laboratory, EGU General Assembly 2022,

Vienna, Austria, 23–27 May 2022, EGU22-908, https://doi.org/10.5194/egusphereegu22-908, 2022.

Mannstein, H., Brömser, A., and Bugliaro, L.: Ground-based observations for the validation of contrails and cirrus detection in satellite imagery, Atmos. Meas. Tech., 3, 655–669, https://doi.org/10.5194/amt-3-655-2010, 2010.

Mannstein, H., Meyer, R., and Wendling, P.: Operational detection of contrails from NOAA-AVHRR data, Int. J. Remote Sens., 20, 1641–1660, https://doi.org/10.1080/014311699212470, 1999.

Märkl, R. S., Voigt, C., Sauer, D., Dischl, R. K., Kaufmann, S., Harlaß, T., Hahn, V., Roiger, A., Weiß-Rehm, C., Burkhardt, U., Schumann, U., Marsing, A., Scheibe, M., Dörnbrack, A., Renard, C., Gauthier, M., Swann, P., Madden, P., Luff, D., Sallinen, R., Schripp, T., and Le Clercq, P.: Powering aircraft with 100 % sustainable aviation fuel reduces ice crystals in contrails, Atmos. Chem. Phys., 24, 3813–3837, https://doi.org/10.5194/acp-24-3813-2024, 2024.

Markowicz, K. M., Witek, M. L.: Simulations of contrail optical properties and radiative forcing for various crystal shapes, J. Appl. Meteorol. Climatol., 50, 1740–1755, https://doi.org/10.1175/JAMC-D-11-071.1, 2011.

Marquart, S., Ponater, M., Mager, F., and Sausen, R.: Future Development of Contrail Cover, Optical Depth, and Radiative Forcing: Impacts of Increasing Air Traffic and Climate Change, J. Climate, 16, 2890–2904, https://doi.org/10.1175/1520-0442(2003)016<2890:FDOCCO>2.0.CO;2, 2003.

Matthes S, Lee DS, De Leon RR, Lim L, Owen B, Skowron A, Thor RN, Terrenoire E.: The effects of supersonic aviation on ozone and climate, Aerospace, 9(1), 41, https://doi.org/10.3390/aerospace9010041, 2022.

Mayer, B., and Kylling, A.: The libRadtran software package for radiative transfer calculations: Description and examples of use, Atmos. Chem. Phys., 5, 1855–1877, https://doi.org/10.5194/acp-5-1855-2005, 2005.

McCloskey, K., Geraedts, S., Van Arsdale, C., and Brand, E.: A human-labeled landsat-8 contrails dataset. In ICML 2021 Workshop on Tackling Climate Change with Machine Learning, https://www.climatechange.ai/events/iclr2023#about, 2021.

Meerkötter, R., Schumann, U., Doelling, D. R., Minnis, P., Nakajima, T., and Tsushima, Y.: Radiative forcing by contrails, Ann. Geophys., 17, 1080–1094, https://doi.org/10.1007/s00585-999-1080-0, 1999.

Meijer, V. R., Kulik, L., Eastham, S. D., Allroggen, F., Speth, R. L., Karaman, S., and Barrett, S. R.: Contrail coverage over the United States before and during the COVID-19 pandemic, Environ. Res. Lett., 17, 034039, https://doi.org/10.1088/1748-9326/ac52f4, 2021.

Minnis, P.: Contrails. In G. R. North (Ed.), Encyclopedia of Atmospheric Sciences (2nd ed., Vol. 2, pp. 121-132). Oxford, UK: Elsevier Ltd., 2015.

Minnis, P., Bedka, S. T., Duda, D. P., Bedka, K. M., Chee, T., Ayers, J. K., Palikonda, R., Spangenberg, D. A., Khlopenkov, K. V., and Boeke, R.: Linear contrail and contrail cirrus properties determined from satellite data, Geophys. Res. Lett., 40, 3220–3226, https://doi.org/10.1002/grl.50557, 2013.

Minnis, P., Schumann, U., Doelling, D. R., Gierens, K. M., and Fahey, D. W.: Global distribution of contrail radiative forcing, Geophys. Res. Lett., 26, 1853–1856, https://doi.org/10.1029/1999GL900391, 1999.

2285 Molod, A., Takacs, L., Suarez, M., and Bacmeister, J.: Development of the GEOS-5 atmospheric
2286   general circulation model: evolution from MERRA to MERRA2, Geosci. Model Dev., 8,
2287   1339–1356, https://doi.org/10.5194/gmd-8-1339-2015, 2015.
2288 Molloy, J., Teoh, R., Harty, S., Koudis, G., Schumann, U., Poll, I. and Stettler, M.E.: Design
2289   principles for a contrail-minimizing trial in the north atlantic, Aerospace, 9(7), p.37,
2290   https://doi.org/10.3390/aerospace9070037, 2022.
2291 Moore, R.H., Thornhill, K.L., Weinzierl, B., Sauer, D., D'Ascoli, E., Kim, J., Lichtenstern, M.,
2292   Scheibe, M., Beaton, B., Beyersdorf, A.J. and Barrick, J.: Biofuel blending reduces particle
2293   emissions from aircraft engines at cruise conditions, Nature, 543(7645), pp.411-415,
2294   https://doi.org/10.1038/nature21420, 2017.
2295 Myhre, G., and Stordal, F.: On the tradeoff of the solar and thermal infrared radiative impact of
2296   contrails, Geophys. Res. Lett., 28, 3119–3122, https://doi.org/10.1029/2001GL013916, 2001.
2297 Myhre, G., Kvalevåg, M., Rädel, G., Cook, J., Shine, K. P., Clark, H., Kärcher, F., Markowicz,
2298   K., Kardas, A., Wolkenberg, P., Balkanski, Y., Ponater, M., Forster, P., Rap, A., and De Leon,
2299   R. R.: Intercomparison of radiative forcing calculations of stratospheric water vapour and
2300   contrails, Meteorol. Z., 18, 585–596, https://doi.org/10.1127/0941-2948/2009/0405, 2009.
2301 Naiman, A. D., Lele, S. K., Wilkerson, J. T., and Jacobson, M. Z.: Parameterization of subgrid
2302   plume dilution for use in large-scale atmospheric simulations, Atmos. Chem. Phys., 10, 2551–
2303   2560, https://doi.org/10.5194/acp-10-2551-2010, 2009.
2304 Naiman, A. D., Lele, S. K., Wilkerson, J. T., and Jacobson, M. Z.: A low order contrail model for
2305   use with global-scale climate models, 47th AIAA Aerospace Science Meeting, Orlando, FL,
2306   2011.
2307 Naiman, A. D., Lele, S. K., and Jacobson, M. Z.: Large Eddy simulations of persistent aircraft
2308   contrails, 49th AIAA Aerospace Science Meeting, Orlando, 2011.
2309 Newinger, C., Burkhardt, U.: Sensitivity of contrail cirrus radiative forcing to air traffic
2310   scheduling, J. Geophys. Res. Atmos., 117, D1020, https://doi.org/10.1029/2011JD016815,
2311   2012.
2312 Neil Y. Chen, N., Sridhar, B., and Ng, H. K.: Prediction and use of contrail frequency index for
2313   contrail reduction strategies, AIAA Guidance, Navigation, and Control Conference, Toronto,
2314   Canada, 2010.
2315 Ng, J. Y. H., McCloskey, K., Cui, J., Brand, E., Sarna, A., Goyal, N., ... and Geraedts, S.:
2316   OpenContrails: Benchmarking Contrail Detection on GOES-16 ABI, arXiv preprint
2317   arXiv:2304.02122, 2023.
2318 Niklaß, M., Grewe, V., Gollnick, V., and Dahlmann, K.: Concept of climate-charged airspaces: a
2319   potential policy instrument for internalizing aviation's climate impact of non-CO2 effects,
2320   Climate Policy, 21, 1066–1085, https://doi.org/10.1080/14693062.2020.1809243, 2021.
2321 Ovarlez, J., van Velthoven, P., Sachse, G., Vay, S., Schlager, H., and Ovarlez, H.: Comparison of
2322   water vapor measurements from POLINAT 2 with ECMWF analyses in high-humidity
2323   conditions, J. Geophys. Res., 105, 3737–3744, https://doi.org/10.1029/1999JD900591, 2000.
2324 Ovarlez, J., Gayet, J.-F., Gierens, K., Strom, J., Ovarlez, H., Auriol, F., Busen, R., and Schumann,
2325   U.: Water vapour measurements inside cirrus clouds in Northern and Southern hemispheres
2326   during INCA, Geophys. Res. Lett., 29, 1813–1817, https://doi.org/10.1029/2002GL016301,
2327   2002.
2328 Palikonda, R., Minnis, P., Duda, D. P., and Mannstein, H.: Contrail coverage derived from 2001
2329   AVHRR data over the continental United States of America and surrounding areas, Meteorol.
2330   Z., 14, 525–536, https://doi.org/10.1127/0941-2948/2005/0055, 2005.

Paoli, R. and Shariff, K.: Contrail Modeling and Simulation, Annu. Rev. Fluid Mech., 48, 393–427, https://doi.org/10.1146/annurev-fluid-010719-060304, 2016.

Penner, J. E., Lister, D. H., Griggs, D. J., Dokken, D. J., and McFarland, M., Eds.: Aviation and the Global Atmosphere, Cambridge University Press, 373 pp., 1999.

Petters, M. D., and Kreidenweis, S. M.: A single parameter representation of hygroscopic growth and cloud condensation nucleus activity, Atmos. Chem. Phys., 7(8), 1961–1971, https://doi.org/10.5194/acp-7-1961-2007, 2007.

Petzold, A., Busen, R., Schröder, F. P., Baumann, R., Kuhn, M., Ström, J., Hagen, D. E., Whitefield, P. D., Baumgardner, D., Arnold, F., Borrmann, S., and Schumann, U.: Near-field measurements on contrail properties from fuels with different sulfur content, J. Geophys. Res. Atmos., 102, 29867–29880, https://doi.org/10.1029/97JD02686, 1997.

Petzold, A., Krämer, M., Neis, P., Rolf, C., Rohs, S., Berkes, F., Smit, H. G. J., Gallagher, M., Beswick, K., Lloyd, G., Baumgardner, D., Spichtinger, P., Nédélec, P., Ebert, V., Buchholz, B., Riese, M., and Wahner, A.: Upper tropospheric water vapor and its interaction with cirrus clouds as seen from IAGOS long-term routine in situ observations, Faraday Discuss, 200, 229–249, https://doi.org/10.1039/C7FD00040A, 2017.

Petzold, A., Hoor, P., Järvinen, E., Lauer, A., Meyer, J., Neuberger, T., Schiller, C., Veselovskii, I., and Woiwode, W.: Ice-supersaturated air masses in the northern mid-latitudes from regular in situ observations by passenger aircraft: vertical distribution, seasonality and tropospheric fingerprint, Atmos. Chem. Phys., 20, 8157–8179, https://doi.org/10.5194/acp-20-8157-2020, 2020.

Poellot, M. R., Arnott, W. P., and Hallett, J.: In situ observations of contrail microphysics and implications for their radiative impact, J. Geophys. Res., 104, 12 077–12 084, https://doi.org/10.1029/1999JD900006, 1999.

Poll DI. On the relationship between non-optimum operations and fuel requirement for large civil transport aircraft, with reference to environmental impact and contrail avoidance strategy, The Aeronautical Journal, Dec;122(1258):1827-70, 2018.

Pomroy, H.R., and Illingworth, J.A.: Ice cloud inhomogeneity: quantifying bias in emissivity from radar observations, Geophys. Res. Lett., 27, 2101–2104, https://doi.org/10.1029/2000GL011429, 2000.

Ponater, M., Marquart, S., and Sausen, R.: Contrails in a comprehensive global climate model: Parameterization and radiative forcing results, J. Geophys. Res. Atmos., 107, ACL 2-1–ACL 2-15, https://doi.org/10.1029/2001JD001227, 2002.

Ponater, M., Bickel, M., Bock, L. and Burkhardt, U.: Towards determining the contrail cirrus efficacy, Aerospace, 8(2), p.42, https://doi.org/10.3390/aerospace8020042, 2021.

Pruppacher, H. R. and Klett, J. D.: Microphysics of Clouds and Precipitation, Atmospheric and Oceanographic Sciences Library, 2nd Edn., Kluwer Academic Publishers, Dordrecht, the Netherlands, ISBN 978-0792344094, 1997.

Pruppacher, H. R. and Klett, J. D.: Microphysics of clouds and precipitation, Kluwer Academic, Norwell, Mass., 2000.

Rädel, G. and Shine, K. P.: Radiative forcing by persistent contrails and its dependence on cruise altitudes, J. Geophys. Res. Atmos., 113, D07105, https://doi.org/10.1029/2007JD009401, 2008.

Rap, A., Forster, P. M., Jones, A., Boucher, O., Haywood, J. M., Bellouin, N., and De Leon, R. R.: Parameterization of contrails in the UK Met Office Climate Model, J. Geophys. Res., 115, D10205, https://doi.org/10.1029/2009JD012152, 2010.

2377 Reutter, P., Konopka, P., Pappalardo, L., Lembras, A., Müller, R., Euler, F., Baklanov, A., and
2378   Hegerl, G.: Ice supersaturated regions: properties and validation of ERA-Interim reanalysis
2379   with IAGOS in situ water vapor measurements, Atmos. Chem. Phys., 20, 787–804,
2380   https://doi.org/10.5194/acp-20-787-2020, 2020.
2381 Righi, M., Hendricks, J., and Sausen, R.: The global impact of the transport sectors on atmospheric
2382   aerosol: simulations for year 2000 emissions, Atmos. Chem. Phys., 13, 9939–9970,
2383   https://doi.org/10.5194/acp-13-9939-2013, 2013.
2384 Righi M, Hendricks J, Beer CG. Exploring the uncertainties in the aviation soot–cirrus effect,
2385   Atmos. Chem. Phys., 21(23), pp.17267-17289, https://doi.org/10.5194/acp-21-17267-2021,
2386   2021.
2387 Roeckner, E., Baeuml, G., Bonventura, L., Brokopf, R., Esch, M., Giorgetta, M., Hagemann, S.,
2388   Kirchner, I., Kornblueh, L., Manzini, E., Rhodin, A., Schlese, U., Schulzweida, U., and
2389   Tompkins, A.: The atmospheric general circulation model ECHAM5. PART I Model
2390   description, Report 349. Max Planck Institute for Meteorology, Hamburg, Germany.
2391 Roosenbrand, E., Sun, J., & Hoekstra, J.: Optimizing Global Flight Altitudes for Contrail
2392   Reduction. Insights from Open Flight and Weather Balloon Data. In: Fifteenth USA/Europe
2393   Air Traffic Management Research and Development Seminar (ATM2023), 2023.
2394 Sanz-Morère, I., Eastham, S. D., Allroggen, F., Speth, R. L., & Barrett, S. R. H.: Impacts of multi-
2395   layer overlap on contrail radiative forcing. Atmos. Chem. Phys., 21, 1649–1681,
2396   doi:10.5194/acp-21-1649-2021, 2021.
2397 Sausen, R., Gierens, K., Ponater, M., & Schumann, U.: A diagnostic study of the global
2398   distribution of contrails. Part I: Present-day climate. Theor. Appl. Climatol., 61, 127–141,
2399   doi:10.1007/s007040050076, 1998.
2400 Sausen, R., Hofer, S. M., Gierens, K. M., Bugliaro Goggia, L., Ehrmanntraut, R., Sitova, I., ... &
2401   Miller, N.: Can we successfully avoid persistent contrails by small altitude adjustments of
2402   flights in the real world?. Meteorol. Z., 2023.
2403 Schmidt, E.: Die Entstehung von Eisnebel aus den Auspuffgasen von Flugmotoren. Schr. Dtsch.
2404   Akad. Luftfahrtforsch., 44, 1–15, 1941.
2405 Schröder, F., Kärcher, B., Duroure, C., Ström, J., Petzold, A., Gayet, J.-F., ... & Borrmann, S.: On
2406   the Transition of Contrails into Cirrus Clouds. J. Atmos. Sci., 57, 464–480, doi:10.1175/1520-
2407   0469(2000)057<0464:OTTOCI>2.0.CO;2, 2000.
2408 Schumann, U., & Graf, K.: Aviation-induced cirrus and radiation changes at diurnal timescales. J.
2409   Geophys. Res., 118, 2404–2421, doi:10.1002/jgrd.50283, 2013.
2410 Schumann, U., & Heymsfield, A.: On the lifecycle of individual contrails and contrail cirrus-Ice
2411   Formation and Evolution in Clouds and Precipitation: Measurement and Modeling Challenges:
2412   Chapter 3, Meteor. Monogr, 3.1–3.24, 2017.
2413 Schumann, U., & Wendling, P.: Determination of contrails from satellite data and observational
2414   results. In: Air Traffic and the Environment-Background, Tendencies and Potential Global
2415   Atmospheric Effects, U. Schumann (Ed.), Lecture Notes in Engineering, Springer-Verlag,
2416   138–153, 1990.
2417 Schumann, U., Baumann, R., Baumgardner, D., Bedka, S. T., Duda, D. P., Freudenthaler, V., ... &
2418   Wang, Z.: Properties of individual contrails: a compilation of observations and some
2419   comparisons. Atmos. Chem. Phys., 17, 403–438, doi:10.5194/acp-17-403-2017, 2017.
2420 Schumann, U., Bugliaro, L., Dörnbrack, A., Baumann, R., & Voigt, C.: Aviation Contrail Cirrus
2421   and Radiative Forcing Over Europe During 6 Months of COVID-19. Geophys. Res. Lett., 48,
2422   doi:10.1029/2021GL096230, 2021.

Schumann, U., Penner, J. E., Chen, Y., Zhou, C., & Graf, K.: Dehydration effects from contrails in a coupled contrail-climate model. Atmos. Chem. Phys., 15, 11179–11199, doi:10.5194/acp-15-11179-2015, 2015.

Schumann, U., Ström, J., Busen, R., Baumann, R., Gierens, K., Krautstrunk, M., ... & Stingl, J.: In situ observations of particles in jet aircraft exhausts and contrails for different sulfur-containing fuels. J. Geophys. Res., 101, 6853–6870, doi:10.1029/95JD00240, 1996.

Schumann, U.: A contrail cirrus prediction model. Geosci. Model Dev., 5, 543–580, doi:10.5194/gmd-5-543-2012, 2012.

Schumann, U.: On conditions for contrail formation from aircraft exhausts. Meteorol. Z., 5, 4–23, doi:10.1127/metz/5/1996/4, 1996.

Schumann, U., Konopka, P., Baumann, R., Busen, B., Gerz, T., Schlager, H., ... & Volkert, H.: Estimate of diffusion parameters of aircraft exhaust plumes near the tropopause from nitric oxide and turbulence measurements. J. Geophys. Res., 100, 147–162, doi:10.1029/94JD01508, 1995.

Siddiqui, N.: Atmospheric Contrail Detection with a Deep Learning Algorithm, Scholarly Horizons: Univ. Minnesota Morris Undergraduate Journal, 7(1), Article 5, doi:10.26757/sh.v7i1.1334, 2020.

Spangenberg, D. A., Minnis, P., Bedka, S. T., Palikonda, R., Duda, D. P., & Rose, F. G.: Contrail radiative forcing over the Northern Hemisphere from 2006 Aqua MODIS data. Geophys. Res. Lett., 40, 595–600, doi:10.1002/grl.50119, 2013.

Spinhirne, J. D., Hart, W. D., & Duda, D. P.: Evolution of the morphology and microphysics of contrail cirrus from airborne remote sensing. Geophys. Res. Lett., 25, 1153–1156, doi:10.1029/97GL03477, 1998.

Sridhar, B., Ng, H. K., & Chen, N. Y.: Aircraft Trajectory Optimization and Contrails Avoidance in the Presence of Winds, in: 10th AIAA Aviation Technology, Integration and Operations Conference (ATIO), Fort Worth, TX, 2010.

Stenke, A., Grewe, V., & Pechtl, S.: Do supersonic aircraft avoid contrails?, Atmos. Chem. Phys., 8, 955–967, doi:10.5194/acp-8-955-2008, 2008.

Stier, P., Feichter, J., Kinne, S., Kloster, S., Vignati, E., Wilson, J., et al.: The aerosol-climate model ECHAM5-HAM. Atmos. Chem. Phys., 5(4), 1125–1156, 2005.

Stocker, T.F., Qin, D., Plattner, G.K., Tignor, M., Allen, S.K., Boschung, J., ... & Midgley, P. M. (Eds.): Climate Change 2013: the Physical Science Basis, Contribution of Working Group I to the Fifth Assessment Report of the Intergovernmental Panel on Climate Change. Cambridge University Press, Cambridge, United Kingdom and New York, NY, USA, 2013.

Stuber, N., Sausen, R., & Ponater, M.: Stratosphere adjusted radiative forcing calculations in a comprehensive climate model. Theor. Appl. Climatol., 68(3–4), 125–135, doi:10.1007/s007040170048, 2001.

Sun, J., & Roosenbrand, E.: Flight Contrail Segmentation via Augmented Transfer Learning with Novel SR Loss Function in Hough Space. arXiv preprint arXiv:2307.12032, 2023 Jul 22.

Taylor, K. E., Williamson, D., & Zwiers, F.: The sea surface temperature and sea-ice concentration boundary conditions for AMIP II simulations, PCMDI report no. 60, program for climate model diagnostics and intercomparison. The University of California, Lawrence Livermore National Laboratory, 2000.

Teoh, R., Schumann, U., Majumdar, A., & Stettler, M.E.: Mitigating the climate forcing of aircraft contrails by small-scale diversions and technology adoption. Environ. Sci. Technol., 54(5), 2941–2950, doi:10.1021/acs.est.9b07102, 2020.

2469   Teoh, R., Engberg, Z., Shapiro, M., Dray, L., & Stettler, M. E. J.: The high-resolution Global
2470   Aviation emissions Inventory based on ADS-B (GAIA) for 2019–2021, Atmos. Chem. Phys.,
2471   24, 725–744, doi:10.5194/acp-24-725-2024, 2024.
2472   Tesche, M., Achtert, P., Glantz, P., & Noone, K. J.: Aviation effects on already-existing cirrus
2473   clouds. Nat. Commun., 7(1), 12016, doi:10.1038/ncomms12016, 2016.
2474   Testa, B., Durdina, L., Edebeli, J., Spirig, C., & Kanji, Z. A.: Contrail processed aviation soot
2475   aerosol are poor ice nucleating particles at cirrus temperatures [Preprint]. EGUsphere,
2476   doi:10.5194/egusphere-2024-151, 2024.
2477   Unterstrasser, S.: Properties of young contrails-A parametrization based on large-eddy
2478   simulations. Atmos. Chem. Phys., 16(4), 2059–2082, doi:10.5194/acp-16-2059-2016, 2016.
2479   Unterstrasser, S., & Sölch, I.: Numerical modeling of contrail cluster formation. Proc. Third Int.
2480   Conf. on Transport, Atmosphere and Climate (TAC-3). Prien am Chiemsee, Germany, DLR,
2481   114–119, 2012.
2482   Unterstrasser, S., & Görsch, N.: Aircraft-type dependency of contrail evolution. J. Geophys. Res.-
2483   Atmos., 119, 14 015–14 027, doi:10.1002/2014JD022083, 2014.
2484   Unterstrasser, S., Gierens, K., Sölch, I., & Wirth, M.: Numerical simulations of homogeneously
2485   nucleated natural cirrus and contrail-cirrus. Part 2: Interaction on a local scale. Meteorol. Z.,
2486   26, 643–661, doi:10.1127/metz/2017/0844, 2017.
2487   Vazquez-Navarro, M., Mannstein, H., & Kox, S.: Contrail life cycle and properties from 1 year of
2488   MSG and SEVIRI rapid scan images. Atmos. Chem. Phys., 15(15), 8739–8749,
2489   doi:10.5194/acp-15-8739-2015, 2015.
2490   Vázquez-Navarro, M., Mannstein, H., & Mayer, B.: An automatic contrail tracking algorithm.
2491   Atmos. Meas. Tech., 3, 1089–1101, doi:10.5194/amt-3-1089-2010, 2010.
2492   Vazquez-Navarro, M., Mayer, B., & Mannstein, H.: A fast method for the retrieval of integrated
2493   longwave and shortwave top-of-atmosphere upwelling irradiances from MSG and SEVIRI
2494   (RRUMS). Atmos. Meas. Tech., 6(10), 2627–2640, doi:10.5194/acp-6-2627-2013, 2013.
2495   Verma, P., & Burkhardt, U.: Contrail formation within cirrus: ICON-LEM simulations of the
2496   impact of cirrus cloud properties on contrail formation. Atmos. Chem. Phys., 22(13), 8819–
2497   8842, doi:10.5194/acp-22-8819-2022, 2022.
2498   Voigt, C., Schumann, U., Jessberger, P., Jurkat, T., Petzold, A., Gayet, J.-F., ... & Fahey, D. W.:
2499   Extinction and optical depth of contrails. Geophys. Res. Lett., 38, L11806,
2500   doi:10.1029/2011GL047189, 2011.
2501   Voigt, C., Schumann, U., Minikin, A., Abdelmonem, A., Afchine, A., Borrmann, S., ... & Curtius,
2502   J.: ML-CIRRUS: The airborne experiment on natural cirrus and contrail cirrus with the high-
2503   altitude long-range research aircraft HALO. Bull. Am. Meteorol. Soc., 98, 271–288,
2504   doi:10.1175/BAMS-D-14-00193.1, 2017.
2505   Weickmann, H.: Formen und Bildung atmosphärischer Eiskristalle. Beitr. Phys. freien Atmos., 28,
2506   33, 1945.
2507   Wilkerson, J. T., Jacobson, M. Z., Malwitz, A., Balasubramanian, S., Wayson, R., Fleming, G., ...
2508   & Lele, S.: Analysis of emission data from global commercial aviation: 2004 and 2006. Atmos.
2509   Chem. Phys., 10(13), 6391–6408, doi:10.5194/acp-10-6391-2010, 2010.
2510   Wolf, K., Bellouin, N., & Boucher, O.: Sensitivity of cirrus and contrail radiative effect on cloud
2511   microphysical and environmental parameters. Atmos. Chem. Phys., 9(21), 14003-14037,
2512   doi:10.5194/acp-9-14003-2009, 2009.
2513   Wuebbles, D., Gupta, M., & Ko, M.: Evaluating the impacts of aviation on climate change. Eos,
2514   Trans. AGU, 88(14), 157-160, doi:10.1029/2007EO140001, 2007.

Wuebbles, D., Forster, P., Rogers, H., & Herman, R.: Issues and uncertainties affecting metrics for aviation impacts on climate. Bull. Amer. Meteor. Soc., 91(4), 491-496, doi:10.1175/2009BAMS2835.1, 2010.

Xie, Y., Yang, P., Liou, K.N., Minnis, P., & Duda, D. P.: Parameterization of contrail radiative properties for climate studies. Geophys. Res. Lett., 39, L00F02, doi:10.1029/2011GL050205, 2012.

Yi, B., Yang, P., Liou, K.N., Minnis, P., & Penner, J. E.: Simulation of the global contrail radiative forcing: A sensitivity analysis. Geophys. Res. Lett., 39, L00F03, doi:10.1029/2011GL050207, 2012.

Yun, Y., Penner, J. E., & Popovicheva, O.: The effects of hygroscopicity on ice nucleation of fossil fuel combustion aerosols in mixed-phase clouds. Atmos. Chem. Phys., 13, 4339–4348, doi:10.5194/acp-13-4339-2013, 2013.

Zängl, G., Reinert, D., Rípodas, P., & Baldauf, M.: The ICON (ICOsahedral Non-hydrostatic) modelling framework of DWD and MPI-M: Description of the non-hydrostatic dynamical core. Q. J. R. Meteorol. Soc., 141(687), 563-579, doi:10.1002/qj.2378, 2015.

Zhou, C., & Penner, J. E.: Aircraft soot indirect effect on large-scale cirrus clouds: Is the indirect forcing by aircraft soot positive or negative? J. Geophys. Res.: Atmos., 119, 11 303–11 320, doi:10.1002/2014JD021821, 2014.